UNIVERSITY OF SOUTHAMPTON

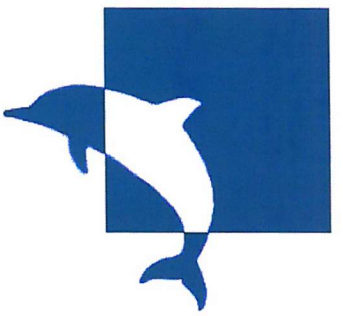

THE SYNTHESIS AND CHARACTERISATION OF COMPLEXES OF TIN AND ANTIMONY

A thesis submitted for the degree of

Master of Philosophy

By

Rina Patel

Department of Chemistry

Southampton

November 2003

ABSTRACT
FACULTY OF SCIENCE
CHEMISTRY
Master of Philosophy

By Rina Patel

The complexes of SnX_4 (X = Cl, Br) with macrocyclic thio- and selenoether ligands ([12]aneS_4, [14]aneS_4, [16]aneS_6, [8]aneSe_2 and [16]aneSe_4) have been synthesised and characterised by multinuclear NMR (^{1}H, ^{119}Sn and ^{77}Se) spectroscopy, IR spectroscopy and elemental analysis. SnI_4 adducts were also studied. Single crystal X-ray diffraction has been employed to structurally characterise [$SnBr_4$([12]aneS_4)], [$SnBr_4$([14]aneS_4)] and [$SnBr_4$([16]aneS_4)], and each reveals a polymeric chain structure. There is a considerable structural dependence on the macrocyclic ring size, as the ring size of the macrocycle is increased the coordination environment at tin(IV) changes, [$SnBr_4$([12]aneS_4)] adopts a *cis*-octahedral geometry at Sn(IV), [$SnBr_4$([14aneS_4)].2/3CH_2Cl_2 and [$SnBr_4$([16]aneS_4)] show a *trans*-octahedral geometry at Sn(IV).

The complex [$SbCl_3$([8]aneSe_2)] has been synthesised and structurally characterised using single crystal X-ray diffraction, the structure reveals [Sb_2Cl_6(η^1-[8]aneSe_2)$_2$] dimers, the dimers are linked together to form an infinite ladder structure. This is the first example involving a *trans* deposition of the Se atom on the Sb(III) acceptor. A range of complexes of the form [$SbCl_5$(L)] where L = $OPMe_3$, $OPPh_3$, $OPMePh_2$, $OAsPh_3$, $SPPh_3$ and $SePPh_3$ and [($SbCl_5$)$_2$L] where L = $Ph_2P(O)CH_2P(O)Ph_2$ and $Ph_2As(O)CH_2As(O)Ph_2$ have been prepared and characterised by multinuclear NMR (^{1}H, ^{31}P and ^{77}Se) spectroscopy, IR spectroscopy and elemental analysis.

A study on the promotion of oxidation of a variety of arylphosphines including Ph_3P, *o*-$C_6H_4(PPh_2)_2$ and $Ph_2P(CH_2)_2PPh_2$ to the corresponding phosphine oxides on reaction with dry air or dioxygen in the presence of catalytic amounts of SnI_4 has been undertaken. The phosphine oxides have been characterised by $^{31}P\{^1H\}$ NMR spectroscopy and IR spectroscopy. The reaction with Ph_3P was conducted using $^{18}O_2$ and the product was shown to be exclusively $Ph_3P^{18}O$ by both IR spectroscopy and EI mass spectrometry, establishing air/dioxygen as the source of the oxygen in the phosphine oxides.

Acknowledgements

I am indebted to my supervisors, Professor Bill Levason and Dr. Gill Reid, for their help, support and enthusiasm during the year of this research, particularly for their time in the collection of multinuclear NMR data.

A large proportion of the discussion in this thesis is based on single crystal X-ray diffraction data, and special mention is due to Melissa Matthews and Lorna Nichols for helping with data collection on the Kappa CCD diffractometer. I would also like to thank Dr. Mike Webster and Gill for their superb advice and guidance in all aspects of crystallography, especially for their help in resolving my crystallographic problems, and Professor Mike Hursthouse and the staff of the EPSRC National Crystallography Service for providing me with regular access to the Kappa CCD diffractometer.

I would also like to thank Matthew Hesford for his time and assistance in the laboratory, and my parents for their encouragement and support throughout the year.

Contents

List of Tables

Chapter 3

Chapter 4

List of Figures

Chapter 1

Chapter 2

Chapter 3

Chapter 4

Abbreviations

Techniques

NMR	Nuclear Magnetic Resonance	ppm	Parts per million
$\{^1H\}$	Proton decoupled	δ	Chemical shift
Dp	Relative receptivity to ^1H	Hz	Hertz
J	Coupling constant	s	Singlet
d	Doublet	t	Triplet
qu	Quintet	m	Multiplet
IR	Infrared	ν	Vibrational frequency
br	Broad	λ	Wavelength
Å	Angstrom (10^{-10} m)		

Solvents

THF	Tetrahydrofuran	DCM	Dichlromethane
CCl_4	Carbon tetrachloride	MeCN	Acetonitrile
DMF	N,N-Dimethylformamide	DMSO	Dimethylsulfoxide

EtOH	Ethanol

Ligands

[9]aneS_3	1,4,7-trithiacyclononane
[12]aneS_4	1,4,7,10-tetrathiacyclododecane
[14]aneS_4	1,4,8,11-tetrathiacyclotetradecane
[16]aneS_4	1,5,9,13-tetrathiacyclohexadecane
[18]aneS_6	1,4,7,10,13,16-hexathiacyclooctadecane
[8]aneSe_2	1,5-diselenacyclooctane
[16]aneSe_4	1,5,9,13-tetraselenacyclohexadecane
[24]aneSe_6	1,5,9,13,17,21-hexaselenacyclotetracosane
cyclen	1,4,7,10-tetraazacyclododecane
cyclam	1,4,8,11-tetraazacyclotetradecane
dmpe	1,2-bis(dimethylphosphino)ethane
dppm	1,2-bis(diphenylphosphino)methane
dppe	1,2-bis(diphenylphosphino)ethane

Miscellaneous

Me	Methyl	Et	Ethyl
^{i}Pr	iso-Propyl	^{n}Pr	n-Propyl
^{n}Bu	n-Butyl	Ph	Phenyl
R	Alkyl or Aryl	*o*	Ortho
p	Para	*m*	Meta
K	Kelvin	mmol	Millimoles

MO	Molecular Orbital
HOMO	Highest Occupied Molecular Orbital
LUMO	Lowest Unoccupied Molecular Orbital
σ^*	Anti-bonding
HSAB	Hard-Soft Acid Base concept
Acac	Acetylacetonate

CHAPTER 1

Introduction

1.1 Elements of Group 14

Group 14 comprises of the elements carbon, silicon, germanium, tin and lead. The expected similarity in the properties between elements in the same group is much less apparent in Group 14, where there is a considerable change in character on descending the group. Carbon is a dull black colour in the form of graphite, or hard and transparent in the form of diamond; silicon and germanium are dull grey or black in colour; tin and lead are shiny and grey in colour. Despite being in the same group the properties of the elements vary considerably on descending the group. Carbon is a non-metal, silicon and germanium are metalloids, and tin and lead are typical metals.

Table 1.1 Some properties of the group 14 elements.[1]

				Ionisation enthalpies (kJ mol^{-1})					
Element	Electronic Structure	mp (°C)	bp (°C)	1st	2nd	3rd	4th	Electro-negativity	Covalent radius (Å)
C	$[He]2s^2 2p^2$	>3550[b]	4827	1086	2353	4618	6512	2.5 – 2.6	0.77
Si	$[Ne]3s^2 3p^2$	1410	2355	786.3	1577	3228	4355	1.8 – 1.9	1.17
Ge	$[Ar]3d^{10}4s^2 4p^2$	937	2830	760	1537	3301	4410	1.8 – 1.9	1.22
Sn	$[Kr]4d^{10}5s^2 5p^2$	231.9	2260	708.2	1411	2942	3928	1.8 – 1.9	1.40[c]
Pb	$[Xe]4f^{14}5d^{10}6s^2 6p^2$	327.5	1744	715.3	1450	3080	4082	1.8	1.44[d]

a. Tetrahedral (*i.e.*, sp^3 radii)

b. Diamond

c. Covalent radius of Sn(II), 1.63 Å

d. Ionic radius of Pb^{2+}, 1.33 (CN 6); of Pb^{4+}, 0.775 Å

In the following summary carbon has been omitted. The group 14 elements occur in two oxidation states, +2 and +4. There is a steady increase in the stability of the +2 oxidation state as the group is descended. The elements in the group have four electrons in the outermost shell, two s electrons and two p electrons. The first four-ionisation energies rise in a fairly even manner, and the fifth ionisation energy is very large, reflecting the removal of an electron from a filled level nearer to the nucleus. Compounds of lead and tin in which the group 14 element has an oxidation number of +2 are regarded as ionic. In these compounds, the Sn^{2+} and Pb^{2+} ions are formed by the

loss of the outermost two electrons, whilst the s electrons remain relatively stable in their filled sub-shell. This is called the 'inert pair effect'.

The Group 14 elements form two series of halides, MX_2 and MX_4. The stability of the MX_2 increases down Group 14; $SiX_2 < GeX_2 < SnX_2 < PbX_2$, the opposite is true for the MX_4; $SiX_4 > GeX_4 > SnX_4 > PbX_4$. The silicon(IV) halides are colourless, volatile liquids, formed by the reaction of silicon or silicon carbide with a halogen. Germanium(IV) halides are easily formed *via* the reaction of GeO_2 with aqueous HX. The tin(IV) halides are formed by the reaction of elemental tin with a halogen under anhydrous conditions. The SnX_4 (X = Cl, Br or I) follow the observed trend of discrete tetrahedral units with $SnCl_4$ as a colourless liquid, $SnBr_4$ as a colourless crystalline solid and SnI_4 as an orange, crystalline solid. SnF_4 which is produced by the reaction of fluorine with tin, is different from the other group 14 tetrahalides in being a white crystalline compound, the structure is polymeric with octahedral coordination about the tin with SnF_6 units joined into planar layers by edge sharing of four equatorial F atoms (Sn-F_μ 2.02 Å) with two further terminal F atoms mutually *trans* (Sn-F_t 1.88 Å).[2] All the group 14 halides are hydroscopic, and are immediately and completely hydrolysed by water.

Figure 1.1 View of the polymeric SnF_4 structure.[2]

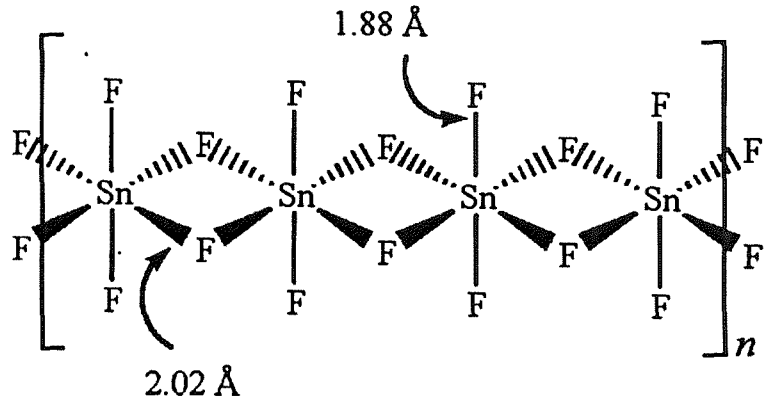

Lewis acidity increases as you progress down the elements of Group 14. The MX_4 molecules possess two vacant d-orbitals, thus they are able to act as electron acceptors. Together with the s- and p-orbitals, these hybridise to form a set of six d^2sp^3 hybrids,[3] adopting the octahedral geometry commonly found in adducts of these MX_4

compounds.[4] There is also a clear trend of decrease in Lewis acidity with halide type, F > Cl > Br > I as the M-X bond becomes less polar and the effective charge on the M centre increases.[5]

1.2 The Elements of Group 15

Group 15 constitutes the third column of the p-block of the periodic table and comprises the elements nitrogen, phosphorus, arsenic, antimony and bismuth (collectively termed the pnictogens or pnictides). Despite being in the same group, the physical and chemical properties show a considerable range. Thus, as the group is descended, nitrogen and phosphorus are non-metals, arsenic and antimony are described as metalloids or semi-metals, and bismuth is considered metallic. Nitrogen, which has the distinction of being gaseous under normal conditions, has been omitted, as there is little resemblance between the characteristics it displays and other Group 15 elements. Table 1.2 shows a selection of the physical properties of the elements in group 15.

Table 1.2 Physical properties of the elements of group 15.[3]

Element	Electronic Configuration	Electronegativity (Allred-Rochow)	Covalent Radius[a] (Å)	Van der Waals Radius (Å)
P	$[Ne]3s^2 3p^3$	2.06	1.10	1.90
As	$[Ar]3d^{10}4s^2 4p^3$	2.20	1.21	2.00
Sb	$[Kr]4d^{10}5s^2 5p^3$	1.82	1.41	2.20
Bi	$[Xe]4f^{14}5d^{10}6s^2 6p^3$	1.67	1.52	2.40

[a] For trivalent state

The common oxidation states for arsenic, antimony and bismuth are +3 and +5. Halogen compounds of phosphorus, arsenic and antimony are numerous and important in synthetic chemistry. The Group 15 elements form two series of halides, MX_3 and MX_5 (M= P, As, Sb or Bi; X = F, Cl, Br or I), although not all are known. Arsenic, antimony and bismuth trihalides comprise 12 compounds that exhibit diversity in their physical and chemical properties, as well as a considerable variation in their structures. Bismuth trifluoride has an ionic lattice with 9-coordinate bismuth. SbF_3 has an

intermediate structure in which SbF_3 molecules (Sb-F = 1.92 Å) are linked through F bridges (Sb---F = 2.61 Å) to give each Sb(III) a very distorted octahedral environment.[3] $BiCl_3$ also possesses a quasi-molecular structure. The other trihalides, AsF_3, $AsCl_3$, $AsBr_3$, $SbCl_3$ and $SbBr_3$ are molecular, and they give pyramidal EX_3 (E = As, Sb) molecules readily in the vapour phase. For the iodides, the solids have close packed arrays of I atoms with E atoms in octahedral interstices but located off-centre so that the incipient EI_3 molecules can be considered to exist. All trihalides except PF_3 are best obtained by direct halogenation, keeping the element in excess, whereas the pentahalides may all be prepared by reaction of the elements with excess halogen.[3]

The pentahalides vary from volatile substances such as PF_5 and AsF_5 to solids, such as PCl_5 and BiF_5. The five-coordinate gas-phase molecules are trigonal bipyramidal. In contrast to the volatile PF_5 and AsF_5, SbF_5 is a highly viscous liquid in which the molecules are associated through F-atom bridges. In solid SbF_5 these bridges result in a cyclic tetramer, which reflects the tendency of Sb(V) to achieve a coordination number of 6. Antimony pentachloride is made by the reaction of Cl_2 with $SbCl_3$ and is stable up to ~140°C. Antimony pentachloride exists in two modifications: above –54.1°C it is trigonal bipyramidal, below –54.1°C it changes reversibly into a double chlorine bridged dimer resulting in an edge shared double octahedral structure ($Cl_4SbCl_2SbCl_4$).[6] The pentafluorides of phosphorous, arsenic, antimony and bismuth are strong Lewis acids.

Much more structurally diverse are compounds of the elements in the +3 oxidation state, as a result of the presence of a lone pair of electrons. The lone pair is an important consideration in the structural chemistry of the Group 15 halides and their complexes. In the gas phase the MX_3 molecules are pyramidal, however in the crystalline state the MX_3 molecules form weak secondary M-X interactions to adjacent units, first proposed by Alcock.[7] Sawyer and Gillespie[8] postulate that these interactions are formed around the direction of maximum electron density of the lone pair, but not directly over it. Galy and Enjalbert[9] examined the structural aspects of MX_3 molecules, and concluded that these species adopt one of three coordination polyhedra: a trigonal antiprism, a bicapped trigonal prism or tricapped trigonal prism. The stereochemical activity of the lone pair are found to decrease in the order As > Sb > Bi, with increasing

coordination number, and with increasing atomic number of the halogen. This is described in more detail in chapter 3.

1.3 Hard and Soft Acids and Bases

Pearson[10] introduced the classification of substances as 'hard' and 'soft' acids and bases, it is an extension of the Lewis and Chatt-Ahrland classifications of metal-ligand interactions.[11]

In general, both acids and bases can be classified as either hard or soft, and it is found that hard acids preferentially bond to (or form adducts with) hard bases and soft acids to soft bases. Hard acids (electron pair acceptors) have no low lying or low energy unfilled orbitals (*i.e.* the LUMO is high in energy) and therefore do not readily form covalent bonds with bases. Hard bases (electron-pair donors) have no high-lying or high-energy orbitals, (*i.e.* the HOMO is low lying in energy) and also do not readily form covalent bonds to acids, but since the acids and bases are usually positively and negatively charged respectively, they tend to bond strongly to each other through ionic interactions. In contrast, soft acids do tend to have low-energy unfilled orbitals (a low energy LUMO), which will readily form covalent bonds, and soft bases tend to have high-energy filled orbitals (a high energy HOMO) which will also easily form covalent bonds. Therefore, the combination of soft acids with soft bases is the one, which maximises a covalent interaction. Acids and bases somewhat intermediate in nature are referred to as *borderline*.

Table 1.3 A selection of hard, soft and borderline acids and bases.[3]

	Hard	Borderline	Soft
Acids	H^+, Li^+, Na^+, Ca^{2+}, Ti^{4+}, Fe^{3+}, As^{3+}, Ga^{3+}, BF_3	NO^+, Fe^{2+}, Cu^{2+}, Pb^{2+}, Zn^{2+}, Ru^{2+}, Sb^{3+}, Bi^{3+}	Tl^+, Cu^+, Au^+, Ag^+, Pd^{2+}, Pt^{2+}, Pt^{4+}, Cd^{2+}, Hg^{2+}, Tl^{3+}, Te^{4+}
Bases	F^-, Cl^-, HO^-, NO^{3-}, H_2O, OR_2, NR_3, ClO_4^-, SO_4^{2-}	Br^-, NO_2^-, N_2, N_3^-, SO_3^{2-}	ER_2 (E = S, Se, Te), $E'R_3$ (E' = P, As, Sb), CO, CN^-

1.4 Macrocyclic Chemistry

For our purposes a macrocyclic ligand may be defined as a cyclic compound with 9 or more members in the ring (including all heteroatoms) and with three or more donor atoms. The properties of the macrocyclic ligand are determined by a number of factors,[12] including the number and type of donor atom (*e.g.* O, N, S, Se, P), the size of the macrocyclic cavity (ring size), the degree of alkylation of donor atoms (*e.g.* for N and P donor macrocycles NR and PR pendant arms), the degree of alkylation of the backbone and the degree of unsaturation/conjugation. Many systems have been studied to-date, including porphyrins, phthalocyanines, crown ethers and aza crowns, containing hard oxygen and nitrogen donors respectively, and thioethers, which incorporate soft sulfur donors.[13,14,15,16,17,18,19]

1.4.1 The Macrocyclic Effect

Macrocyclic chemistry has developed over the years as a result of the inherent stability of complexes of macrocyclic ligands. Early in the development of coordination chemistry it was found that complexes with polydentate ligands were subjectively and quantitatively more stable than complexes with monodentate ligands, this phenomenon was described as the chelate effect.[12] The effect was found to be sequential and the stability increased as more donors were incorporated into the polydentate ligands. Just as chelating n-dentate ligands give a more stable complex than n-unidentate ligands of similar type due to the chelate effect, a macrocyclic ligand gives even more stable

complexes than the most similar n-dentate open chain ligand due to the 'macrocyclic effect' first observed by Cabbiness and Margerum,[20] who quantified it for Cu(II) aza macrocyclic systems. However, the origins of the macrocyclic effect are not clearly defined. Macrocyclic complexes are usually both thermodynamically stable and chemically inert.

1.4.2 Kinetic Stability[21]

The uptake of a macrocycle or an open chain analogue by a metal ion is expressed as follows:

$$M^{2+}_{(aq)} + L \rightleftharpoons ML^{2+} \qquad K = k_f/k_d$$

The k_f and k_d terms refer to the second order formation constant and first order dissociation constant respectively. The stability constant K, defined as the ratio of k_f/k_d is a reflection of the stability of the complex. It was found that both the formation and especially the dissociation constants (k_f and k_d respectively) are considerably lower in macrocyclic complexes than in for the analogous non-macrocyclic systems, resulting in a larger rate constant K. For simple ligand complexes, the formation rate is often controlled by the solvent exchange rate of the solvated metal ion. This can be ascribed to the differences in flexibility of the coordinative bonds in the two types of systems. Dissociation requires elongation and cleavage of the M-L bonds, which is inhibited in the macrocyclic complex since M-L cleavage leads to a distortion throughout the whole ring. In contrast, M-L cleavage in an open chain polychelate is much easier, involving an "unzipping mechanism".[12]

1.4.3 Thermodynamic Stability

In comparing the thermodynamics of the uptake of the macrocycle compared to the analogous open chain ligand it is convenient to consider the Gibbs Free Energy term, $\Delta G = \Delta H - T\Delta S$. In the following example,[22] ΔG for the reaction at 298K is -33.67 kJ mol^{-1}. This arises from the enthalpic, ΔH,[21] and the entropic, $T\Delta S$[23], terms.

$$[NiL]^{2+} + [14]aneN_4 \rightleftharpoons [Ni([14]aneN_4)]^{2+} + L$$

$$L = H_2N(CH_2)_2NH(CH_2)_3NH(CH_2)_2NH_2$$

The Entropic Contribution

The value of the entropic term $T\Delta S$ in the above reaction is 13.2 kJ mol^{-1}.[22] The entropic effect arises due to the higher entropy from the open chain analogue in its free form compared to the entropy for the free macrocycle in its uncoordinated form. This is partly due to the ring structure of the macrocycle. For the macrocycle, which is compact and rigid in its 'free' form, coordination to a metal ion only leads to a small reduction in the rotational and vibrational degrees of freedom. However, the open chain analogue exhibits greater configurational entropy in the free form than in the coordinated form. Thus, there is a net gain in entropy upon release of the acyclic ligand into solution.

The Enthalpic Contribution

The different solvation energies of the open-chain and macrocyclic ligands may play a crucial role in determining the enthalpic contribution. For example, in the above reaction ΔH = -20.5 kJ mol^{-1}.[22] Solvation occurs more readily for the open chain ligand compared to the analogous macrocycle, which in its uncoordinated form is more rigid and compact. As a result, macrocyclic coordination leads to a favourable term in the above reaction. The variability of the enthalpy term appears to reflect a number of influences, an important concern is any difference in the energy of the bonds between the metal ions and the respective ligands involved. Changes in ligand conformation on complexation are also important, as is the size of the macrocyclic cavity.

Preorganisation

Preorganisation of the lone pairs also contributes to the macrocyclic effect. Solid state X-ray structural studies show that in many thioether macrocycles the S-donors adopt *exo*-conformations,[24] with the S atom lone-pairs directed away from the cavity, thus minimising lone-pair repulsions. Therefore, coordination of a metal within the cavity requires a conformational rearrangement to the *endo* form. This requires

energy, thus the macrocyclic effect may be very small. In contrast to the conformation adopted by most of the free macrocylic thioethers, the sulfur atoms in [9]aneS_3 are *endodentate*.[25] The X-ray structure of [9]aneS_3 shows that all the S atom lone pairs are in an ideal orientation for facial coordination to a metal. In an attempt to investigate the distortion of the ring upon complexation, [Mo(CO_3)([9]aneS_3)] was prepared and structurally characterised.[26] The features of most interest in this structure are those that describe the distortion of the cyclic polythioether upon coordination to the metal. Uncomplexed [9]aneS_3 compensates for the repulsive interaction between the sulfurs by increasing the S-C-C'-S' torsion angle. An increase in this angle effects an increase in the inter-sulfur distance and also rotates the interior lone pair on the sulfur away from the molecules rotational axis (Figure 1.2).

Figure 1.2 Diagram of 'free' [9]aneS_3 displaying the orientation of the lone pairs.

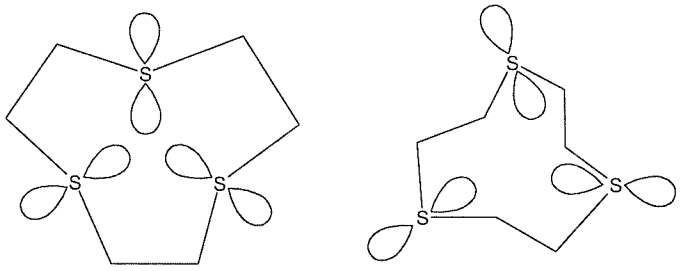

The S-C-C'-S' torsion angle and the rotation of the ring on the metal tricarbonyl fragment are related to the metal sulfur orbital overlap. The S-C-C'-S' torsion angle for uncomplexed [9]aneS_3 is 58°. The torsion angle for [Mo(CO_3)([9]aneS_3)] is 48°. The reduction in this torsion angle is the result of stabilisation provided by the formation of metal-sulfur bonds, which partly overcomes the repulsion between the sulfur lone-pairs. Stronger shorter metal sulfur bonds would result in a smaller torsion angle.[26]

1.5 Synthesis of Macrocyclic Chalcogenoethers

There are two major methods for the synthesis of macrocycles:

High Dilution Methods

One widely adopted method involves the use of high dilution reaction conditions, the macrocyclic ring closure mechanism is undertaken at high levels of

dilution to keep the concentrations of the reagents low and therefore maximise cyclisation over polymerisation. It is usually necessary to ensure that the reactants are mixed very slowly and slow, consecutive addition of the reactants must be maintained over hours or days. Many of the reactive precursors are water sensitive and it is essential to work under strictly anhydrous reaction conditions. Also, if stereoisomers are possible, this route will typically yield mixtures, which may be difficult to separate. Figure 1.4 describes the preparation of a 14-membered S_4-donor macrocycle, which is best performed at high dilution.

Metal Template Synthesis

One of the problems with the synthesis of macrocycles is the conformation control in bringing the two ends of a chain together in the final cyclisation step. The 'template effect' is a widely used strategy, which circumvents these problems. The idea is that a metal ion will coordinate to the donor atoms and pre-organises the various intermediates in the conformation required to give the desired cyclic products. Reactions yield a macrocyclic complex and demetallation is required to release the free macrocycle. Curtis[27] reported the first of a number of pioneering template reactions for macrocyclic systems. In the Curtis synthesis, a yellow crystalline product was observed to result from the reaction of $[Ni(1,2\text{-diaminoethane})_3]^{2+}$ and dry acetone. The yellow product was shown to be a mixture of the isomeric complexes (a) and (b) described in Figure 1.3.[28]

Figure 1.3 A diagram to show the isomeric macrocyclic complexes formed in the Curtis synthesis.

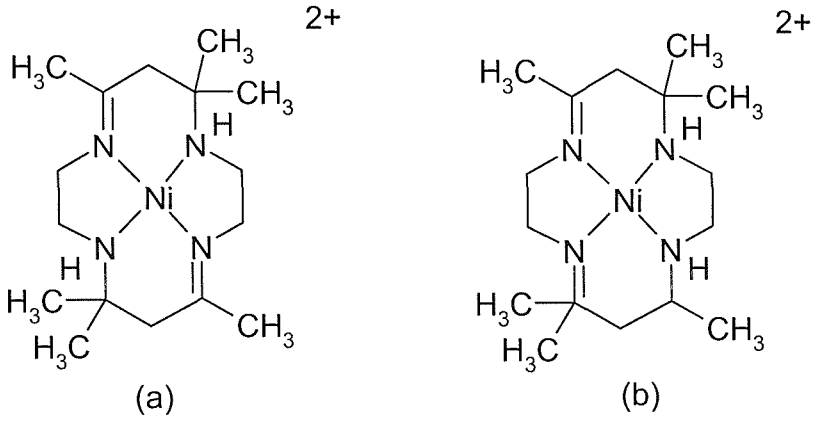

The removal of a macrocycle from its coordinated metal ion is a frequent procedure in macrocyclic ligand synthesis (demetallation). The addition of excess acid may lead to the demetallation of an amine-containing macrocycle. For chemically labile systems, the acid will protonate the amine functions as they dissociate from the metal ion and thus 'scavenge' the macrocycle as its *N*-protonated form. Demetallation may be induced by addition of a strongly competing ligand to a solution of the macrocyclic complex (the cyanide ion or ethylenediaminetetraacetate are frequently used). In some cases when the sulfide or hydroxide ion is employed as the scavenging ligand, the metal may be removed as an insoluble precipitate (metal sulfide or hydroxide) leaving the metal-free macrocycle in the supernatant liquid.[12]

The disadvantages of this process are that not all metal ions can act as templates and macrocyclic complexes tend to be non-labile hence it is difficult to obtain the free macrocycles *via* demetallation.

- **Macrocyclic Thioethers**

Synthetic routes to the chalcogenoethers used in this study are discussed below. The macrocyclic thioethers used in these studies were obtained commercially from Aldrich. Prior to developments in the procedures adopted for the synthesis of thioether macrocycles, they were only obtainable in low yields, therefore it is worth reviewing the major synthetic routes adopted for these ligands.

The typical route for the synthesis of thioether macrocycles is *via* high dilution techniques, whereby large volumes of the solvent are used thus favouring cyclisation over polymerisation. One of the first thiacrowns to be prepared was [18]aneS_6, which was isolated in less than a 2% yield. Ochrymowycz who had developed purification methods for the macrocyclic thioethers, later improved this to *ca.* 30%. However, the route employed the use of sulfur mustard derivatives requiring extreme care in handling.[29]

The initial yields for the formation of [12]aneS_4 were 4%[30] and 6.3%[29], 16%[30] for [14]aneS_4 and 7.5%[31] for [16]aneS_4. These were later improved ([12]aneS_4: 88%, [14]aneS_4: 72% and [16]aneS_4: 76%) due to the development of Cs_2CO_3/DMF-

promoted cyclisation. Thiols were found to be deprotonated readily by Cs_2CO_3 and $CsHCO_3$ in DMF to form caesium thiolates, which are relatively soluble. It is assumed that cyclisation occurs in two steps (Figure 1.4). The Cs_2CO_3 was suspended in 500 cm^3 dry DMF, to this well stirred solution held at 45-50°C were added simultaneously and slowly a solution of dithiol in 100cm^3 of DMF and a solution of dibromide in 100 cm^3 of DMF. The total time of addition was 12-15 hours. The effect of caesium in promoting intramolecular cyclisation is assumed to lie in the second step with the rate constant k_2. The smaller alkali metal cations do not promote cyclisation to the same extent and are seen to give more oligomeric products at the cost of cyclisation.[32]

Figure 1.4 Synthetic route to the cyclic thioether [14]aneS_4.[32]

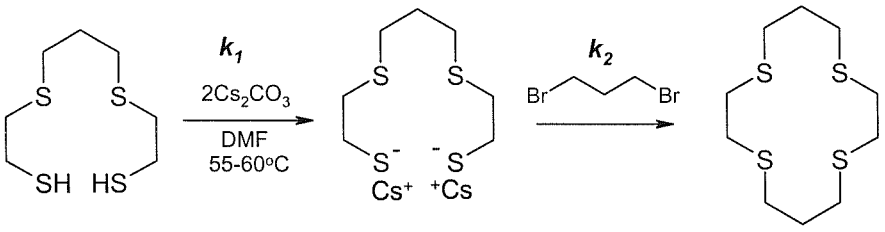

A template-based high yield synthesis of [9]aneS_3 has also been reported. During a study of the reactions of molybdenum(0) carbonyl complexes with multidentate organosulfur ligands, $(NMe_4)_2[Mo(CO)_3(SC_2H_4SC_2H_4S)]$ was obtained from $[Mo(CO)_3(CH_3CN)_3]$ and $(NMe_4)_2(SC_2H_4SC_2H_4S)$; subsequent alkylation with 1,2-dibromoethane gave $[Mo(CO)_3([9]aneS_3)]$, treatment of the complex with further $(NMe_4)_2(SC_2H_4SC_2H_4S)$ liberates free [9]aneS_3 and regenerates the complex $(NMe_4)_2[Mo(CO)_3(SC_2H_4SC_2H_4S)]$.[33]

- **Macrocyclic Selenoethers**

In 1989 Pinto and co-workers[34] described the preparation of the cyclic selenoethers [8]aneSe_2, [16]aneSe_4 and [24]aneSe_6. The following section summarises the methodology employed during the reaction procedures required in the synthesis of selenoether macrocycles (Figure 1.5). The synthesis of $NCSe(CH_2)_3SeCN$ is accomplished by the reaction of slightly greater than two molar equivalents of KSeCN

with one molar equivalent of $Br(CH_2)_3Br$ in dry DMF. The reaction to produce macrocycles is performed at low temperature. Ammonia is condensed into the flask *via* a Me_2CO/solid CO_2 slush bath at *ca.* 195K. Addition of $NCSe(CH_2)_3SeCN$ and sodium produces a solution of $NaSe(CH_2)_3SeNa$ and NaCN. A slight excess of $Br(CH_2)_3Br$ in THF is added dropwise over 3 hours with the slush bath mantained at 223K. This gradually produces a precipitate of NaBr and NH_3 is evaporated. Distilled water is added to the mixture to dissolve the precipitate, and a yellow solution results *via* extraction with dichloromethane. The mixture containing the cyclic selenoethers is purified by column chromatography on silica with an eluting mixture of 19:1 hexane: ethyl acetate. The first ligand to be eluted from the column is [8]aneSe_2 with a R_f value of 0.65. The second is [16]aneSe_4 (R_f= 0.4). The third ligand is [24]aneSe_6 (R_f = 0.1).

Figure 1.5 Synthetic Route to the Cyclic Selenoethers [8]aneSe_2, [16]aneSe_4, and [24]aneSe_6.[34]

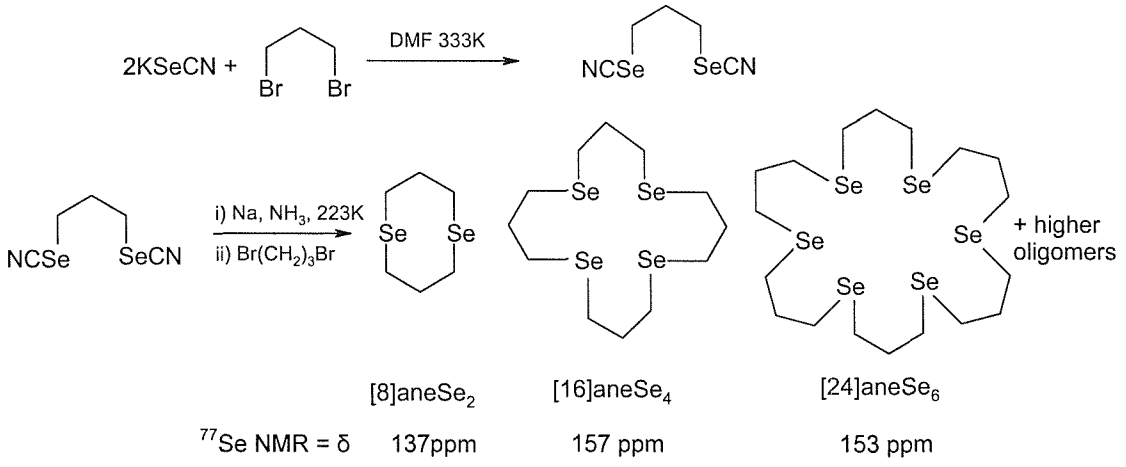

The preparations of [12]aneSe_3 and [20]aneSe_5 involve stepwise introduction of the Se atoms, with ring closure occurring *via* a high dilution cyclisation of $NaSe(CH_2)_3SeNa$ (generated in situ) with $TsO(CH_2)_3\{Se(CH_2)_3\}_nOTs$, n = 1 or 3 respectively (Figure 1.6).[35]

Figure 1.6 Synthetic route to the cyclic selenoether [12]aneSe$_3$.[35]

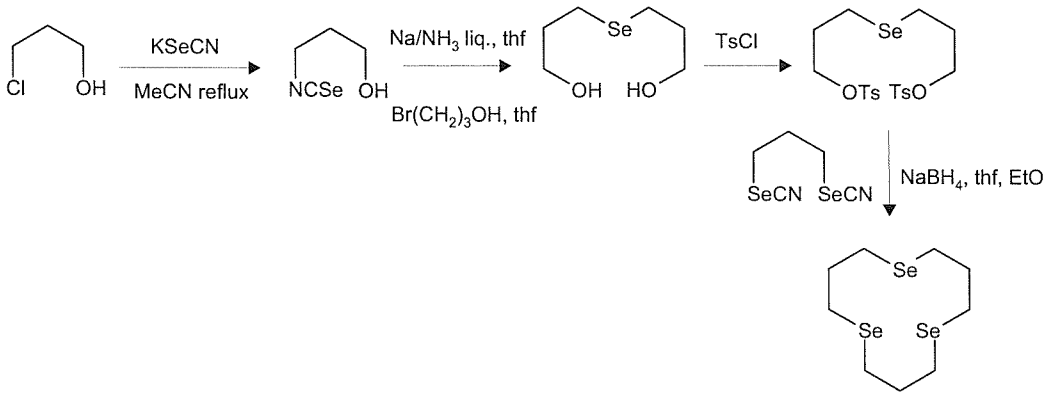

- **Acyclic thio- and seleno-ethers**

MeS(CH$_2$)$_n$SMe (n = 2 or 3)[36]

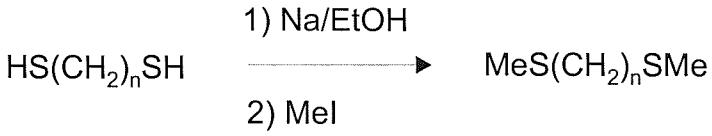

n = 2, ^{77}Se NMR = δ 121 ppm
n = 3, ^{77}Se NMR = δ 74 ppm

The acyclic dithioethers used were readily prepared by reaction of the appropriate dithiol with sodium in ethanol, followed by treatment of the disodium salt with methyl iodide. Fractionation *in vacuo* affords the ligands as colourless (n = 2) or pale yellow (n = 3) liquids in > 70% yield.[36]

MeSe(CH$_2$)$_n$SeMe (n = 2 or 3)[37]

A number of routes for the preparation of acyclic diselenoethers exist in the literature, with early examples reported by Greenwood[38] and Westland.[39] The diselenoethers may also be obtained by reaction of the appropriate α, ω-dichloroalkane

with a frozen THF solution of MeSeLi, prepared from MeLi and Se powder. The pale yellow liquid ligands are isolated in >70% yield by fractionation *in vacuo*.[37]

1.6 Bonding in Chalcogenoether Complexes[40]

The ground-state electronic configuration of the donor atoms in ER_2 species (E = S, Se, Te) is $ns^2np^4nd^0$. Two of these electrons are used in bonding, leaving four electrons to occupy non-bonding atoms on the chalcogen atom. In thioethers, bonding can be accounted for by sp^3 hybridisation; the degree of hybridisation falls moving to Se and Te. Thus, two hybrid lone pair orbitals are available for donation; one or both of which may form a σ–bond resulting in a bridging R_2E group. One orbital may also behave as a π-donor to a suitable metal d-orbital, particularly to electron poor metals however there is no good evidence that this is a significant component of the bonding. For R_2E, the E atom could behave as a π-acceptor either into the lowest empty d-orbital as in the original Chatt model,[41] the bonding can be described in terms of donation into the E-C σ*-antibonding orbital, analogous to the Orpen-Connelly model[42] for PR_3 species. It is possible that to electron-rich metal centres the second lone pair will be a source of π-repulsion in M-ER_2.

A detailed study using extended Huckel MO theory was undertaken by Schumann and co-workers,[43] experimental studies on $[\eta^5\text{-}C_5H_5)Fe(CO)_2L]^+$ cations where L is a Group 15 or 16 donor ligand, showed that within Group 16 both the inertness and the stability of the Fe-E bond increased Te>>Se>S>O. It was concluded that π-effects are insignificant, and that the unusually strong binding of telluroethers is due to enhanced σ-donation. More recent studies on $[Mn(CO)_3X(L\text{-}L)]$ (L-L = dithioether, diselenoether, or ditelluroether) and $[Mn(CO)_3(tripod)]^+$ (tripod = $MeC(CH_2EMe)_3$, E = S, Se or Te) have been undertaken.[44] Analysis of the force constants resulting from the IR spectra of the $Mn(CO)_3$ groups and the magnitude of the NMR chemical shifts (^{55}Mn, ^{77}Se, ^{125}Te) show similar trends, with increased electron density at the manganese centre S<Se<<Te. Similar trends are also observed in $[M(CO)_4(L\text{-}L)]$ complexes of Group 6 carbonyls.[45] For low valent metals the spatial extension of the d-orbitals will be such that good overlap with the large Te σ-orbital is attainable, as the metal oxidation state increases, the metal becomes harder and the orbitals contract, which would decrease bonding to the large soft tellurium. Thus

telluroethers are unable to bond to high oxidation state metals. It is apparent that within Group 16 the relative donor strength varies with the metal acceptor, to high or medium oxidation state metals it is S<Se>Te, whereas to low valent centres it is S<Se<<Te.[46]

1.7 Pyramidal Inversion

Acyclic thio-, seleno- and telluro-ethers can bind *via* one of two lone pairs; therefore, different invertomers are possible. In solution the molecules are able to switch between invertomers, either by a dissociative route or *via* pyramidal inversion. *Abel et al.*[47] first studied pyramidal inversion using ^{1}H NMR spectroscopy with $[PtCl_2\{MeS(CH_2)_2SMe\}]$. It was found that the inversion process was slow on the NMR timescale, such that the protons were non-equivalent and the *meso* and *dl* invertomers could be indentified. Typical activation energies are in the range 35 – 100 $kJmol^{-1}$.[48]

Figure 1.7 *meso* and *dl* invertomers for $[PtCl_2\{MeS(CH_2)_2SMe\}]$[47]

The activation energy for this process is low, and $^{195}Pt\{^{1}H\}$ coupling is retained at higher temperatures, and it was therefore proposed that the mechanism for inversion is *via* a planar transition state with both lone pairs bonded to the metal.[49,50] In comparison to the *trans* monodentate complexes, pyramidal inversion in bidentate complexes occurs at significantly higher temperatures. The *trans* effect seen for the halide ions in these complexes is found to be in the order Cl < Br < I.

Figure 1.8 Proposed mechanism for pyramidal inversion in $[PtCl_2\{MeS(CH_2)_2SMe\}]$[49,50]

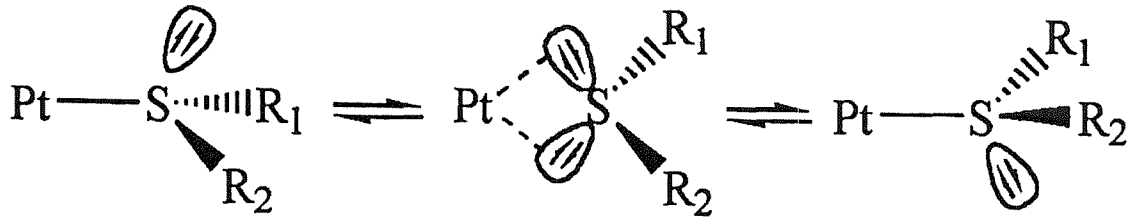

1.8 Complexes of Thio- and Selenoether Macrocyclic Ligands

This section aims to provide a general overview of the complexes of thio- and selenoether macrocyclic ligands with p-block halides. Using selected examples, the discussion will concentrate on structurally characterised complexes. A more detailed review of the literature specifically regarding Sn(IV), Sb(III) and Sb(V) halide complexes is made in the relevant chapter.

The diverse structures exhibited by complexes of p-block halides with acyclic and macrocyclic thio- seleno- and telluro-ethers have been reviewed in detail by Levason and Reid.[51] The only examples of aluminium complexes to be reported are $[AlMe_3([12]aneS_4)]_n$ (Figure 1.9)[52] and $[(AlMe_3([14]aneS_4)]$.[53] However both complexes show structural features that appear frequently throughout the p-block complexes. The former exhibits *exo* coordination to the $AlMe_3$ fragment through one S atom. The environment at Al(III) is a distorted trigonal bipyramid via a further secondary Al-S interaction from an adjacent $[AlMe_3([12]aneS_4)]$ unit. This leads to an infinite one dimensional chain polymer. In contrast, $[(AlMe_3([14]aneS_4)]$ involves four terminal exocyclic $AlMe_3$ fragments one coordinated to each of the S-donor atoms. This gives rise to a tetrahedral geometry at Al(III).

Figure 1.9 View of $[AlMe_3([12]aneS_4)]$.[52]

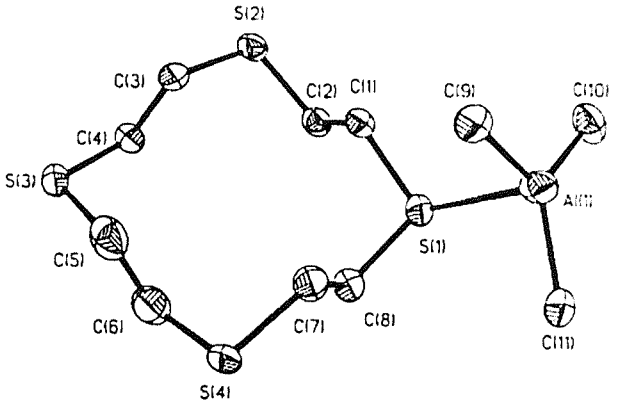

Wieghardt and co-workers[54] have reported the preparation of the complex $[InCl_3([9]aneS_3)]$. No structural data has been obtained for this complex, however it is likely to involve *fac*-coordination by $[9]aneS_3$ giving a *pseudo*-octahedral monomer. The crystal structure of $[InMe_3(L)]_n$ (L = 1,4-dithiane) involves infinite chains of trigonal bipyramidal In(III), with equatorial Me groups and axial coordination to bridging dithiane ligands.[55]

Complexes of thallium are also known, $[Tl([9]aneS_3)]PF_6$,[56] $[Tl([18]aneS_6)]PF_6$,[57] $[Tl([18]aneN_2S_4)]PF_6$[57] and $[Tl([24]aneS_8]PF_6$.[58] In all the compounds only the +1 oxidation state is seen. Much less regular motifs and variable coordination numbers are observed in the structures of these thallium(I) complexes and secondary interactions are significant. $[Tl([9]aneS_3)]PF_6$ reveals tridentate $[9]aneS_3$ coordinated to a single thallium, infinite chains are generated due to a further Tl-S secondary interaction to an adjacent $[Tl([9]aneS_3)]^+$ unit. The chains are cross-linked *via* a further series of four weak secondary Tl-F interactions to PF_6^- anions, thus giving eight coordinate Tl(I). The selenoether complexes $[Tl\{MeSe(CH_2)_3SeMe\}]PF_6$ and $[Tl\{MeSe(CH_2)_2SeMe\}]$ have recently been structurally characterised.[59] In the latter species each Tl(I) centre is coordinated to four Se atoms from different selenoethers, giving a distorted tetrahedral geometry. Each Se atom uses its second lone pair to coordinate to an adjacent Tl centre, therefore generating a 3D network containing Tl_2Se_2 rhomboids. This is the first structural evidence for this doubly bridging coordination mode in diselenoether ligand chemistry. The anions in this species occupy the channels within the cationic 3D framework, providing five weak Tl-F contacts per

Tl centre, from three $[PF_6]^-$ anions, one of which interacts *via* the three F's from a triangular face, while the other two interact *via* a single F atom each. This combination leads to a nine-coordinate geometry at each Tl centre.

A considerable number of lead complexes have been reported in the literature. The compounds $[Pb([9]aneS_3)_2(ClO_4)_2]$,[60] and $[Pb([28]aneS_8)(ClO_4)_4]$[58] have been prepared by the reaction of $Pb(ClO_4)_2$ with the respective macrocycles. The structure of the complex $[Pb([9]aneS_3)_2(ClO_4)_2]$ (Figure 1.10) shows eight-coordination at Pb(II) due to two $[9]aneS_3$ ligands and two weakly associated η^1-coordinated ClO_4^- ligands. The overall geometry is a square antiprism and the lone pair on Pb(II) is stereochemically inactive. The structure of $[Pb([9]aneS_3)_2(ClO_4)_2]$ is also eight co-ordinate about the Pb(II) metal centres, which are bonded to four adjacent thioether donor atoms; the coordination environment is completed by two μ-O_2ClO_2 and one η^2-O_2ClO_2.

Figure 1.10 View of the crystal structure of $[Pb([9]aneS_3)_2(ClO_4)_2]$.[60]

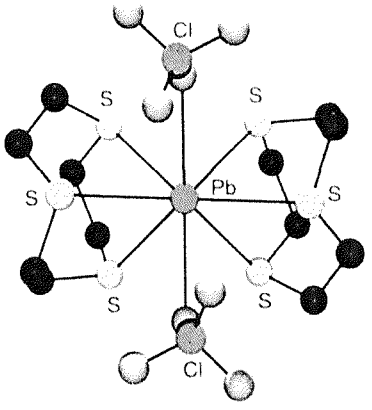

1.9 Physical Measurements

The complexes formed in this study were all characterised using a combination of techniques. Microanalyses were collected for the solids isolated, *via* the University of Strathclyde microanalysis laboratory. The other methods of characterisation were infrared spectroscopy, single crystal X-ray diffraction and NMR spectroscopy (^1H, ^{119}Sn, $^{13}C\{^1H\}$, $^{77}Se\{^1H\}$, and $^{31}P\{^1H\}$).

1.9.1 Nuclear Magnetic Resonance Spectroscopy (NMR)

NMR spectroscopy has been a major characterisation technique in these studies. Multinuclear NMR spectroscopy, with a low temperature attachment has enabled the dynamic processes occurring in solution to be probed. A brief discussion of the nuclei studied is given.

$^{77}Se\{^{1}H\}$ NMR Spectroscopy[61]

The element selenium has six naturally occuring isotopes: ^{74}Se (0.89%), ^{76}Se (9.02%), ^{77}Se (7.58%), ^{78}Se(23.52%), ^{80}Se(49.82%) and ^{82}Se(9.19%). Only one of them, ^{77}Se is NMR active having a nuclear spin quantum number of I = ½, *i.e.* it has no quadropolar moment, and high resolution NMR spectroscopy is possible.^{77}Se has a relative receptivity to the proton of 5.26 x 10^{-4} and the shifts are referenced to neat Me_2Se which is assigned δ 0 ppm. It has however, been found that the chemical shifts of Me_2Se are relatively sensitive to solvent and concentration. In fact, variations of about 10 ppm for ^{77}Se can occur with solvent and temperature for any resonance. A high chemical shift is observed with electron rich substituents. When an M-Se σ bond is formed on coordination to a metal centre, the Se centre is deshielded and the resulting shift is usually to high frequency.

$^{31}P\{^{1}H\}$ NMR Spectroscopy[62]

Phosphorus has a 100% abundance of ^{31}P with spin I = ½ and a relative receptivity to the proton of 6.6 x 10^{-2}, making the nucleus very useful for studies incorporating metal-phosphine complexes. Chemical shifts are referenced to an external 85% aqueous H_3PO_4 solution. The chemical shifts of the phosphines are largely dependant upon the nature of the substituent. If the substituents are electron-poor a high frequency shift is observed, the opposite is true for electron-rich substituents when a low frequency shift is observed. When a phosphine is coordinated to a metal centre the formation of a M-P σ bond involves the transfer of electron density away from the phosphine to the metal, causing deshielding of the ^{31}P nucleus. This results in a shift to higher frequency of the coordinated phosphine. The size of the coordination shift is found to be dependent upon the metal centre and also, for

multidentate phosphines, the size of the chelate ring formed. The term ΔR is used to describe the effect of the chelate ring size upon the chemical shift of the coordination complex and has been reviewed by Garrou.[63] It is defined as the difference between the coordination chemical shift, Δ, of a *cis*-disubstituted phosphine complex (*cis*-$[SnX_4(Me_3P)_2]$) and the observed coordination chemical shift of an equivalent phosphorus atom in a chelate complex (e.g. $\Delta(SnX_4(dmpe)])$ - $\Delta(cis\text{-}[SnX_4(Me_3P)_2])$). In general with four- and six- membered chelate rings give negative ΔR values, whereas in a five- member chelate ring ΔR is positive, for example in the series of complexes $[PtMe_2\{Ph_2P(CH_2)_nPPh_2\}]$ where n = 1– 4, the ΔR values are –52.2, +24.1, -14.1 and –0.7 respectively.[63]

^{119}Sn NMR Spectroscopy

Tin has three nuclei suitable for study by NMR spectroscopy, ^{115}Sn, ^{117}Sn and ^{119}Sn. All three nuclei have spin I = ½. ^{115}Sn is very rarely used due to its low natural abundance (0.35%). Both ^{117}Sn and ^{119}Sn have similar relative receptivities ^{117}Sn = 3.5 x 10^{-3}, ^{119}Sn = 4.5 x 10^{-3}, and similar natural abundances, (^{117}Sn 7.6% and ^{119}Sn 8.6%,) but it is the ^{119}Sn due to its slight advantage in both respects which is commonly studied. ^{119}Sn chemical shifts are referenced to neat Me_4Sn (δ 0). ^{119}Sn also possesses a large magnetogyric ratio, γ = -9.9707 x 10^7 rad T^{-1} S^{-1}, thus the observed resonances are greatly effected by signal diminution from the NOE (Nuclear Overhauser Effect).[64] For most nuclei this ratio is positive and has the effect of enhancing the signal by an amount defined by:

$$NOE_{\max} = 1 + \frac{\chi_s}{2\chi_I}$$

χ_s = magnetogyric ratio of observed species

χ_I = magnetogyric ratio of irradiated species

A negative effect is observed when a negative magnetogyric ratio is placed into this equation, *i.e.* signal diminuation. In order to remove the NOE and reduce very long spin-lattice relaxation times, a paramagnetic centre such as $Cr(acac)_3$ is added. This is

achieved by providing a second relaxation mechanism, which over-rides the nuclear dipole-dipole relaxation process.

1.9.2 Infra-red Spectroscopy

Previous studies of tin(IV) halide complexes have shown that the ν(Sn-X) bands lie within the regions 340 - 290 cm^{-1} for X = Cl and 240 - 190 cm^{-1} for X = Br.[65] The Sb(V) chloride complexes were found to show several features assigned as ν(Sb-Cl) in the range 400 - 300cm^{-1}. Therefore, in order to access the region, nujol mulls of the samples are supported on caesium iodide plates, which are transparent across the range 4000 – 180 cm^{-1}, spectra were recorded using a Perkin – Elmer 983G spectrophotometer. The group theory for both sets of complexes is described in more detail in the relevant chapters. In order to find the number of IR active bands to be expected, the reduction formula is applied to the reducible representation of symmetry operations within the molecules.

Figure 1.5 Group theory reduction formula.

$$n_i = \frac{1}{h}\Sigma g_i \chi_I \chi_r$$

h = number of operations in the group

g_i = number of symmetry operations in the class

χ_I = character of the irreducible representation

χ_r = character of the reducible representation

1.10 Aims of this study

The aims of this research were to synthesise and characterise a variety of SnX_4 (Cl, Br and I) complexes with a variety of thio- and seleno-ether macrocycles. These complexes have been characterised using spectroscopic techniques and, in a number of

cases, structurally using single crystal X-ray diffraction. By using multinuclear NMR spectroscopic techniques incorporating variable temperature studies, it has been possible to study the dynamic processes of ligand dissociation in solution for the Sn(IV) halide complexes. The data obtained for a variety of complexes from their X-ray structural analysis has permitted correlations to be drawn between the solution and solid states. The effects of altering the halide species and the macrocyclic ring size have also been studied and conclusions have been drawn from the results.

Using single crystal X-ray diffraction a homologous series ($BiCl_3$, $SbCl_3$ and $AsCl_3$) of [8]aneSe_2 complexes have been structurally characterised and conclusions have been drawn on the different factors affecting the structures and structural trends and more specifically the extent of the lone pair activity within these neutral adducts. The preparation of a range of antimony pentachloride complexes with phosphine oxide, phosphine sulfide, phosphine selenide and arsine oxide ligands are described in chapter 3. The main focus of this study was to re-examine specific known examples, and obtain full characterisation, extending these studies to look at antimony pentachloride complexes of the parent phosphine and arsine ligands.

Chapter 4 details a study on the promotion of oxidation of a variety of arylphosphines including Ph_3P, *o*-$C_6H_4(PPh_2)_2$ and $Ph_2PCH_2CH_2PPh_2$ to the corresponding phosphine oxides on reaction with dry air or dioxygen in the presence of catalytic amounts of SnI_4. A detailed examination of the $^{31}P\{^1H\}$ NMR spectroscopy, IR spectroscopy and in some cases EI mass spectrometry is presented.

1.11 References

[1] F. A. Cotton and G. Wilkinson, *Advanced Inorganic Chemistry*, 5th edition, Wiley, New York, 1988.

[2] R. Hoppe and W. Dahne, *Naturwissenschaften*, 1962, **49**, 254.

[3] N. C. Norman, *Periodicity and the P-block Elements*, (Ed. J. Evans), Oxford University Press, Oxford, 1995.

[4] J-M. Dumas and M. Gomel, *Bull. Soc. Chim. France*, 1974, **10**, 1885.

[5] P.G. Harrison, in P. G. Harrison (Editor), *The Chemistry of Tin*, Blackie, New York, 1989, p. 30.

[6] S. Haupt and K. Seppelt, *Z. Anorg. Allg. Chem.*, 2002, **628**, 729.

[7] N. W. Alcock, *Adv. Inorg. Chem. Radiochem.*, 1972, **15**, 1.

[8] J. F. Sawyer and R. J. Gillespie, *Prog. Inorg. Chem.*, 1986, **34**, 65.

[9] J. Galy and R. J. Enjalbert, *J. Solid State Chem.*, 1982, **44**, 1.

[10] R. G. Pearson, *Coord. Chem Rev.*, 1990, **100**, 403 and references therein.

[11] G. N. Lewis, *J. Am. Chem. Soc.*, 1913, **35**, 1448; S. Ahrland, J. Chatt and N. R. Davies, *Q. Rev. Chem. Soc.*, 1958, **12**, 265.

[12] L. F.Lindoy, *The Chemistry of Macrocyclic Ligand Complexes*, Cambridge University Press, Cambridge, 1989.

[13] C. J. Pederson, *J. Am. Chem. Soc.*, 1967, **89**, 7017.

[14] G. Shoham, W. N. Lipscomb and U. Olsher, *J. Am. Chem. Soc*, 1983, **105**, 1247

[15] M. A. Bush and M. R. Truter, *J. Chem. Soc., Perkin. Trans. II.*, 1972, 341.

[16] P. R. Mallinson and M. R. Truter, *J. Chem. Soc., Perkin. Trans. II.*, 1972, 1818.

[17] S. A. Zuchman, G. M. Freeman, D. E. Troutner, W. A. Volkert, R. A. Holmes, D. G. VanDerveer and E. K. Barefield, *Inorg. Chem.*, 1981, **20**, 2386.

[18] M. Micheloni, P. Paoletti, L. Siegfried-Hertli and T. A. Kaden, *J. Chem. Soc., Dalton. Trans*, 1985, 1169.

[19] V. B. Pett, L. L. Diaddario, E. R. Dockal, P. W. Corfield, C. Ceccarelli, M. D. Glick, L. A. Ochrymowycz and D. B. Rorabacher, *Inorg. Chem*, 1983, 3661.

[20] D.K. Cabbiness and D. W. Margerum, *J. Am. Chem. Soc.*, 1969, **91**, 6540; D.K. Cabbiness and D. W. Margerum, *J. Am. Chem. Soc.*, 1970, **92**, 2151.

[21] F. P. Hinz and D. W. Margerum, *Inorg. Chem.*, 1974, **13**, 2941.

[22] M. Micheloni, P. Paoletti and A. Sabatini, *J. Chem. Soc., Dalton. Trans.*, 1983, 1189.

[23] M. Kodama and E. Kimura, *J. Chem. Soc., Dalton. Trans.*, 1976, 2341.

[24] N. K. Dalley, J. S. Smith, S. B. Larson, K. L. Matheson, J. J. Cristensen, and R. M. Izatt, *J. Chem. Soc., Chem. Commun.*, 1975, 84; R. E. DeSimone, and M. D. Glick, *J. Am. Chem. Soc.*, 1976, **98**, 762.

[25] R. S. Glass, G. S. Wilson, W. N. Setzer, *J. Am. Chem. Soc*, 1980, **102**, 5068.

[26] M. T. Ashby and D. L. Lichtenberger, *Inorg. Chem.*, 1985, **24**, 636.

[27] N. F. Curtis, *J. Chem. Soc.*, 1960, 4409.

[28] N. F. Curtis and D. A. House, *Chemistry. Ind. (London)*, 1961, 1708; N. F. Curtis, Y. M. Curtis and H. K. J. Powell, *J. Chem. Soc, A.*, 1966, 1015.

[29] L. Ochrymowycz, C. P. Mak and J. D. Michna, *J. Org. Chem.*, 1974, **39**, 2079.

[30] W. Rosen and D. H. Busch, *Inorg. Chem.*, 1970, **9**, 262.

[31] W. Rosen and D. H. Busch, *J. Am. Chem. Soc.*, 1969, **91**, 4694.

[32] J. Buter and R. M. Kellogg, *J. Org. Chem.*, 1981, **46**, 4481.

[33] D. Sellmann and L. Zapf, *J. Organomet. Chem.*, 1985, 57.

[34] R. J. Batchelor, F. W. B. Einstein, I. D. Gay, J-H. Gu, B. D. Johnston and B. M. Pinto, *J. Am. Chem. Soc.*, 1989, **111**, 6582.

[35] I. Cordova-Reyes, E. vandenHoven, A. Mohammed and B. M. Pinto, *Can. J. Chem.*, 1995, **73**, 113.

[36] F. R. Hartley, W. Levason, C. A. McAuliffe, S. G. Murray and H. E. Soutter, *Inorg. Chim. Acta*, 1979, **35**, 265.

[37] D. J. Gulliver, E. G. Hope, W. Levason, G. L. Marshall and S. G. Murray, *J. Chem. Soc., Perkin Trans. II*, 1984, 429.

[38] E. E. Aynsley, N. N. Greenwood and J. B. Leach, *Chem. Ind. (London),* 1966, 379.

[39] A. D. Westland and L. Westland, *Can. J. Chem.*, 1965, **43**, 426.

[40] W. Levason, S. D. Orchard and G. Reid, *Coord. Chem. Rev.*, 2002, **225**, 159.

[41] J. Chatt, *Nature*, 1950, **165**, 637.

[42] A. G. Orpen, N. G. Connelly, *J. Chem. Soc., Chem. Commun.*, 1985, 1310.

[43] H. Schumann, A. M. Arif, A. L. Rheingold, C. Janaik, R. Hoffmann, N. Kuhn, *Inorg. Chem.*, 1991, **30**, 1618.

[44] W. Levason, S. D. Orchard and G. Reid, *Organometallics*, 1999, **18**, 1275; W. Levason, S. D. Orchard and G. Reid, *J. Chem. Soc., Dalton. Trans.*, 1999, 823.

[45] A. J. Barton, W. Levason and G. Reid, *J. Organomet. Chem*, 1999, **579**, 235.

[46] W. Levason, S. D. Orchard, G. Reid and J. M. Street, *J. Chem. Soc., Dalton. Trans.*, 2000, 2537.

[47] E. W. Abel, R. P. Bush, F. J. Hopton and C. R. Jenkins, *J. Chem. Soc., Chem. Commun.*, 1966, 58.

[48] E. W. Abel, S. K. Bhargava and K. G. Orrell, *Prog. Inorg. Chem.*, 1984, **32**, 1.

[49] P. Haake and P. C. Turley, *J. Am. Chem. Soc.*, 1967, **89**, 4611; P. Haake and P. C. Turley, *J. Am. Chem. Soc.*, 1967, **89**, 4617.

[50] J. H. Eekhof, H. Hoegeveen, R. M. Kellogg and E. Klie, *J. Organomet. Chem.*, 1978, **161**, 183.

[51] W. Levason and G. Reid, *J. Chem. Soc., Dalton Trans.*, 2001, 2953.

[52] G. H. Robinson and S. A. Sangokoya, *J. Am. Chem. Soc.*, 1988, **110**, 1494.

[53] G. H. Robinson, H. Zhang and J. L. Atwood, *Organometallics*, 1987, **6**, 887.

[54] K. Wieghardt, M. Kliene-Boynann, B. Nuber and J. Weiss, *Inorg Chem.*, 1986, **25**, 1654.

[55] J. Blank, H. -D. Hausen, W. Schwarz and J. Weidlein, *J. Organomet. Chem.*, 1993, **443**, 154.

[56] A. J. Blake, J. A. Greig and M. Schröder, *J. Chem. Soc., Dalton Trans.*, 1991, 529.

[57] A. J. Blake, G. Reid and M. Schröder, *J. Chem. Soc., Dalton. Trans.*, 1992, 2987.

[58] A. J. Blake, D. Fenske, W. –S. Li, V. Lippolis and M. Schröder, *J. Chem. Soc., Dalton. Trans.*, 1998, 3961.

[59] N. J. Hill, W. Levason, M. E. Light and G. Reid, *Chem. Commun.*, 2003, 110.

[60] H-J. Kuppers, K. Wieghardt, B. Nuber and J. Weiss, *Z. Anorg., Allg. Chem.*, 1989, **577**, 155.

[61] H. Duddeck, *Progress in Nuclear Magnetic Resonance Spectroscopy*, 1995, **27**, 1.

[62] *Multinuclear NMR*, Ed. J. Mason, Plenum, New York, 1987.

[63] P. E. Garrou, *Chem Rev.*, 1981, **81**, 229.

[64] *NMR and the Periodic Table*, R. K. Harris and B. E. Mann (Editors), Academic Press, London, 1978, p. 402 (^{77}Se); p. 10 (NOE); p. 342 (^{119}Sn).

[65] A. R. J. Genge, W. Levason and G. Reid, *J. Chem. Soc., Dalton. Trans.*, 1997, 4479; S. E. Dann, A. R. J. Genge, W. Levason and G. Reid, *J. Chem. Soc., Dalton. Trans.*, 1997, 2207; S. E. Dann, A. R. J. Genge, W. Levason and G. Reid, *J. Chem. Soc., Dalton. Trans.*, 1996, 4471.

CHAPTER 2

Tin(IV) Halide Complexes of Thioether and Selenoether Macrocycles

2.1 Introduction

In contrast to the rapid growth of phosphine and arsine coordination chemistry, the development of chalcogenoether coordination chemistry has been slow. In recent years thioether macrocycles have attracted considerable interest, with compounds containing a variety of ring sizes and denticities being prepared. Selenium and tellurium chemistry has also developed rapidly over the past 30 years or so. The growing interest in these systems may, in part, be credited to the emergence of reliable synthetic routes to the ligands and the increasing availability of FT-NMR to study their solution behaviour. For example, both ^{77}Se and ^{125}Te possess nuclei with a spin quantum number which is non-zero (I = ½,), ^{77}Se has a natural abundance of 7.6 % and a relative receptivity to the proton of 5.26 x 10^{-4}, ^{125}Te has a natural abundance of 7.0 % and a relative receptivity to the proton of 2.21 x 10^{-3}, making them a valuable tool in NMR spectroscopic studies. Sulphur does not have a convenient NMR active nucleus for studies to be undertaken. Recent studies have provided evidence for the enhanced ligating properties of the heavier telluroether and selenoether ligands compared to the much more widely explored thioethers, especially to low valent transition metal centres.

The coordination chemistry of macrocyclic and polydentate thioether and selenoether ligands has been studied in detail with the p-block (Group 13-15) halides. The presence of an electron pair on the p-block element, which may or may not be stereochemically active and the frequent occurrence of 'secondary bonding interactions' have lead to highly unusual and interesting structural motifs and polynucleur assemblies. Examples include 6-coordinate monomers, through to one- two- and three dimensional network infinite polymers.[1]

There are no reported examples of complexes of germanium halides with thio- or selenoether ligands. However there are examples of complexes of $GeCl_4$ with few phosphorus and arsenic donor ligands. A range of tertiary phosphines and tertiary arsines were reacted with $GeCl_4$ in both a 1:1 and 2:1 stoichiometric ratio in diethyl ether solution. In the presence of a tertiary phosphine ligand a redox reaction occurs to produce the ionic Ge(II) complexes $[R_3PCl][GeCl_3]$. The crystal structure of $[Bu_3^nPCl][GeCl_3]$ revealed no interaction between the cation and the anion, in direct contrast to the only other reported complex of this stoichiometry $[Pr^i_3PBr][GeBr_3]$. No

reaction was observed between PPh_3 and $GeCl_4$. The reaction of $AsMe_3$ with $GeCl_4$ in both a 1:1 and 2:1 stoichiometric ratios produced the molecular *trans*-octahedral Ge(IV) complex, $[GeCl_4(AsMe_3)_2]$, the first crystallographically characterised arsine complex. No reaction occurred between $GeCl_4$ and $AsPh_3$.[2]

In the case of tin(IV) halides, complexes with O and N donors of Group 15 have long been known and there has been recent interest in phosphine donor ligands.[3,4,5,6]A range of phosphine and diphosphine complexes have been prepared and characterised by vibrational and Mőssbauer spectroscopy and X-ray crystallography.[3,4,5,6,7,8,9,10,11] The formation of adducts of the form $MX_4.nL$ reported in the literature provided substantial evidence of the tendancy of the Group 14 halides to adopt a maximum covalency of six through the formation of coordinate bonds with sufficiently strong electron donors. In the case where 1:2 adducts are formed, the possibility of *cis-trans* isomerism arises. X-ray crystallography has established the complexes $[SnCl_4(POCl_3)_2]$, $[SnCl_4(Me_2SO)_2]$, $[SnCl_4(SeOCl_2)_2]$ and $[SnCl_4(MeCN)_2]$ as *cis*-octahedral species. However, reaction of SnX_4 (where X = Cl or Br) with ligands of the type R_3P in solution readily forms the 1:2 *trans*-$[SnX_4(PR_3)_2]$ complex. The complexes have been assigned a *trans*-stereochemistry based on the observation of the D_{4h}, spectral pattern of metal halogen stretching frequencies (two Raman active and one infrared active) in the vibrational spectra.[12] This assignment was confirmed by the single crystal X-ray diffraction study of *trans*-$[SnCl_4(PEt_3)_2]$;[13] the air sensitive $[SnI_4(PPr^n_3)_2]$[9] also reveals a *trans* structure.

Figure 2.1 View of the structure *trans*-$[SnI_4(PPr^n_3)_2]$.[9]

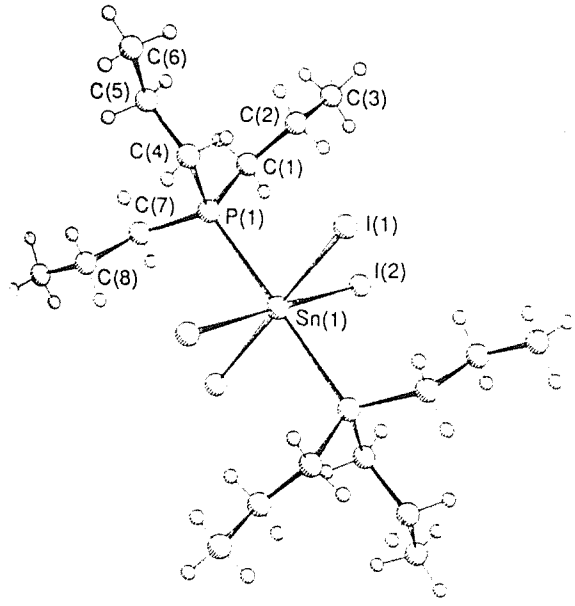

The complexes of bidentate phosphines have also been studied. Sarikhaya[11] has used vibration spectroscopy to examine a range of SnX_4 complexes with bidentate phosphines, $R_2P(CH_2)_nPR_2$ (where R = Me, Et or Ph for n = 2; R = Me or Et for n = 3). The IR spectra of these complexes exhibit four ν(Sn-X) consistent with C_{2V} symmetry. This assignment is confirmed by the X-ray crystal analysis of *cis*-$[SnCl_4(Ph_2P(CH_2)_2PPh_2)]$ by Kunkel and Dehnicke.[10] When examining the reaction between $Ph_2PCH_2PPh_2$ and $SnCl_4$ Dakternieks *et al.*[14] found that a chelate structure is not formed, instead a 1:2 complex is formed with two mutually *trans* η^1 $Ph_2PCH_2PPh_2$ ligands. Genge and co-workers[15] further studied the complexes of bidentate phosphine ligands with SnX_4. A range of complexes of type $[SnX_4(L\text{-}L)]$ (where X = Cl, Br or I; L-L = $Me_2P(CH_2)_2PMe_2$, $Ph_2P(CH_2)_2PPh_2$ and *o*-$C_6H_4(PPh_2)_2$) were prepared. IR spectroscopy showed four ν(Sn-X) consistent with C_{2V} symmetry. A detailed study of the variable temperature $^{119}Sn\{^1H\}$ and $^{31}P\{^1H\}$ NMR spectroscopy of the complexes was also undertaken. It was found that methyl substituted ligands formed more stable compounds than the phenyl substituted versions, and that complexes involving a five-membered chelate ring were more stable than those featuring four- or six- membered chelate rings. The studies also illustrated that the stability of the complexes formed decreases with the SnX_4 acceptor: X = Cl > Br >>I.

A large amount of work has been carried out to investigate the complexes of the tin(IV) halides with monodentate arsines using IR and ^{119}Sn Mőssbauer techniques.[3,7,8,16,17] The studies confirm the formation of the *trans* isomer as the major species in 1:2 $[SnX_4(AsR_3)_2]$ systems. Studies on complexes of bidentate arsine ligands with SnX_4 were undertaken by Genge,[18] who synthesised a range of complexes of type $[SnX_4(L\text{-}L)]$ (where X = Cl, Br or I for L-L = *o*-$C_6H_4(AsMe_2)_2$; X = Cl or Br for L-L = $Ph_2As(CH_2)_2AsPh_2$). IR spectroscopy of the complexes suggests chelate formation with four ν(Sn-X) bands observed, consistent with C_{2V} symmetry. Red-brown crystals of $[SnI_4(o\text{-}C_6H_4(AsMe_2)_2)]$ were obtained. The structure (Figure 2.2) shows a distorted *cis*-octahedral geometry at the tin, composed of chelating diarsine and four iodines. This being the first structurally characterised example of a tin-arsine complex.

Figure 2.2 View of the structure of $[SnI_4(o\text{-}C_6H_4(AsMe_2)_2)]$.[18]

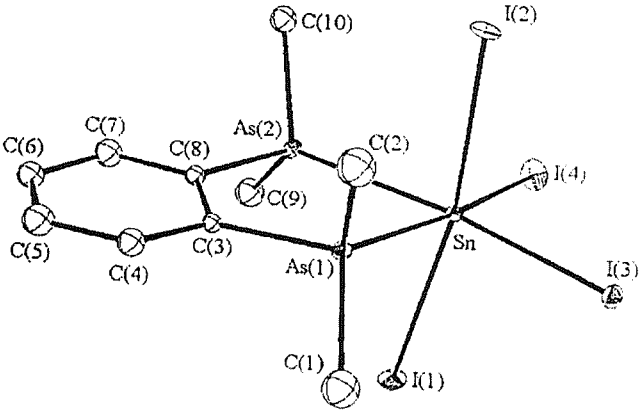

Studies with Group 16 donor ligands are more limited. Tin(IV) halides can readily coordinate two neutral S-, Se-, or Te-atoms to give discrete *pseudo* octahedral complexes. The complexes *cis*- and *trans*-$[SnCl_4(Me_2S)_2]$ have been studied in detail by Merbach and co-workers.[19,20,21,22,23] By carrying out a combination of variable pressure proton NMR and magnetisation transfer ^{119}Sn NMR spectroscopy experiments they were able to study the intermolecular *cis-trans* isomerisation process in solution. A systematic investigation on the coordination chemistry of mono- and bi-dentate dithio- and diseleno-ether ligands with tin(IV) tetrahalide Lewis acids has been undertaken by Genge and co-workers.[24,25,26] The complexes $[SnX_4L_2]$ (where X = Cl, Br or I; L =

Me_2S or Ph_2S) and $[SnX_4(SeR_2)_2]$ (where X = Cl or Br, R = Me or Ph; X = I, R = Me) have been formed by the reaction of SnX_4 with two molar equivalents of the thio- or seleno-ether ligand in anhydrous CH_2Cl_2. Single crystal X-ray diffraction studies on *trans*-$[SnX_4(SeMe_2)_2]$ confirms a distorted octahedral geometry at Sn(IV).

Figure 2.3 View of the structure *trans*-$[SnBr_4(SeMe_2)_2]$.[25]

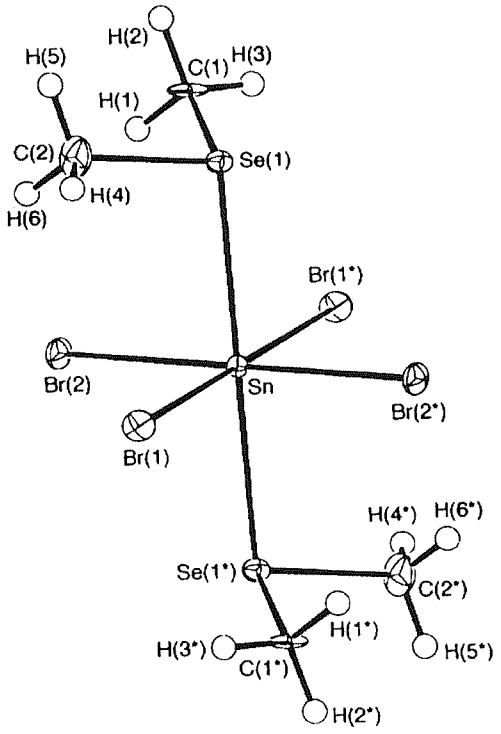

Reaction of SnX_4 with the dithioether, L-L in dry $CHCl_3$ gave the six-coordinate species $[SnX_4(L\text{-}L)]$ (where X = Cl, L-L = $MeS(CH_2)_nSMe$, *o*-$C_6H_4(SMe)_2$ or $PhS(CH_2)_nSPh$ (n = 2 or 3)). Reaction of SnX_4 (X = Cl or Br) with diselenoether ligands in dry $CHCl_3$ produced complexes of type $[SnX_4(L\text{-}L)]$ (where X = Cl, L-L = $MeSe(CH_2)_nSeMe$ (n = 1, 2 or 3), $PhSe(CH_2)_nSePh$ (n = 2 or 3), *o*-$C_6H_4(SeMe)_2$; X = Br, L-L = $MeSe(CH_2)_3SeMe$ (n = 2 or 3) and *o*-$C_6H_4(SeMe)_2$). These complexes have been characterised by a combination of variable temperature ^1H, $^{119}Sn\{^1H\}$ and $^{77}Se\{^1H\}$ NMR, IR spectroscopy and microanalyses. Single crystal X-ray diffraction studies have also been undertaken on some of the complexes.

The complexes $[SnCl_4(MeSCH_2SMe)]$ and $[SnCl_4(MeSeCH_2SeMe)]$ were the first examples showing bidentate chelation of the methylene-bridged dithio- and

diseleno-ethers, which more commonly act as bridging bidentate ligands to transition metals.[27] The single-crystal structure of $[SnCl_4(MeSCH_2SMe)]$ shows a mononuclear Sn(IV) species involving a highly distorted octahedral S_2Cl_4 donor set, with the dithioether ligand coordinated in a bidentate fashion to give a four membered chelate ring. The coordinated dithioether adopts the *dl* configuration with the Me-groups directed to the opposite sides of the SnS_2Cl_2 plane. The structure of $[SnCl_4(MeSeCH_2SeMe)]$ adopts a similar arrangement, with the exception that the Me-groups adopt a *meso* configuration. The variable temperature NMR studies demonstrate the acceptor ability of $SnCl_4 > SnBr_4 > SnI_4$, and that dissociation in solution increases with donor type S < Se.

Figure 2.4 View of the structure of $[SnCl_4\{MeS(CH_2)_2SMe\}]$.[24]

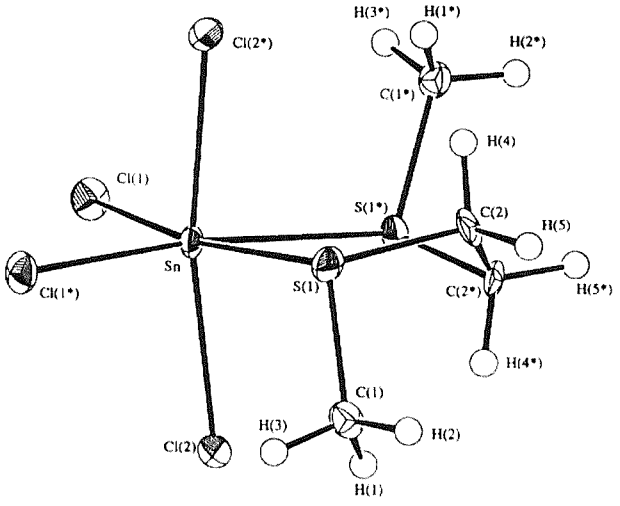

Prior to this work the only reported macrocyclic thioether complexes with Sn(IV) were those reported by Willey and co-workers.[28] Two new Sn(IV) compounds $[SnCl_3([9]aneS_3)]_2[SnCl_6]$ and $[(SnCl_4)_2([18]aneS_6)]$ were isolated. The complex $3SnCl_4.2[9]aneS_3$ is produced by reaction in MeCN, and consists of discrete $[SnCl_3([9]aneS_3)]^+$ cations and $[SnCl_6]^{2-}$ anions in the ratio 2:1. The cation incorporates terdentate coordination of $[9]aneS_3$ to an $SnCl_3^+$ unit with a resulting *fac*-octahedral geometry. In the neutral molecule of $[(SnCl_4)_2([18]aneS_6)]$, the hexathia crown acts as a bidentate (S.S') chelating ligand to separate $SnCl_4$ units located at opposite ends of the cavity and on opposite sides of the ring plane. Again the six-coordinate geometry favoured by Sn(IV) is preserved at the expense of the limited ring attachment. $[(SnCl_4)_2([18]aneS_6)]$ is highly distorted in order to accommodate the two $SnCl_4$ units.

In the same paper Willey *et al.*[28] stated that $SnCl_4$ does not react with the macrocyclic thioethers [12]aneS_4 or [15]aneS_5 in anhydrous MeCN solution.

Figure 2.5 View of the $[SnCl_3([9]aneS_3]^+$ cation.[28]

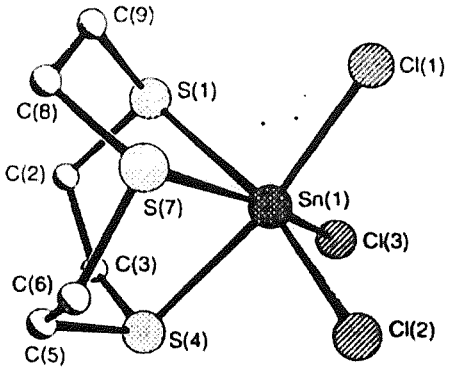

Figure 2.6 Molecular structure of $2SnCl_4.[18]aneS_6$.[28]

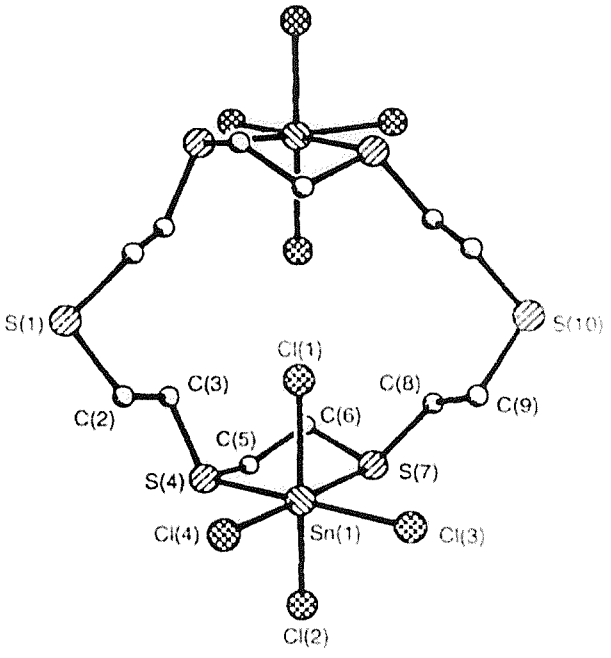

The following work reported here provides a detailed investigation into the behaviour of tin(IV) halides ($SnCl_4$ and $SnBr_4$) with macrocyclic thio- and selenoether ligands ([12]aneS_4, [14]aneS_4, [16]aneS_4, [8]aneSe_2, [16]aneSe_4). The influences of the ligating modes and variation of ring size and donor set on the species produced are also

studied. Multinuclear ^{1}H and $^{119}Sn\{^{1}H\}$ NMR spectroscopy allowed the study of the dynamic processes that occur in solution for the tin(IV) halide complexes of the Group 16 ligands. By studying the analogous selenoether complexes it is possible to draw conclusions of the relative stabilities of the compounds. Infrared spectroscopy and single crystal X-ray diffraction have been used to study the behaviour of these complexes in the solid state.

Figure 2.7 Principle macrocyclic ligands discussed in this work.

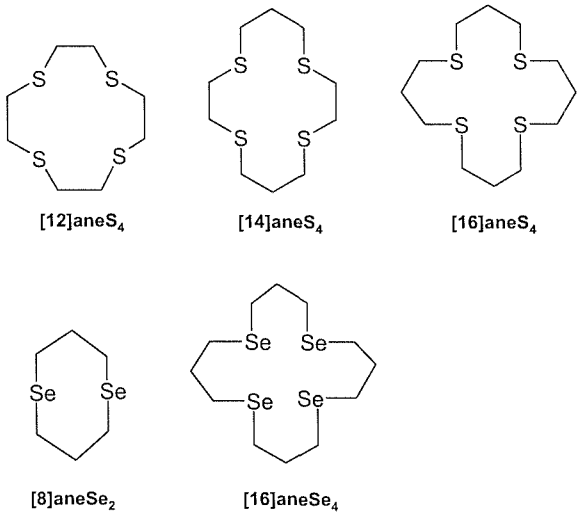

2.2 Results and Discussion

2.2.1 Synthesis and Properties of the Macrocyclic Tin(IV) complexes

A range of complexes of type $[(SnCl_4)_2L]$ (where L= [12]aneS$_4$, [14]aneS$_4$ and [16]aneS$_4$), $[SnBr_4(L)]$ (where L= [12]aneS$_4$, [14]aneS$_4$, [16]aneS$_4$ and [16]aneSe$_4$) and $[SnCl_4(L)]$ (where L=[8]aneSe$_2$ and [16]aneSe$_4$) have been prepared by the reaction of two molar equivalents of SnX_4 with one molar equivalent of the thioether or selenoether macrocyclic ligand in rigorously anhydrous CH_2Cl_2. The complexes were isolated in good yield (>70 %) by filtration, washing with CH_2Cl_2 and drying in *vacuo*. The $[(SnCl_4)_2$[n]aneS$_4]$ complexes were formed as powdered white solids, whereas the $[SnBr_4$([n]aneS$_4)]$ complexes were powdered yellow solids. The $SnBr_4$/[8]aneSe$_2$ system yielded solids of varying composition and a pure compound could not be isolated. The $[SnI_4$([9]aneS$_3)]$ complex was prepared by the reaction of one molar

equivalent of SnI_4 with one molar equivalent of [9]aneS_3 under the same conditions to form a powdered purple solid. EDX analysis of the product also confirms the presence of Sn, I and S approximately in the expected ratios. The product was too poorly soluble for NMR studies to be undertaken. Due to the low Lewis acidity of the SnI_4, attempts to react SnI_4 with [12]aneS_4 under similar conditions resulted only in the isolation of the parent macrocycle. Synthesis of SnX_4 (where X = Cl or Br) complexes of [9]aneS_3 were also attempted using the same method, however due to the poor solubility of the complexes formed structural characterisation was not undertaken. The same method of synthesis was also employed for the study of $GeCl_4$ with [9]aneS_3 and [12]aneS_4 but infrared spectroscopy of the white solids obtained showed the absence of v(Ge-Cl) stretches, and resembled the infrared spectra of the starting ligands. The melting point of the solid also corresponded to that of the parent macrocycle [9]aneS_3 (experimental mp. = 82 – 84 °C). The solid tin complexes formed were indefinitely stable in sealed tubes or in a dry box, but decompose quickly in moist air, and are very easily hydrolysed by traces of water in solution. Therefore all samples were stored and manipulated in a dry, nitrogen purged glove box.

For the tin(IV) halide systems studied, two possible symmetries at Sn(IV) were anticipated. *Trans*-[SnX_4(L-L)] will exhibit D_{4h} symmetry, while *cis*-[SnX_4(L-L)] exhibits C_{2V} symmetry, based on the assumption that only two macrocyclic donor atoms are coordinated. By applying the reduction formula to the reducible representation of the symmetry operations within the molecule it is possible to find the IR bands to be expected. Thus for molecules of the type *cis*-[$SnX_4(L_2)$] with C_{2V} symmetry the reducible representation is:

C_{2V}	E	C_2	σ_v	σ_v'
Γ_{Sn-X}	4	0	2	2

which, when the reduction formula is applied predicts four active bands ($2A_1 + B_1 + B_2$) in the far infrared region. For molecules of the type *trans*-[$SnX_4(L_2)$] with D_{4h} symmetry the reducible representation is:

D_{4h}	E	$2C_4$	C_2	$2C_2'$	$2C_2''$	i	$2S_4$	σ_h	$2\sigma_v$	$2\sigma_d$
Γ_{Sn-X}	4	0	0	2	0	0	0	4	2	0

which when the reduction formula is applied predicts one active band (E_u) in the far infrared region.

Infrared spectroscopy of the SnX_4 complexes of the thio- and selenoethers reveal up to four features in the far infrared region (Table 2.1). For the chloro complexes these range between 332-300 cm^{-1}, which are assigned to the Sn-Cl stretching modes, consistent with a *cis*-disubstituted octahedral geometry. For example, the *cis*-disubstituted complexes $[SnCl_4\{MeS(CH_2)_2SMe\}]$ exhibit ν(Sn-X) at 326, 316, 307, and 301 cm^{-1}.[24] The Sn-Br stretching modes occur at a much lower frequency. The Sn-Cl and Sn-Br bands in the macrocyclic complexes are not so well resolved and therefore it is difficult to determine exactly how many stretches are present in the spectra. Thus it is difficult to assign the stereochemistry conclusively on the basis of these data alone. The majority of the bands are attributed to ligand absorptions, which are shifted slightly on coordination of SnX_4. The absence of an absorption in the range 3600 – 3100 cm-^{1} confirms that water is not present in the bulk samples.[29]

Table 2.1 IR Spectroscopic data for the tin(IV) halide complexes

Complex	Colour	v(Sn-X) cm^{-1} [a]
$[(SnCl_4)_2([12]aneS_4)]$	White	334, 320, 312
$[(SnCl_4)_2([14]aneS_4)]$	White	332, 328, 323
$[(SnCl_4)_2([16]aneS_4)]$	White	332, 327, 316, 300
$[SnBr_4([12]aneS_4)]$	Yellow	221 (br)
$[SnBr_4([14]aneS_4)]$	Yellow	223 (br)
$[SnBr_4([16]aneS_4)]$	Yellow	223 (br)
$[SnCl_4([8]aneSe_2)]$	Orange	333, 320, 314, 300
$[SnCl_4([16]aneSe_4)]$	Yellow	332, 327, 316, 305
$[SnBr_4([16]aneSe_4)]$	Orange	223 (br)

a = Recorded as nujol mulls supported between CsI plates.

2.2.2 Single Crystal X-Ray Diffraction Studies

In order to attempt to identify the trends in the geometric parameters, and to correlate these with the observed behaviour within solution NMR (by variable temperature ^{119}Sn and ^{1}H NMR spectroscopy) single crystal X-ray structure analyses on several of the complexes were undertaken. Pale yellow crystals of $[SnBr_4([12]aneS_4)]$ and $[SnBr_4([16]aneS_4)]$ were obtained by slow evaporation of the solutions in CH_2Cl_2 solution in the glove box. Crystals of $[SnBr_4([14]aneS_4)].2/3CH_2Cl_2$ were obtained by careful layering of a CH_2Cl_2 solution of $SnBr_4$ with a CH_2Cl_2 solution of $[14]aneS_4$ in a N_2-filled dry glove box. Details of the crystallographic data collection and refinement parameters are given in Table 2.2.

Table 2.2 Crystallographic Data and Refinement Parameters.

	$[SnBr_4([12]aneS_4)]$	**$[SnBr_4([14]aneS_4)].2/3CH_2Cl_2$**	**$[SnBr_4([16]aneS_4)]$**
Formula	$C_8H_{16}Br_4S_4Sn$	$C_{10.67}H_{21.33}Br_4Cl_{1.33}S_4Sn$	$C_{12}H_{24}Br_4S_4Sn$
MWt	678.78	763.45	734.88
Crystal System	orthorhombic	triclinic	orthorhombic
Space Group	C*mcm*	P-*1*	P*ca*2_1
a/Å	10.5135(3)	11.2865(3)	19.4987(7)
b/Å	8.3306(3)	11.5634(3)	10.0624(3)
c/Å	19.6638(7)	13.3067(4)	10.9104(3)
α/°	90	104.8650(10)	90
β/°	90	103.4750(10)	90
γ/°	90	92.8590(10)	90
U/ Å^3	1722.23(10)	1621.19(8)	2140.66
Z	4	3	4
μ(Mo-Kα)/mm^{-1}	11.227	9.119	9.042
Unique reflections	1069	7125	4590
Obs. reflections With [$I > 2\sigma(I)$]	991	5762	4105
R1 [$I > 2\sigma(I)$]	0.0412	0.0467	0.0535
R1 (all data)	0.0447	0.0635	0.0626
wR2 (all data)	0.1072	0.1077	0.1380

Common Data: T = 120K; λ(Mo-Kα) = 0.71073 Å; $R1 = \Sigma||F_o|-|F_c||/\Sigma|F_o|$; $wR2 = [\Sigma w(F_o^2-F_c^2)^2/\Sigma wF_o^4]^{½}$

Table 2.3 Selected bond lengths (Å) and angles (°) for $[SnBr_4([12]aneS_4)]$

	Bond Lengths/ Å
Sn(1)-Br(1)	2.5582(7)
Sn(1)-Br(2)	2.5407(7)
Sn(1)-S(2)	2.7697(17)

	Bond Angles/ °
Br(2)-Sn(1)-Br(2')	102.09(4)
Br(2)-Sn(1)-Br(1)	92.69(1)
Br(1)-Sn(1)-Br(1'')	171.43(4)
Br(2)-Sn(1)-S(2')	167.48(4)
Br(2)-Sn(1)-S(2)	90.43(3)
Br(1)-Sn(1)-S(2)	86.65(2)
S(2)-Sn(1)-S(2')	77.05(7)

Symmetry operations: prime(') = x, y, ½ -z; double prime('') = -x, y,z

Figure 2.8 View of a portion of the chain structure in [$SnBr_4$([12]aneS_4)] with the numbering scheme adopted.

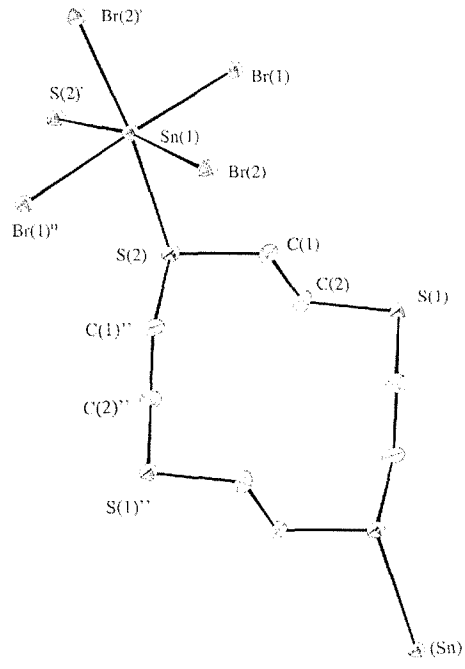

The structure for [$SnBr_4$([12]aneS_4)] (Figure 2.8) shows a distorted *cis*-octahedral geometry at Sn(IV), with S coordination occurring to two distinct bridging thiacrowns. This generates an infinite polymer structure with alternate S- atoms in each macrocycle coordinating to the $SnBr_4$ unit (Figure 2.11). The Sn-S bond distance of 2.7697(17) Å and the Sn-Br bond distances of 2.5582(7) Å (Br *trans* Br) and 2.5406 Å (Br *trans* S) determined for this study are in good agreement with the structurally characterised complex [$SnBr_4${$MeS(CH_2)_3SMe$}] [24,25]d(Sn – S) = 2.700(7) Å, d(Sn – Br) (Br *trans* Br) = 2.562(3) Å and d(Sn-Br) (Br *trans* S) = 2.533(3) Å. In both cases d(Sn – Br) for Br *trans* to Br is longer than the d(Sn – Br) for Br *trans* to S reflecting the greater *trans* influence of Br over S(thioether). The Sn – S bond distance is also of interest, we see that the shortest distance occurs for the six membered ring species [$SnBr_4${$MeS(CH_2)_3SMe$}], suggesting coordination of the 6-membered bidentate is preferred to coordination of the macrocycle.

Table 2.4 Selected bond lengths (Å) and angles (°) for $[SnBr_4([14]aneS_4)].2/3CH_2Cl_2$

	Bond Lengths/ Å
Sn(1)-Br(1)	2.5660(6)
Sn(1)-Br(2)	2.5661(6)
Sn(1)-S(1)	2.6565(16)
Sn(2)-Br(3)	2.5614(7)
Sn(2)-Br(4)	2.5887(6)
Sn(2)-S(3)	2.6050(17)
Sn(3)-Br(5)	2.5625(7)
Sn(3)-S(5)	2.6371(17)
Sn(3)-S(5)	2.6371(17)

	Bond Angles/°
Br(1)-Sn(1)-Br(2)	90.79(2)
Br(1)-Sn(1)-S(1)	89.31(4)
Br(2)-Sn(1)-S(1)	92.27(4)
Br(3)-Sn(2)-Br(4)	90.60(2)
Br(3)-Sn(2)-S(3)	84.53(4)
Br(4)-Sn(2)-S(3)	93.64(4)
Br(6)-Sn(3)-Br(5)	90.50(2)
Br(6)-Sn(3)-S(5)	96.70(4)
Br(5)-Sn(3)-S(5)	95.58(4)

Figure 2.9 View of the chain structure in $[SnBr_4([14]aneS_4)].2/3CH_2Cl_2$ with the numbering scheme adopted.

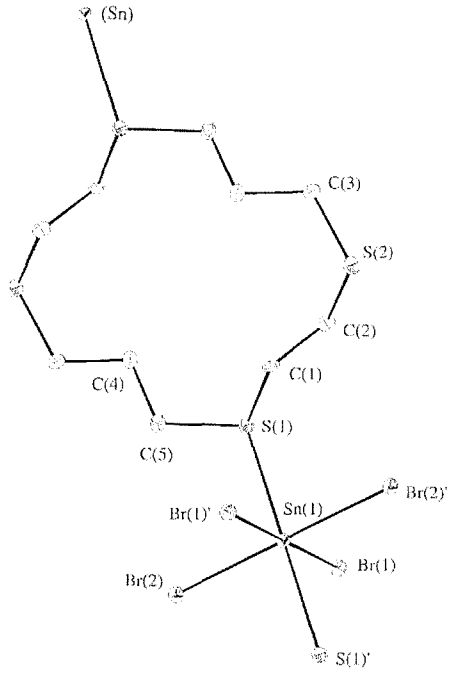

The structure of $[SnBr_4([14]aneS_4)].2/3CH_2Cl_2$ (Figure 2.9) reveals three independent Sn containing molecules in the asymmetric unit, along with an unbound CH_2Cl_2 solvent molecule. On symmetry expansion of the species parallel, infinite chain polymers are generated (Figure 2.12). The structure shows a *trans*-octahedral geometry at Sn through four Br atoms in a plane with S coordination occurring at two distinct bridging thiacrowns. The macrocycle uses every alternate S atom to bridge the tin centres. The *trans* configuration at tin is unusual for Sn(IV) thioether complexes and contrasts with the *cis* arrangement adopted by the 12-membered ring. The Sn-Br bond distances lie in the range 2.5614(7)-2.5887(6) Å, the Sn-S bond distances are 2.605(2), 2.637(2) and 2.656(2) Å. The Sn-S bond distances are considerably shorter than the Sn-S bond distance of 2.7697(17) Å in $[SnBr_4([12]aneS_4)]$ The only other examples of complexes adopting the *trans* configuration at Sn(IV) are $[SnCl_4(\eta^1\text{-}L)_2]$[30] (where L = 1,5-dithiacyclooctane), d(Sn-S) = 2.602(1) Å and $[SnBr_4(Me_2S)_2]$[12] d(Sn-S) = 2.65(1) Å, the Sn-S bond distances observed in $[SnBr_4([14]aneS_4)].2/3CH_2Cl_2$ are comparable.

Table 2.5 Selected bond lengths (Å) and angles (°) for $[SnBr_4([16]aneS_4)]$.

	Bond Lengths/ Å
Sn(1)-Br(1)	2.5625(13)
Sn(1)-Br(2)	2.5528(13)
Sn(1)-Br(3)	2.5774(12)
Sn(1)-Br(4)	2.5489(12)
Sn(1)-S(4')	2.641(2)
Sn(1)-S(1)	2.693(2)

	Bond Angles/°
Br(4)-Sn(1)-Br(2)	177.61(4)
Br(4)-Sn(1)-Br(1)	88.98(5)
Br(2)-Sn(1)-Br(1)	90.96(3)
Br(4)-Sn(1)-Br(3)	89.86(3)
Br(2)-Sn(1)-Br(3)	90.36(5)
Br(1)-Sn(1)-Br(3)	175.87(4)
Br(4)-Sn(1)-S(4')	92.88(5)
Br(2)-Sn(1)-S(4')	84.75(6)
Br(1)-Sn(1)-S(4')	96.53(6)
Br(3)-Sn(1)-S(4')	87.48(6)
Br(4)-Sn(1)-S(1)	91.56(7)
Br(2)-Sn(1)-S(1)	90.83(7)
Br(1))-Sn(1)-S(1)	89.60(7)
Br(3)-Sn(1)-S(1)	86.47(7)
S(4')-Sn(1)-S(1)	172.49(10)

Figure 2.10 View of a portion of the chain structure in $[SnBr_4([16]aneS_4)]$ with the numbering scheme adopted.

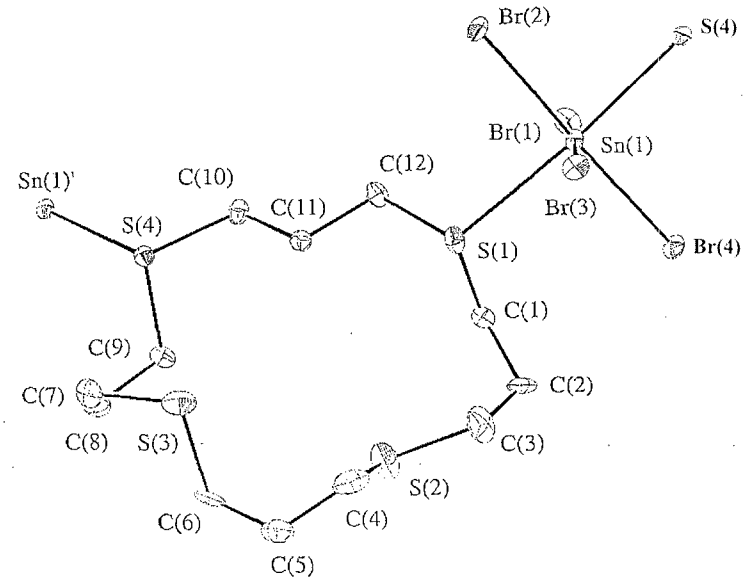

The crystal structure obtained for $[SnBr_4([16]aneS_4)]$ (Figure 2.10) shows a *trans* configuration at tin(IV), involving coordination to Sn(IV) *via* four Br atoms, and two S atoms from different thiacrowns. The macrocycles then bridge to adjacent Sn centres, the $[16]aneS_4$ uses adjacent S atoms in the ring, thus generating a one-dimensional 'zig-zag' coordination polymer (Figure 2.13). This is unlike the structures described previously. The Sn-Br distances are all similar and lie in the range 2.5489(12) - 2.5774(12) Å, the Sn-S bond distances are 2.641(2) and 2.693(2) Å. The $Sn\text{-}S_{trans}^{S}$ bond distances found in the two *trans* species are slightly shorter than for the bidentate complex *cis*-$[SnBr_4\{MeS(CH_2)_3SMe\}]$[24] and significantly shorter than in the 12-membered complex $[SnBr_4([12]aneS_4)]$. Thus suggesting that the 12-membered macrocycle and the 6-membered chelate ring are less favourable for coordination to the Sn(IV) centre than the 14- and 16-membered macrocycles.

Figure 2.11 View of a portion of the 1D polymer structure of $[SnBr_4([12]aneS_4)]$.

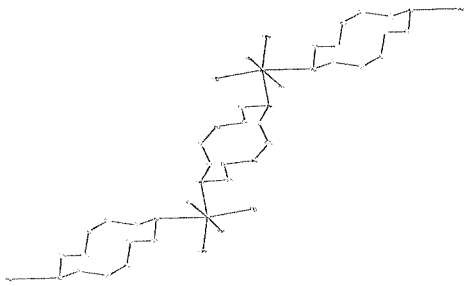

Figure 2.12 View of a portion of the 1D polymer structure of $[SnBr_4([14]aneS_4)]$.

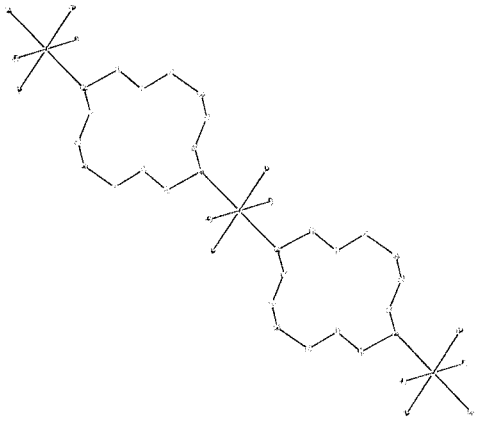

Figure 2.13 View of a portion of the 1D polymer structure of $[SnBr_4([16]aneS_4)]$.

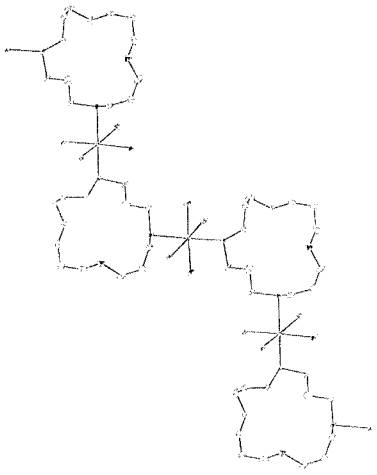

For comparison the exodentate complex $[(SnCl_4)_2([18]aneS_6)]$ is described. The 2:1 complex involves neutral $SnCl_4$ fragments coordinated in an *exo* fashion to two adjacent S-donor atoms of the macrocycle giving *pseudo* octahedral coordination at tin, Sn-S = 2.535(10)-2.689(13) Å.[28]

In summary, the crystal structures of the complexes $[SnBr_4([n]aneS_4)]$ (n = 12, 14 or 16) all exhibit *exo* coordination to the $SnBr_4$ *via* two S atoms from different macrocyclic units, forming a one-dimensional chain polymer. However, as the macrocyclic ring size is increased there is a marked difference in the coordination environment at tin, and in the binding mode. These are the first examples of Sn(IV) complexes with chalcogenoether ligands that adopt extended structures. The occurrence of the polymeric structures may in part be a result of the ability of the macrocycles to act as bridging ligands *via exo* coordination or due to the complexes being poorly soluble and as a result crystallising preferentially from solution. We also see that the Sn-S and Sn-Br bond distances are comparable to those observed in all of the bidentate thio-, seleno- and telluro-ether complexes, with the Sn-X bond distances *trans* to X being considerably longer than those *trans* to S, ascribed to a *trans* influence on the hard Sn(IV) centre of X > S. The *trans* X-Sn-X is also less than 180° expected for a regular octahedron, with the SnX_2 unit bending towards the neutral ligand, *e.g.* in $[SnBr_4([12]aneS_4)]$ *trans* Br-Sn-Br is 171.43(4)° and in $[SnBr_4([16]aneS_4)]$ *trans* Br-Sn-Br is 177.61(4)°.

Figure 2.14 A diagram to illustrate the SnX_2 unit bending towards the neutral ligand.

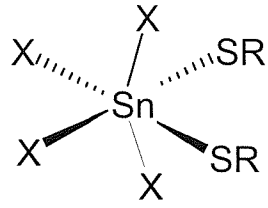

2.2.3 Variable Temperature Solution ^{1}H and ^{119}Sn NMR studies

Although only moderately soluble, ^{1}H NMR spectra were recorded in a rigorously anhydrous non-coordinating solvent (CD_2Cl_2) to avoid competition from the solvent for coordination to the tin. At 295K the tin(IV) complexes of the macrocyclic thio- and seleno-ethers are expected to undergo exchange *via* a dissociative process, which is rapid on the NMR timescale. As a result in the NMR spectra recorded at 295K only resonances for free ligand are observed. Resonances for each complex can clearly be shown to broaden on cooling, and the spectra become complicated, with splitting appearing. For the $SnBr_4$/[n]aneS_4 systems the resonance for the free ligand broadens, signifying that for this system the low temperature limit has not yet been reached. However, some splitting of the peaks is apparent suggesting coordination of the macrocycle. No ^{119}Sn NMR resonances were observed for the bromides at 295K or 183K.

Figure 2.15 ^{1}H NMR spectrum of [$SnBr_4$([12]aneS_4)] at 300K and 183 K in CD_2Cl_2 solution.

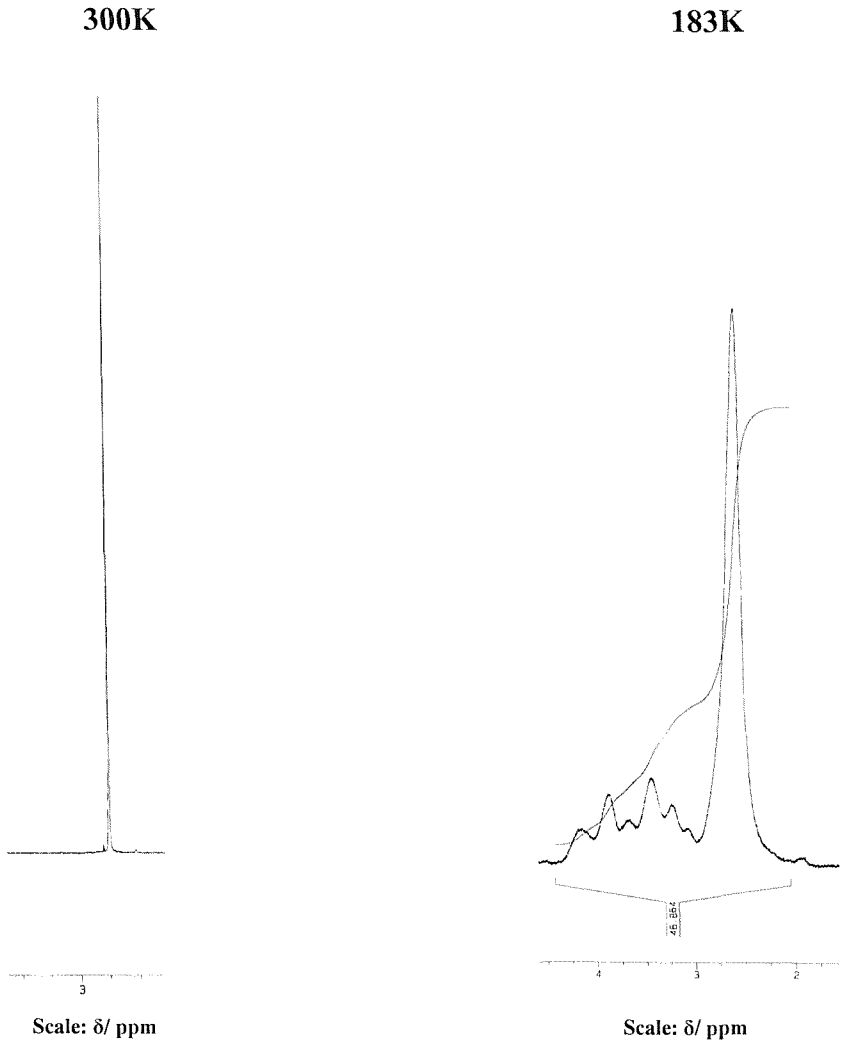

The $SnCl_4$/[n]aneS_4 systems are also extensively dissociated at 295K showing ^{1}H spectra similar to free macrocycle. Cooling to *ca.* 243-223K leads to exchange slowing. Resonances shift to a higher frequency compared to that of the parent macrocycle, thus providing evidence for coordination. The resonances are still not well enough resolved at 183K to allow for structural determination. No resonances were observed in the ^{119}Sn NMR spectra at 295K. A significant ^{119}Sn resonance becomes apparent on cooling to 183 K at δ–564, δ-603 and δ–543 for [12]-, [14]- and [16]-aneS_4 respectively; however the poor solubility of the complex coupled with the low sensitivity of the ^{119}Sn nucleus means that minor species may not be detected. ^{119}Sn

resonances for the complexes are seen to shift to low frequency by *ca.* 50 – 110 ppm on changing S for Se.

Table 2.6 ^{119}Sn NMR spectroscopic data for the tin(IV) halide complexes

Complex	^{119}Sn (δ)/ppm
$[(SnCl_4)_2([12]aneS_4)]$	-564
$[(SnCl_4)_2([14]aneS_4)]$	-603
$[(SnCl_4)_2([16]aneS_4)]$	-543
$[SnCl_4([8]aneSe_2)]$	-656
$[SnBr_4([16]aneSe_4)]$	-644

The chemical shift of the tin resonances obtained from studies on the bidentate thio- and seleno-ethers are similar to those obtained in these studies, *e.g.* $[SnCl_4\{MeS(CH_2)_3Me_2S\}]$[24] shows a broad tin resonance at 300K (δ -567) which sharpens on cooling and below *ca.* 220K shows two closely spaced resonance attributable to the *meso* and *dl* invertomers, the behaviour of $[SnCl_4\{MeS(CH_2)_2SMe\}]$ is similar, a broad tin resonance is apparent at 300K (δ -560). None of the $[SnX_4$(diselenoether)] complexes exhibit a ^{119}Sn-{^{1}H} resonance at 300K; on cooling resonances were initially observed as broad peaks which sharpened and in most cases resolved into two signals at 180K, consistent with the presence of *meso* and *dl* invertomers *e.g.* $[SnCl_4\{MeSe(CH_2)_2SeMe\}]$ shows tin resonances at δ –680 and δ -683 (180K).

The ^{1}H NMR spectrum of $[SnCl_4([8]aneSe_2)]$ at 295K shows broad resonances at 3.42, 3.27 and 1.71 ppm, which appear to sharpen on cooling. On cooling to 183K ^{77}Se{^{1}H} and ^{119}Sn resonances were detected δ(^{77}Se{^{1}H}) = 287 and δ(^{119}Sn{^{1}H}) = -656. The shift to high frequency of the ^{77}Se{^{1}H} resonance of the complex compared to 'free' ligand (δ(^{77}Se{^{1}H}) = 137)[31] suggests that both Se atoms are coordinated and thus the structure adopted may be a *cis*-chelated monomer in solution.

Similarly to the thioether macrocyclic complexes of tin(IV), at 295K the ^{1}H NMR spectrum of the tetraselenoether complex $[SnCl_4([16]aneSe_4)]$ shows extensive

dissociation. However, at 183K resonances for both coordinated and uncoordinated regions of the macrocycle are apparent. At 183K the $^{77}Se\{^{1}H\}$ NMR spectrum reveals two resonances of approximately equal intensity at 290 and 157 ppm, consistent with coordinated and un-coordinated selenoether groups. On the basis of these data a likely structure of $[SnCl_4([16]aneSe_4)]$ in solution is a 1:1 adduct involving the *cis*-octahedral coordination at Sn *via* two adjacent Se atoms of the ring, leaving the other two uncoordinated (Figure 2.16).

Figure 2.16 A View of the Proposed Structure of $[SnCl_4([16]aneSe_4)]$.

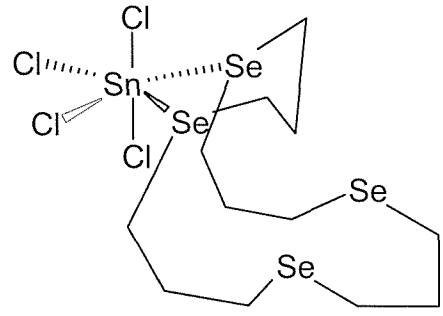

$[SnBr_4([16]aneSe_4)]$ is extensively dissociated even at low temperatures, which is clearly displayed by the ^{1}H NMR spectrum. No ^{119}Sn or $^{77}Se\{^{1}H\}$ spectra were obtained at 183K, owing to either the poor solubility of the complex in CD_2Cl_2 solution.

In summary, solution NMR spectroscopy shows that all the tetrathia and tetraselena macrocyclic complexes are extensively dissociated at 298K. While the bromo derivatives are still largely dissociated at 183K, spectra of the chloro complexes show much less dissociation. Dissociation is greater for the selenoether systems than the thioethers, as observed in previously reported examples. ^{1}H NMR also confirm the absence of a resonance corresponding to H_2O suggesting that the bulk samples are not the product of hydrolysis.

2.2.4 Crystallographic Studies on $[Sn_2Cl_6(OH)_2(H_2O)_2].3H_2O$ and $[SnCl_4(H_2O)_2].H_2O$

Efforts to grow good quality crystals of the $SnCl_4$/[n]aneS_4 systems suitable for X-ray diffraction proved unsuccessful. Attempts to grow crystals from the slow evaporation of the filtrates obtained from the reactions of [12]aneS_4 and [14]aneS_4 with $SnCl_4$ in the glove box formed a few colourless crystals of $[Sn_2Cl_6(OH)_2(H_2O)_2].3H_2O$ and $[SnCl_4(H_2O)_2].H_2O$ respectively, which were found to be a result of hydrolysis. Hydrolysis is a very common problem, which is also seen in the Sn(IV) chemistry studied by Genge[15]. These hydrolysis products are very minor species, the bulk of the samples isolated are $[(SnCl_4)_2$[n]ane$S_4]$ complexes, confirmed by the absences of H_2O stretching modes in the infrared spectra and a resonance assigned to H_2O in the ^1H NMR spectra.

Examples of the $[SnCl_4(H_2O)_2]$ are known in the literature, the crystal structures differ by their solvate. Tin tetrachloride pentahydrate $[SnCl_4(OH_2)_2].3H_2O$ is the only example in which water is the solvate.[32] Other structures are solvated with crown-ethers[33] or diethyl gluterate.[34] For example, when a mixture of two equivalents of $SnCl_4$ and one equivalent of 18-crown-6 in methanol were refluxed for two hours followed by cooling to -20°C, the neutral 1:1 adduct $SnCl_4$.18-crown-6.$2H_2O$ was formed. Recrystallisation of this complex from methanol-chloroform (1:1) gives the complex $SnCl_4$.18-crown-6.$4H_2O$, the crystal structure of which contains octahedral $Sn(OH_2)_2Cl_4$ units, in which the two water molecules occupy *cis* positions. Szafert[34] attempted to form the compound $[Sn_2Cl_8\{\mu\text{-}C_3H_6(CO_2Et)_2\}_2].2CH_2Cl_2$ by the direct reaction of $SnCl_4$ with diethyl gluterate, however due to the influence of moisture during the recrystallisation of this compound *cis*-$[SnCl_4(H_2O)_2].C_3H_6(CO_2Et)_2$ was obtained. Its crystal structure revealed a monomeric complex of Sn(IV) in which each atom is surrounded octahedrally by four chlorine atoms and two water oxygen atoms. A non-coordinated ester molecule is hydrogen bonded through the carbonyl oxygen atoms to one water molecule.

Examples of the solvated dimer $[Sn_2Cl_6(OH)_2(H_2O)_2]$ are also known. Crystal structures of (a) $[Sn_2Cl_6(OH)_2(H_2O)_2].3C_4H_8O_2$, (b) $[Sn_2Cl_6(OH)_2(H_2O)_2].4C_{10}H_{18}O$ and (c) $[Sn_2Cl_6(OH)_2(H_2O)_2].4H_2O$[32] have been determined. The hydroxo-bridged

dimers are based on *fac*-octahedral coordination. In (a) all H atoms of the dimer participate in bonds to 1,4-dioxan and each dioxan O atom participates in one hydrogen bond, resulting in a layer structure. In (b) each ligand of the dimer participates in one hydrogen bond to an oxygen atom of the bulky cyclic ether 1,8-cineole; there is no extended structure. In (c) hydrogen bonding to lattice water links the dimers into chains, which are cross-linked by Cl-H_2O bonds.

Details of the crystallographic data collection and refinement parameters of $[Sn_2Cl_6(OH)_2(H_2O)_2].3H_2O$ and $[SnCl_4(H_2O)_2].H_2O$ are given in Table 2.7. The unit cell of $[SnCl_4(H_2O)_2].H_2O$ looks orthorhombic but the systematic absences do not fit into any orthorhombic space group therefore it was taken as monoclinic. Hydrogen atoms of the water are difficult to find, therefore hydrogen atoms were located on the electron density map and restrained with the DFIX command 0.84(2) Å, the H(2b)-O(2)-Sn(1) angle is acute therefore it was concluded that H2b is in an unreasonable position and was eliminated from the calculations.

Table 2.7 Crystallographic Data

	$[Sn_2Cl_6(OH)_2(H_2O)_2].3H_2O$	$[SnCl_4(H_2O)_2].H_2O$
Formula	$H_{12}Cl_6O_7Sn_2$	$H_6Cl_4O_3Sn$
MWt	574.18	314.54
Crystal System	Monoclinic	Monoclinic
Space Group	C2/c	$P2_1/c$
a/Å	12.159(3)	6.3581(10)
b/Å	7.3535(15)	11.0600(15)
c/Å	17.122(4)	11.883(2)
α/°	90.00	90.00
β/°	95.73(1)	90.0079(9)
γ/°	90.00	90.00
U/ Å^0	1523.24(50)	834.39(20)
Z	4	4
μ(Mo-Kα)/mm^{-1}	4.339	4.271
Unique reflections	1728	1857
Obs. Reflections With $[I > 2\sigma(I)]$	1502	1820
*R*1 $[I > 2\sigma(I)]$	0.0287	0.0350
*R*1 (all data)	0.0358	0.0357
*wR*2 (all data)	0.0638	0.0832

Common Data: T = 120K; λ(Mo-Kα) = 0.71073 Å; $R1 = \Sigma|F_o|-|F_c|/\Sigma|F_o|$; $wR2 = [\Sigma w(F_o^2-F_c^2)^2/ \Sigma wF_o^4]^{½}$

Table 2.8 Selected bond lengths (Å) and angles (°) for *cis*-tetrachlorobis(aqua)tin(IV) monohydrate $[SnCl_4(H_2O)_2].H_2O$.

	Bond Lengths/ Å
Sn(1)-O(1)	2.140(3)
Sn(1)-O(2)	2.165(3)
Sn(1)-Cl(1)	2.3998(11)
Sn(1)-Cl(2)	2.3421(12)
Sn(1)-Cl(3)	2.3812(12)
Sn(1)-Cl(4)	2.3850(12)

	Bond Angles/°		**Bond Angles/°**
O(1)-Sn(1)-O(2)	83.50 (14)	O(1)-Sn(1)-Cl(1)	91.60(10)
O(1)-Sn(1)-Cl(2)	86.08(10)	O(2)-Sn(1)-Cl(1)	174.65(9)
O(2)-Sn(1)-Cl(2)	85.58(10)	Cl(2)-Sn(1)-Cl(1)	96.25(4)
O(1)-Sn(1)-Cl(3)	83.60(10)	Cl(3)-Sn(1)-Cl(1)	91.80(4)
O(2)-Sn(1)-Cl(3)	85.55(9)	Cl(4)-Sn(1)-Cl(1)	94.27(4)
Cl(2)-Sn(1)-Cl(3)	167.08(4)	Sn(1)-O(1)-H(1A)	115(5)
O(1)-Sn(1)-Cl(4)	173.29(11)	Sn(1)-O(1)-H(1B)	113(5)
O(2)-Sn(1)-Cl(4)	90.51(10)	H(1A)-O(1)-H(1B)	123(7)
Cl(2)-Sn(1)-Cl(4)	96.50(4)	Sn(1)-O(2)-H(2A)	112(5)
Cl(3)-Sn(1)-Cl(4)	92.95(4)	H(3A)-O(3)-H(3B)	102(8)

Figure 2.17 View of the structure of *cis*-tetrachlorobis(aqua)tin(IV) monohydrate with numbering scheme adopted.

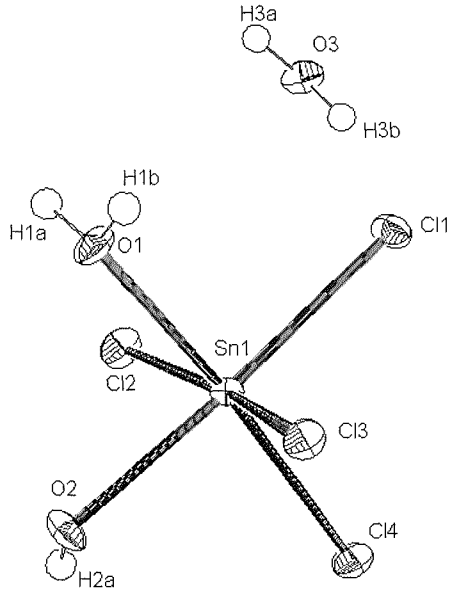

$[SnCl_4(H_2O)_2].H_2O$ is a monomeric Sn(IV) complex in which the Sn(IV) is in an octahedral environment and the two water molecules occupy *cis* positions. A non-coordinated water molecule is hydrogen bonded to one coordinated water molecule. The Sn-Cl bond distances for the complex lie in the range 2.3421(12) – 2.3998(11) Å, these bond distances are very similar to the Sn-Cl bond distances in the structure $[SnCl_4(H_2O)_2].3H_2O$ which lie in the range 2.383(5) – 2.401(4) Å.[33] The hydrogen bond distances H1b-O3 (1.86(2) Å) and O1-O3 (2.689(5) Å) are in good agreement with $[SnCl_4(H_2O)_2].3H_2O$ where O-O lie in the range 2.71(2) – 2.78(2) Å.

Table 2.9 Selected bond lengths (Å) and angles (°) for di (μ-hydroxo)bis(trichloroaquatin(IV)) trihydrate $[Sn_2Cl_6(OH)_2(H_2O)_2].3H_2O$

	Bond Lengths/ Å
Sn(1)-O(1)	2.071(2)
Sn(1)-O(2)	2.133(3)
Sn(1)-Cl(1)	2.3679(9)
Sn(1)-Cl(2)	2.3937(10)
Sn(1)-Cl(3)	2.3464(9)

	Bond Angles/°		**Bond Angles/°**
O(1)-Sn(1)-O(1)	84.25(9)	Cl(3)-Sn(1)-Cl(2)	96.02(4)
O(1)-Sn(1)-Cl(3)	163.96(7)	Cl(1)-Sn(1)-Cl(2)	94.12(3)
O(2)-Sn(1)-Cl(3)	88.67(8)	Sn(1)-O(1)-H(1)	123(3)
O(1)-Sn(1)-Cl(1)	93.72(6)	Sn(1)-O(2)-H(2A)	122(4)
O(2)-Sn(1)-Cl(1)	86.46(7)	Sn(1)-O(2)-H(2B)	120(3)
Cl(3)-Sn(1)-Cl(1)	100.21(3)	H(2A)-O(2)-H(2B)	118(5)
O(1)-Sn(1)-Cl(2)	90.84(7)	H(3A)-O(3)-H(3B)	109(5)
O(2)-Sn(1)-Cl(2)	175.09(7)		

Figure 2.18 View of the structure of di (μ-hydroxo)bis(trichloroaquatin(IV)) trihydrate with numbering scheme adopted.

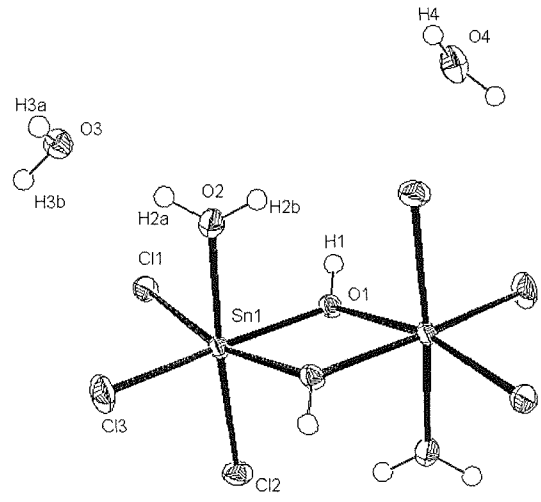

$[Sn_2Cl_6(OH)_2(H_2O)_2].3H_2O$ is a hydroxo-bridged dimer in which Sn(IV) adopts a *fac*-octahedral geometry. The Sn-Cl bond distances lie in the range 2.3464(9) – 2.3937(10) Å, which are in good agreement with the Sn-Cl bond distances in the structure $[Sn_2Cl_6(OH)_2(H_2O)_2].4H_2O$ in which the Sn-Cl bond distances lie in the range 2.356(4) – 2.371(4) Å. The hydrogen bond distances H1-O3 (1.88(2) Å), H2a-O3 (1.78(2) Å), H3b-O4 (1.93(2) Å), O1-O3 (2.699(3) Å), O2-O3 (2.624(4) Å) and O3-O4 (2.756(3) Å) are consistent with the hydrogen bond distance values literature for the structure $[Sn_2Cl_6(OH)_2(H_2O)_2].4H_2O$ where the O-O hydrogen bond distances lie in the range 2.67 – 2.87 Å.

2.2.5 Conclusions

The products $[(SnCl_4)_2([n]aneS_4)]$ (n = 12, 14, 16) and $[SnBr_4([n]aneS_4)]$ have been prepared in high yield by reaction of 2 mol. equiv. of the tin(IV) halide with 1 mol. equiv. of the parent macrocycle in anhydrous CH_2Cl_2. The 1:1 species $[SnX_4([16]aneSe_4)]$ (where X = Cl, or Br) is afforded by similar reactions of $[16]aneSe_4$ with 2 mol. equiv. of SnX_4, while $[SnCl_4([8]aneSe_2)]$ is obtained by the reaction of $[8]aneSe_2$ with 1 mol. equiv. of $SnCl_4$. A detailed examination of the variable temperature ^1H and ^{119}Sn NMR spectra over the range 298K – 183K has been presented, solution NMR spectroscopy shows that all the macrocyclic complexes

extensively dissociate at 298K. The bromo complexes are still largely dissociated at 183K, however the chloro derivatives are much less dissociated, ^{119}Sn NMR data are consistent with one major species in solution at low temperature. Far IR spectroscopy indicates that the choro complexes are all *cis*-octahedral tin species. Single crystal X-ray diffraction studies on $[SnBr_4([12]aneS_4)]$, $[SnBr_4([14]aneS_4)].2/3CH_2Cl_2$ and $[SnBr_4([16]aneS_4)]$ shows that each adopts a polymeric chain structure. There is however a considerable structural dependence on the macrocyclic ring size, as the ring size of the macrocycle is increased the coordination environment at tin(IV) changes, $[SnBr_4([12]aneS_4)]$ adopts a *cis*-octahedral geometry at Sn(IV), $[SnBr_4([14]aneS_4)].2/3CH_2Cl_2$ and $[SnBr_4([16]aneS_4)]$ show a *trans*-octahedral geometry at Sn(IV).

2.3 Experimental

Infrared spectra were recorded as Nujol mulls between CsI plates, using a Perkin Elmer 983 IR spectrometer over the range 4000 – 180 cm^{-1}. ^{1}H NMR spectra were recorded in $CDCl_3$ or CD_2Cl_2 using a Bruker DPX400 spectrometer, while $^{77}Se\{^1H\}$ and ^{119}Sn NMR spectra used a Bruker DPX400 spectrometer operating at 76.33 and 149.02 MHz and are referenced to neat external Me_2Se and Me_3Sn respectively. Microanalyses were obtained from the University of Strathclyde Microanalytical Laboratory. Tin tetrahalides and the thioether macrocycles were obtained from Aldrich and used as received. The $[8]aneSe_2$ and $[16]aneSe_4$ were prepared by the literature method.[31] Standard Schlenk techniques and anhydrous solvents were used throughout, and all preparations and manipulations were performed under a N_2 environment, also rigorously anhydrous solvents were used (CH_2Cl_2 distilled from CaH_2). Isolated yields were typically 60-70% in each case.

2.3.1 Preparations

[$(SnCl_4)_2$([12]aneS$_4$)]. [12]aneS$_4$ (0.05 g, 0.2 mmol) was dissolved in anhydrous CH_2Cl_2 (20 cm^3) under an atmosphere of dry N_2 and the solution further degassed. Two molar equivalents of $SnCl_4$ (0.05 cm^3, 0.4 mmol) was added to the ligand solution and stirred at room temperature for *ca.* 30 mins. Concentration of the reaction mixture in vacuo formed a white solid. The solution was decanted from the solid, which was subsequently washed with CH_2Cl_2 and dried *in vacuo*. Calc. for $C_8H_{16}Cl_8S_4Sn_2$: C, 12.6; H, 12.6. Found: C, 12.9; H, 2.1%. ^{1}H NMR (CD_2Cl_2, 253K: δ 3.50, 2.74 (1:1, both broad, coord. and uncoord. SCH_2). ^{119}Sn NMR (CD_2Cl_2, 223K): δ –564. IR/cm^{-1}: 334, 320, 312 (Sn-Cl).

[$(SnCl_4)_2$([14]aneS$_4$)]. Procedure as for [$(SnCl_4)_2$([12]aneS$_4$)], but using [14]aneS$_4$. White solid. Calc. for $C_{10}H_{20}Cl_8S_4Sn_2.CH_2Cl_2$: C, 15.1; H, 2.6%. Found: C, 14.3; H, 3.1%. ^{1}H NMR (CD_2Cl_2, 223K): δ 3.74, 3.61, 3.53 (coord. SCH_2), 2.99, 2.85 (uncoord. SCH_2), 2.12, 2.03 (SCH_2CH_2). ^{119}Sn NMR (CD_2Cl_2, 223K): δ –603. IR/cm^{-1}: 332, 328, 323 (Sn-Cl).

[$(SnCl_4)_2$([16]aneS$_4$)]. Procedure as for [$(SnCl_4)_2$([12]aneS$_4$)], but using [16]aneS$_4$. White solid. Calc. for $C_{12}H_{24}Cl_8S_4Sn_2$: C, 17.6; H, 3.0. Found: C, 17.4; H, 3.0%. ^{1}H NMR (CD_2Cl_2, 193K): δ 3.40, 3.03, 3.58, 2.05, 1.81 (coord. and uncoord. SCH_2 and CH_2). ^{119}Sn NMR (CD_2Cl_2, 193K): δ –543. IR/cm-1: 332, 327, 316, 300 (Sn-Cl).

[$SnBr_4$([12]aneS$_4$)]. To a solution of [12]aneS$_4$ (0.05 g, 0.2 mmol) in anhydrous CH_2Cl_2 (20 cm^3) was added $SnBr_4$ (0.175g, 0.4 mmol) and the resulting solution was stirred at room temperature for *ca.* 30 mins. Concentration of the reaction mixture in vacuo afforded a yellow precipitate, which was filtered washed with CH_2Cl_2 and dried in vacuo. Calc. for $C_8H_{16}Br_4S_4Sn_1$: C, 14.2; H, 2.4. Found: C, 14.5; H, 2.1%. ^{1}H NMR (CD_2Cl_2, 300K): δ 2.75 (*s*); (183K): δ 3.0-4.3 (br, *m*, coord. SCH_2), 2.60 (br, *s*, uncoord. SCH_2). IR/cm^{-1}: 221 (br, Sn-Br).

[$SnBr_4$([14]aneS_4)]. Procedure as for [$SnBr_4$([12]aneS_4)], but using [14]aneS_4. Yellow solid. Calc. for $C_{10}H_{20}Br_4S_4Sn_1$: C, 17.0; H, 2.9. Found: C, 16.9; H, 2.6%. ^{1}H NMR (CD_2Cl_2, 300K): δ 2.79 (*s*, SCH_2CH_2S), 2.67 (*t*, $SCH_2CH_2CH_2$), 1.95 (*q*, $CH_2CH_2CH_2$); (183K): δ 3.73, 3.33 (coord. SCH_2), 2.80 (br, uncoord. SCH_2), 2.15 (br, SCH_2CH_2). IR/ cm^{-1}: 223 (br, Sn-Br).

[$SnBr_4$([16]aneS_4)]. Procedure as for [$SnBr_4$([12]aneS_4)], but using [16]aneS_4. Yellow solid. Calc. for $C_{12}H_{24}Br_4S_4Sn_1$: C, 19.6; H, 3.3. Found: C, 20.2; H, 3.2%. ^{1}H NMR (CD_2Cl_2, 300K): δ 2.66 (*t*, SCH_2), 1.95 (*q*, SCH_2CH_2); (183K): δ 3.30, 2.77, 2.57, 2.12 (all broad). IR/cm^{-1}: 223 (br, Sn-Br).

$NCSe(CH_2)_3SeCN$ Dry KSeCN (9.71 g, 67.2 mmol) was suspended in dry DMF (100 cm^3) was added under N_2. The solution was heated to 333K, and $Br(CH_2)_3Br$ (3.3 cm^3, 32 mmol) was added slowly dropwise over the course of 20 minutes, and the mixture heated (5 hrs). The resulting mixture was filtered to remove the insoluble material, and the resulting solution was vacuum distilled to remove the DMF solvent. The resulting oil was dried *in vacuo* (24 hrs) to afford a pale orange solid. $^{77}Se\{^1H\}$ NMR spectrum (68.68 MHz, DMF, 298K): δ 214; ^{1}H NMR spectrum (300 MHz, $CDCl_3$, 298K): δ 3.2 (4H, m, $SeCH_2CH_2$), 2.5 (2H, m, $SeCH_2CH_2$); $^{13}C\{^1H\}$ NMR Spectrum (75.47 MHz, $CDCl_3$, 298K): δ 101 (SeCN), 27.9 ($SeCH_2CH_2$) and 31.9 ($SeCH_2CH_2$).

[8]aneSe_2, [16]aneSe_4, [24]aneSe_4 Dry THF was added to a 500 cm^3 three necked round bottom flask under N_2. Ammonia (200 cm^3) was condensed into the flask (using a slush bath of Me_2CO and solid CO_2 pellets at *ca.* 195K). A small piece of sodium was added to the mixture followed by $NCS(CH_2)_3SeCN$ (7.257 g, 28 mmol) in a small amount of dry THF (10 cm^3) to give an orange brown solution. Sodium metal (2.55 g, 11 mmol) was then added in small pieces to afford a colour change to blue. At this point a pressure equalising funnel was fitted and a solution containing dry THF (150 cm^3) and $Br(CH_2)_3Br$ (6.34 g, 31 mmol) was added to the reaction vessel slowly drop wise over a period of 3 hours with the slush bath maintained a 223K, to afford an orange solution and a white precipitate. This was then left to warm to room temperature and subsequently stirred under N_2 for 20 hours. To the resulting mixture was added distilled water (300 cm^3), which dissolved the precipitate. Extraction with CH_2Cl_2 (3 x 100 cm^3) afforded a yellow solution, which upon solvent removal *in vacuo* produced an

orange oil. The oil was separated on a silica column (MN Kieselgel 60, 230 400 mesh) of length 40 cm and diameter 3.5 cm using a 19:1 hexane: ethyl acetate mixture. The first ligand to be eluted from the column was [8]aneSe$_2$ with an R_f value of 0.65. The second was [16]aneSe$_4$ (R_f = 0.4) and the third ligand was [24]aneSe$_6$ (R_f = 0.1). ^{77}Se{^{1}H} NMR spectrum (68.68 MHz, CH_2Cl_2, 298K): δ 137 ([8]aneSe$_2$), 157 ([16]aneSe$_4$) and 153 ([24]aneSe$_4$).

[SnCl$_4$([8]aneSe$_2$)]. To a solution of [8]aneSe$_2$ (0.05 g, 0.207 mmol) in degassed CH_2Cl_2 (20 cm^3) was added one molar equivalent of $SnCl_4$ (0.09 g, 0.207 mmol) and the resulting solution was stirred at room temperature for *ca.* 30 mins. Concentration *in vacuo* afforded an orange solid, which was filtered, washed with CH_2Cl_2 and dried in vacuo. Calc. for $C_6H_{12}Cl_4Se_2Sn_1$: C, 14.3; H, 2.4. Found: C, 14.1; H, 2.2 %. ^{1}H NMR (CD_2Cl_2, 300K): δ 3.42, 3.27, 1.71 (br). ^{77}Se-{^{1}H} NMR (CD_2Cl_2, 183K): δ 287. ^{119}Sn NMR (CD_2Cl_2, 183K): δ –656. IR/cm^{-1}: 333, 320, 314, 300 (Sn-Cl).

[SnCl$_4$([16]aneSe$_4$)]. Procedure as for [SnCl$_4$([8]aneSe$_2$)], but using [16]aneSe$_4$. Yellow solid. Calc. for $C_{12}H_{24}Cl_4Se_4Sn_1$: C, 19.4; H, 3.3 %. Found: C, 19.2; H, 3.7 %. ^{1}H NMR (CD_2Cl_2, 183K): δ 3.0-3.5 (br, *m*, coord, $SeCH_2$), 2.65 (br, *s*, uncoord. $SeCH_2$), 1.7-2.1 (br, *m*, coord. $SeCH_2CH_2$), 1.86 (br, *s*, uncoord. $SeCH_2CH_2$). ^{77}Se{^{1}H} NMR (CD_2Cl_2, 183K) : δ 290, 157 (1:1 ratio of coord. uncoord. Se). ^{119}Sn NMR (CD_2Cl_2, 183K): δ -644. IR/cm^{-1}: 332, 327, 316, 305 (Sn-Cl).

[SnBr$_4$([16]aneSe$_4$)]. Method as for [SnBr$_4$([12]aneS$_4$)], but using [16]aneSe$_4$. Orange solid. Calc. for $C_{12}H_{24}Br_4Se_4Sn_1$: C, 15.6; H, 2.6 %. Found: C, 14.4; H, 2.6 %. ^{1}H NMR (CD_2Cl_2, 183K): see text. IR/cm^{-1}: 223 (br, Sn-Br).

[SnI$_4$([9]aneS$_3$)]. [9]aneS$_3$ (0.05 g, 0.277 mmol) was dissolved in anhydrous CH_2Cl_2 (20 cm^3) under an atmosphere of dry N_2 and the solution further degassed. SnI_4 (0.173 g, 0.277 mmol) was added to the ligand solution and stirred at room temperature *ca.* 30 mins. The reaction mixture was concentrated *in vacuo* to from a deep purple precipitate, which was filtered and washed with CH_2Cl_2. Calc. for $C_6H_{12}S_3I_4Sn_1$: C, 8.9; H, 1.5 %. Found: C, 8.8; H, 1.3 %.

2.4 References

[1] W. Levason and G. Reid, *J. Chem. Soc., Dalton Trans.*, 2001, 2953.

[2] S. M. Godfrey, I. Mushtaq and R. G. Pritchard, *J. Chem. Soc., Dalton Trans.*, 1999, 1319.

[3] J. A. C. Allison and F. G. Mann, *J. Chem. Soc.*, 1949, 2915.

[4] I. R. Beattie, *Q. Rev. Chem. Soc.*, 1963, **17**, 382.

[5] W. Levason and C. A. McAuliffe, *Coord. Chem. Rev.*, 1976, **19**, 173.

[6] J. D. Dumas and M. Gomel, *Bull. Soc. Chim. France*, 1974, 1885.

[7] P. G. Harrison, B. C. Lane and J. J Zuckerman, *Inorg. Chem.*, 1972, **11**, 1537.

[8] D. Cunningham, M. J. Frazer and J. D. Donaldson, *J. Chem. Soc. A.*, 1971, 2049.

[9] N. Bricklebank, S. M. Godfrey, C. A. McAuliffe and R. G. Pritchard, *J. Chem. Soc., Chem. Commun.,* 1994, 695; N. Bricklebank, S. M. Godfrey, C. A. McAuliffe and K. C. Molloy, *J. Chem. Soc., Dalton Trans.,* 1995, 1593.

[10] F. Kunkel, K. Dehnicke, H. Goesmann and D. Fenske, *Z. Naturforsch., Teil B.*, 1995, **50**, 848.

[11] F. Sarikhaya, *Synth. React. Inorg. Met. Org. Chem.*, 1989, **19**, 641.

[12] I. R. Beattie and G. A. Ozin, *J. Chem. Soc. A.,* 1970, 370; D. K. Frieson and G. A Ozin, *Can. J. Chem.,* 1973, **51**, 2685.

[13] G. G. Mather, G. M. McLaughlin and A. Pidcock, *J. Chem. Soc., Dalton Trans.,* 1973, 1823.

[14] D. Dakternieks, Hongjian Zhu and E. R. T. Tiekink, *Main Group Metal Chem.*, 1994, **17**, 519.

[15] A. R. J. Genge, Ph.D Thesis, University of Southampton, 1999.

[16] R. Rivest, S. Singh and C. Abraham, *Can. J. Chem.*, 1967, **45**, 3137.

[17] N. Ohkaku and K. Nakamato, *Inorg. Chem.*, 1973, **12**, 2446.

[18] A. R. J. Genge, W. Levason and G. Reid, *Inorg. Chim. Acta.*, 1999, **288**, 142.

[19] S. J. Ruzicka and A. E. Merbach, *Inorg. Chim. Acta.*, 1976, **20**, 221.

[20] S. J. Ruzicka and A. E. Merbach, *Inorg. Chim. Acta.*, 1977, **22**, 191.

[21] S. J. Ruzicka, C. M. P. Favez and A. E. Merbach, *Inorg. Chim. Acta*, 1977, **23**, 239.

[22] C. T. G. Knight and A. E. Merbach, *J. Am. Chem. Soc.*, 1984, **106**, 804.

[23] C. T. G. Knight and A. E. Merbach, *Inorg. Chem.*, 1985, **24**, 576.

[24] S. E. Dann, A. R. J. Genge, W. Levason and G. Reid, *J. Chem. Soc., Dalton Trans.*, 1996, 4471.

[25] S. E. Dann, A. R. J. Genge, W. Levason and G. Reid, *J. Chem. Soc., Dalton Trans.*, 1997, 2207.

[26] A. R. J. Genge, W. Levason and G. Reid , *J. Chem. Soc., Dalton Trans.*, 1997, 4549.

[27] A. R. J. Genge, W. Levason and G. Reid , *J. Chem. Soc., Dalton Trans.*, 1997, 4479.

[28] G. R. Willey, A. Jarvis, J. Palin and W. Errington, *J. Chem. Soc., Dalton Trans.*, 1994, 255.

[29] D. H. Williams and I. Fleming, *Spectroscopic Methods in Organic Chemistry*, McGray-Hill, London, 1995.

[30] M. M. Olmstead, K. A. Williams and K. Musker, *J. Am. Chem. Soc.*, 1982, **104**, 5567.

[31] R. J. Batchelor, F. W. B. Einstein, I. D. Gay, J. Gu, B. D. Johnston and B. M. Pinto, *J. Am. Chem. Soc.*, 1989, **111**, 6582.

[32] J. C. Barnes, H. A. Sampson and T. J. R. Weakley, *J. Chem. Soc., Dalton Trans.*, 1980, 949.

[33] P. A. Cusack, B. N. Patel and P. J. Smith, *J. Chem. Soc., Dalton Trans.*, 1984, 1239.

[34] P. Sobota, S. Szafert and T. Glowiak, *J. Chem. Soc., Dalton Trans.*, 1996, 439.

CHAPTER 3

Complexes of Antimony Trichloride and Antimony Pentachloride

3.1 Complexes of Arsenic(III), Antimony(III) and Bismuth(III)

3.1.1 Introduction

A general overview of the Lewis acid – Lewis base chemistry of As(III), Sb(III) and Bi(III) is discussed in chapter 1. Recent work has shown that the heavy p-block trihalide Lewis acids of group 15 MX_3 (M = arsenic(III), antimony(III) and bismuth(III)) readily form complexes with polydentate and macrocyclic thio- and selenoether ligands to give a diverse range of structural motifs. These compounds show a structural dependence on the ligand donor type, denticity, architecture and whether the ligand is acyclic or macrocyclic.

In general the structures are derived from a combination of primary and secondary M-X and M-E (E = S, Se and Te) bonding interactions; the concept of primary and secondary bonding interactions was first introduced by Alcock.[1] As well as normal or primary bonds, many metalloids and non-metal compounds exhibit longer directional interactions, shorter than van der Waals but significantly longer than primary bonds. The donor-acceptor model[2,3]is convenient in describing bonding in main group complexes. Carmalt and Norman[4] have described an account of this model as applied to Group 15 compounds. In primary M-X bonding, the σ orbital is polarised towards the more electronegative X and the corresponding M-X σ* antibonding orbital is polarised towards M. The antibonding orbital may behave as an acceptor orbital towards a Lewis base or a bridging halide from a monomer unit if the orbital lies low enough in energy. The electronegativity of both M and X and the match in orbital size will influence the extent and strength of the secondary bonding, since both are reflected in the energy of the antibonding orbital. Further diversity exists due to a lone pair based on M, the presence of which is apparent from structural irregularities, e.g. voids in the coordination sphere or distortions in bond lengths and bond angles. In the complexes discussed the geometries are often quite distorted, although it is difficult to decide in many cases (particularly with M = Sb or Bi) whether it is the effect of the lone pair or the consequence of ligand geometry.

Very recently, investigations of the coordination chemistry of AsX_3 (X = Cl, Br or I) with thio- and seleno-ether ligands has been undertaken.[5,6] Complexes of AsX_3 with $MeS(CH_2)_2SMe$, [9]aneS_3, [14]aneS_4, [8]aneSe_2, [16]aneSe_4 and [24]aneSe_6 have been isolated and characterised. These complexes were prepared by the reaction of the arsenic(III) halide in anhydrous CH_2Cl_2 (X = Cl, Br) or THF (X = I) solutions with one molar equivalent of the ligand. The crystal structure of [$AsCl_3$([9]aneS_3)] is unusual in that the As(III) lone pair is effectively stereochemically inactive. The structure shows six-coordinate monomers involving the thiacrown capping the face of the As(III) atom, with three mutually *fac* chlorine atoms completing the donor set, to establish a distorted geometry with d(As-S) = 2.720(4) – 2.861(4) Å (Figure 3.1).

Figure 3.1 View of the crystal structure of [$AsCl_3$([9]aneS_3)].[5]

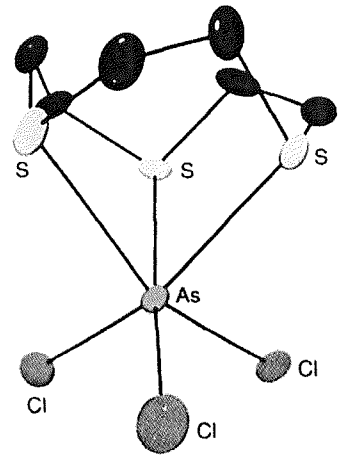

The structure of [$AsCl_3$([8]aneSe_2)][7] reveals an infinite one-dimensional ladder, comprising near-planar As_2Cl_6 units linked by bridging [8]aneSe_2 molecules. This is the first example of an AsX_3-chalcogenoether complex that adopts a mutually *trans* deposition for the chalcogen atoms (Figure 3.2), and is discussed in more detail in section 3.1.2.

Figure 3.2 View of the crystal structure of $[AsCl_3([8]aneSe_2)]$.[7]

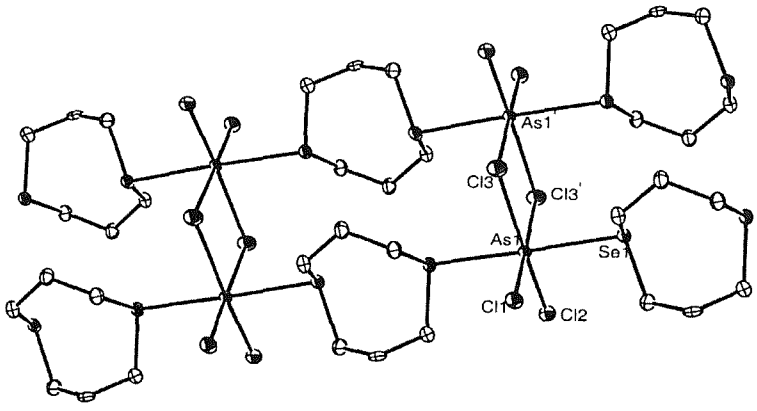

The 2:1 adduct $[(AsCl_3)_2[16]aneSe_4]$ adopts a sheet polymer structure with five-coordinate As(III) coordinated to three terminal Cl's and two Se donor atoms from *exo*-coordination to two different macrocyclic rings. This results in an octahedron about the As metal centre with one vacant vertex, which is assumed to be occupied by the As-based lone pair, d(As-Se) = 2.7840(7), 2.7840(7) Å. The structure $[(AsCl_3)_4[24]aneSe_6]$ unexpectedly adopts an As : ligand stoichiometry of 4 : 1. The $[(AsCl_3)_4[24]aneSe_6]$ is new in revealing both *exo* and *endo* coordination of the As(III) centres and forms discrete molecules. An As_2Cl_6 μ-chloro-bridged dinuclear unit is coordinated within the macrocycle, giving a distorted octahedral Se_2Cl_4 coordination environment at the *endo* As atoms. The *exo* As centres adopt a different coordination number and geometry. Those *exo* to the ring form four-coordinate distorted sawhorse units through coordination to three terminal Cl's and a single Se atom. The lone pair on the *exo* As atoms is assumed to occupy the third equatorial vertex of a 'trigonal bipyramid'. The hexaselenoether macrocycle therefore uses all six Se donor atoms to bind to the As centres; two pairs of adjacent Se atoms chelate to the As centres of the endocyclic dinuclear fragment, with each of the two remaining, mutually *trans* Se atoms co-ordinating η^1 (*exo*) to discrete $AsCl_3$ units, $d(As\text{-}Se)_{endo}$ = 2.994(2), 3.005(2); $d(As\text{-}Se)_{exo}$ = 3.091 Å (Figure 3.3).[8]

Figure 3.3 View of the Crystal Structure of $[(AsCl_3)_4[24]aneSe_6]$.[8]

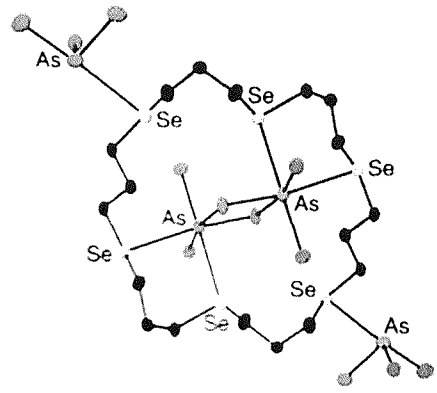

The arsenic halides have poorer acceptor properties compared with either the antimony(III) halides or the bismuth(III) halides. The As(III) atom is much smaller than its heavier congeners, the stereochemical implications of which are illustrated by the fact that while seven-coordination is observed in thio- and seleno-ether complexes of Sb(III) and Bi(III), the maximum coordination number observed for As(III) in the literature is six. A consequence of the smaller radius is the increased hardness of the AsX_3 unit compared to SbX_3 or BiX_3 (in terms of the HSAB principle described in chapter 1). Arsenic(III) halides appear to represent the lower limit of Lewis acidity for MX_3 species toward neutral Group 16 donor ligand systems, as in PX_3 the combination of increased hardness, lower Lewis acidity and smaller radius means that there are no structural reports of thio-, seleno- or telluro-ether complexes with PX_3 acting as a Lewis acid.[6]

The Southampton group has undertaken studies on antimony(III) halide complexes with thio- and seleno-ether ligands.[9] The crystal structures of the antimony(III) halide complexes $[SbBr_3\{MeS(CH_2)_3SMe\}]$, $[SbCl_3\{MeS(CH_2)_3SMe\}]$, $[SbCl_3\{MeSe(CH_2)_3SeMe\}]$, $[(SbBr_3)_2[(14]aneS_4)]$, $[SbCl_3\{MeC(CH_2SMe)_3\}]$, $[SbI_3\{MeC(CH_2SMe)_3\}]$, $[SbBr_3\{MeC(CH_2SeMe_3\}]$ and $[(SbBr_3)_2[(16]aneSe_4)]$ all exhibit infinite one- or two-dimensional networks which are assembled from distorted five or six coordinate Sb(III) with primary Sb-X bonding, secondary Sb-S or Sb-Se interactions and retention of the pyramidal SbX_3 unit found in the parent halides. The cyclic selenoethers [8]aneSe$_2$, [16]aneSe$_4$ and [24]aneSe$_6$ form 1:1 or very occasionally 1:2 macrocycle : SbX_3 complexes. The crystal structure of the complex

$[(SbBr_3)_2[(16]aneSe_4)]$ (Figure 3.4) shows a two dimensional array derived from $[16]aneSe_4$ molecules coordinated in an exocyclic fashion to four Sb centres, each of which bind to another selenoether macrocycle. The geometry at Sb is five-coordinate *via* primary interactions to three *fac* terminal Br atoms and secondary interactions to two *cis* Se atoms from different macrocycles, giving a distorted square-pyramidal coordination environment. The Sb-Br bond distances lie in the range 2.537 (1)–2.687(1) Å and the Sb-Se bond distances lie in the range 2.989(1) – 3.193(1) Å. The Sb-Se distances in $[(SbBr_3)_2[(16]aneSe_4)]$ are shorter than those in $[SbCl_3\{MeSe(CH_2)_3SeMe\}]$, however this may be due to the lower coordination number of the former.[9]

Figure 3.4 View of a portion of the two-dimensional sheet adopted by $[(SbBr_3)_2([16]aneSe_4)]$. [9]

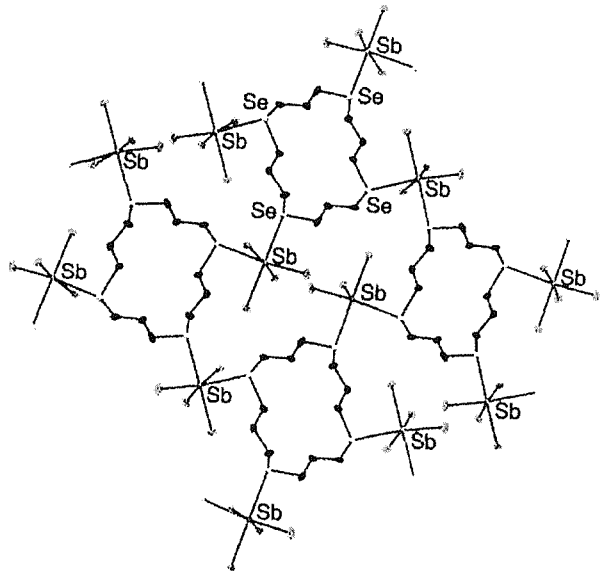

The structures adopted by the antimony(III) species are contrasted with those observed for related bismuth(III) species. Willey and co-workers have described a small number of Bi(III) complexes involving macrocyclic thioethers, including $[BiCl_3([9]aneS_3)]$,[10] $[BiCl_3([12]aneS_4)]$[11] and $[BiCl_3([18]aneS_6)]$.[12] The crystal structures of $[BiCl_3([12]aneS_4)]$ and $[BiCl_3([18]aneS_6)]$ all show a pyramidal MX_3 unit bound in an endocyclic manner to four or six co-planar sulfur donors from the macrocycle respectively to give an approximate half-sandwich structure. The structure

of the related $[(BiCl_3)_2([24]aneS_4)]$[13] complex is comprised of two distinct $BiCl_3$ units bound to five sulfur donors (two of which bridge the bismuth atoms). The $BiCl_3$ units are disposed on opposite sides of the mean plane of the crown (Bi-S 3.134(2) – 3.313(2) Å). In these complexes weak secondary interactions exist between Bi-S (*c.a.* 3.2 Å) which essentially replace the weak, secondary Bi-Cl interactions evident in the parent pyramidal $BiCl_3$. Macrocyclic ligands offer enhanced binding properties over acyclic counterparts and often exhibit different binding modes. Structural studies have shown that these macrocyclic Bi species are discrete molecular entities, with coordination numbers varying from six to nine.

Genge and co-workers have investigated Bi(III) complexes of acyclic thioethers, and the complex $[Bi_4Cl_{12}(MeS(CH_2)_3SMe)_4]_n.nH_2O$ has been reported. The complex was prepared by reaction of $BiCl_3$ with one molar equivalent of $MeS(CH_2)_3SMe$ in CH_2Cl_2. The structure involves $Bi_4Cl_{12}(\eta^1\text{-}MeS(CH_2)_3SMe)_4$ tetrameric units which are linked by bridging dithioether ligands to give a three-dimensional polymeric network. Each Bi(III) ion is therefore coordinated to two terminal Cl atoms, Bi-Cl_{term} = 2.538(7) and 2.533(7) Å, two μ^2 Cl atoms, Bi-$Cl_{bridging}$ = 2.913(7) and 2.969(6) Å and two S donors from different bridging dithioether ligands, Bi-S = 2.857(7) and 2.977(7) Å. The geometry at each Bi(III) metal centre approximates to an octahedron, with an open triangular face, which is assumed to be occupied by the Bi lone pair. The Bi_4Cl_4 core is an eight membered heterocycle, which adopts an open cradle conformation (Figure 3.5).

Figure 3.5 View of the $BiCl_4$ core of $[Bi_4Cl_{12}(MeS(CH_2)_3SMe)_4]_n.nH_2O$ illustrating the open cradle conformation. The dashed lines indicate the secondary Bi---Cl interactions.[14]

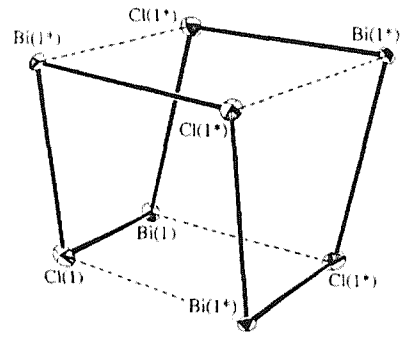

Other bismuth trihalides (BiX_3, X = Cl, Br or I) react with a range of thio- and seleno-ether ligands L-L in anhydrous MeCN solution to yield compounds with either a 1:1, 1:2 or 2:1 Bi:L-L ratio.[15] Structural studies on $[BiBr_3\{MeE(CH_2)_3EMe\}]$ (E = S or Se) and $[BiCl_3\{MeSe(CH_2)_3SeMe\}]$ revealed that all of these species adopt an infinite two-dimensional sheet array derived from planar Bi_2X_6 units linked by bridging dithio- or diseleno-ether ligands which occupy mutually *trans* coordination sites, giving a distorted octahedral geometry at Bi(III). In the complex $[BiBr_3\{MeS(CH_2)_3SMe\}]$ the coordination geometry around Bi(III) is derived from two terminal Br (2.697(2), 2.719(2) Å), two bridging Br (2.980(2), 2.931(4) Å) and two S-donors from mutually *trans* bridging thioether ligands (2.880(4), 2.931(4) Å). While the Bi-Br distances are comparable with those in the related compounds, the Bi-S bond distances are shorter than for the macrocyclic thioether complexes, [10,11,12] indicating stronger interactions for the complexes described here. The structure of $[BiBr_3\{MeS(CH_2)_2SMe\}_2]$ reveals a discrete molecular compound which adopts a 7-coordinate distorted pentagonal bipyramidal geometry involving two chelating $MeS(CH_2)_2SMe$ ligands. This arrangement is also found for the iodide analogue.[15] The compound $[BiBr_3\{MeSe(CH_2)_3SeMe\}]$ is isostructural with $[BiBr_3\{MeS(CH_2)_3SMe\}]$, with Bi-Se distances of 3.028(2) and 2.978(3) Å. The Bi-Se distances in these compounds are shorter than (or in some cases similar to) the macrocyclic thioether complexes of BiX_3 described previously. This suggests that while the Bi-S interactions are described as

weak, secondary interactions, those involving Se donors are considerably stronger, and it is presumed that they reflect the orientation of the bismuth lone pair which, is towards the thioether ligand in the macrocyclic derivatives, but towards the bridging Br ligands in the compounds described above. The shorter Bi-Se distances are a result of the larger and more diffuse ionic radius of selenium, and are within the sum of the ionic radii of Bi^{3+} and Se^{2-} (3.01 Å).

Altering the terminal substituent on the dithioether also has a dramatic effect upon the structure adopted. Reaction of $BiBr_3$ with the Ph-substituted ligand $PhS(CH_2)_2SPh$ generated a very different structural arrangement in which chains of almost mutually orthogonal Bi_2Br_2 'rectangles' are cross-linked by bridging dithioether ligands to yield infinite sheets of formula $[Bi_2Br_6\{PhS(CH_2)_2SPh\}]$. The donor set around the bismuth ions comprises four bridging Br (2.693(3) – 3.274(3) Å), one terminal Br (2.596(2) Å) and one thioether S- donor (3.082(6) Å), giving a distorted octahedral geometry. With the tripodal ligands L_3 ($MeC(CH_2SMe)_3$ or $MeC(CH_2SeMe)_3$) compounds of stoichiometry $[BiX_3(L_3)]$ were obtained. The crystal structure of $[BiCl_3\{MeC(CH_2SeMe)_3\}]$ shows Bi_2Cl_6 subunits linked by bridging selenoether ligands to give a two-dimensional sheet. The bismuth(III) ion is 7-coordinate, with the donor set comprising two bridging Cl (2.776(8), 3.151(10) Å), one bidentate selenoether (2.622(9), 2.55(1) Å) and one monodentate selenoether (3.117(4) Å).[15]

Studies have also been undertaken on Bi(III) complexes of macrocyclic selenoether ligands. [16] Treatment of BiX_3 (X = Cl or Br) with one molar equivalent of [8]$aneSe_2$, [16]$aneSe_4$ and [24]$aneSe_6$ yielded species of the formula $[BiX_3(L)]$. The crystal structures of $[BiCl_3([8]aneSe_2)]$ and $[BiBr_3([16]aneSe_4)]$ have been determined. $[BiCl_3([8]aneSe_2)]$ reveals an infinite one-dimensional ladder structure derived from almost co-planar Bi_2Cl_6 dimer units linked by four bridging cyclic [8]$aneSe_2$ 'uprights'. The Se-donor atoms adopt mutually *trans* coordination sites on each Bi ion (Figure 3.6). The bond lengths and bond angles are discussed in more detail in section 3.1.2.

Figure 3.6 View of the structure of a portion of the infinite one-dimensional ladder adopted by $[BiCl_3([8]aneSe_2)]$.[16]

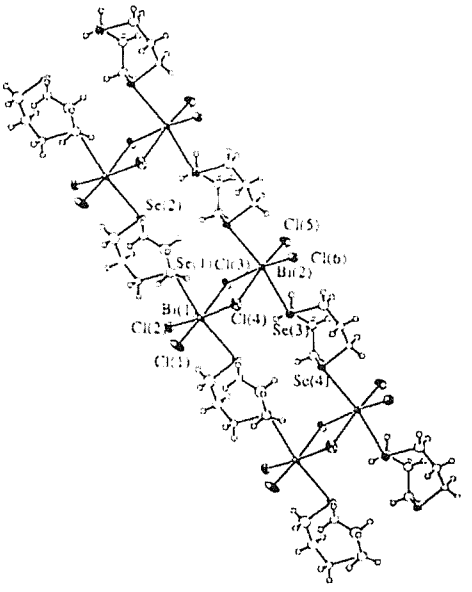

A very similar motif is observed for $[BiBr_3([16]aneSe_4)]$, the one dimensional infinite arrangement is derived from almost planar Bi_2Br_6 units, with each Bi linked to the next Bi_2Br_6 units by bridging $[16]aneSe_4$. Coordination is *via* one Se-donor atom to each Bi. The macrocycles are bonded *via* mutually *trans* selenium donors and adopt an exocyclic conformation. Within this centrosymmetric structure each Bi is coordinated *via* a *trans*-Se_2Br_4 donor set, d(Bi-Se) = 2.952(2) and 3.095(2) Å , d(Bi-Br) = 2.693(2) – 3.058(2) Å . There are two mutually *trans* Se atoms within each $[16]aneSe_4$ unit which remain un-coordinated. To date, these are the only examples of complexes with *trans* coordination by the thio-, seleno- and telluroether ligands to the Bi(III) metal centre.[16]

The first donor-acceptor complexes of Sb(III) and Bi(III) with telluroether ligands have also been reported.[17] The reactions of various MX_3 (M = As, Sb, Bi; X = Cl, Br, I) with $MeTe(CH_2)_3TeMe$ in anhydrous MeCN solution (or THF for X = I) were investigated. Reaction with As(III) halides did not yield isolable products. However, Sb

and Bi halides allowed the isolation of the analytically pure complexes $[SbX_3\{MeTe(CH_2)_3TeMe\}]$ (X = Br or I), $[BiCl_3\{MeTe(CH_2)_3TeMe\}]$ and $[BiBr_3(PhTeMe\}]$. The isolated solids are poorly soluble in chlorocarbons, MeCN and $MeNO_2$, thus to date the only structurally characterised example involving a telluroether is $[BiBr_3(PhTeMe)]$ (Figure 3.7). Red crystals of this material were obtained by slow evaporation from a MeCN solution of $BiBr_3$ which had been layered with an equimolar solution of PhTeMe in CH_2Cl_2. The structure reveals a planar asymmetric $Br_2Bi(\mu\text{-}Br)_2BiBr_2$ dimer unit with one PhTeMe ligand coordinated apically to each Bi and occupying mutually *anti* positions. Long contacts between bromines *via* the open Bi vertex enables adjacent units to be linked to give an infinite chain of $Bi_2Br_6(PhTeMe)_2$ dimers in a step-like arrangement.

Figure 3.7 View of the crystal structure $[BiBr_3(PhTeMe)]$.[17]

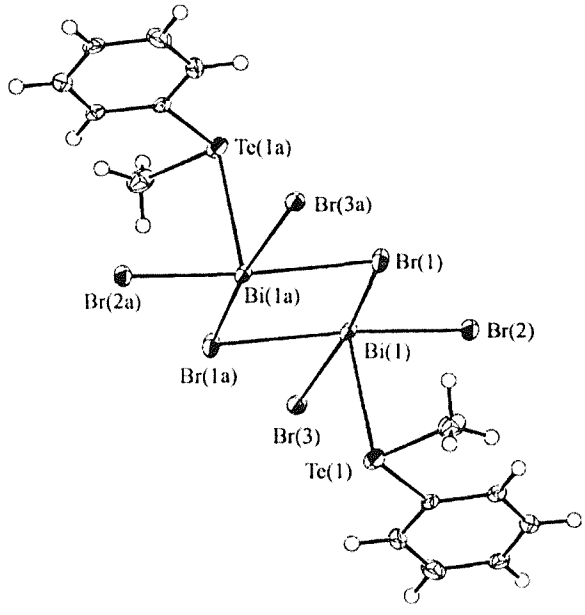

In summary, the MX_3 complexes of thio- seleno- and telluroether ligands adopt a diverse range of structures with rich coordination chemistry. It is clear from previous work in the Southampton laboratories that changes in X, E and M, ligand denticity and architecture all influence the structures adopted in a complex way and predicting structures is not simple. Comparisons of a closely related family of neutral donor-acceptor compounds of As(III), Sb(III) and Bi(III) would enable us to probe more

directly the different factors affecting the structures and the structural trends with M(III), however to date there are no known studies of this nature in the literature.

3.1.2 Results and Discussion

The complexes $[AsCl_3([8]aneSe_2)]$[7] and $[BiCl_3([8]aneSe_2)]$[16] are known in the literature and both have been structurally characterised in the Southampton laboratories. The aim of this particular piece of work is to complete the family of compounds by establishing the structure of $[SbCl_3([8]aneSe_2)]$. This would allow the structural effects within a closely related family of neutral seleno-ether complexes, which differ only in the identity of the acceptor atom to be probed for the first time. The same method of synthesis and solvents were used in the formation of all MX_3 complexes of $[8]aneSe_2$. It is also important to note that all data collections were made at the same temperature (120K), hence structural differences are not simply due to temperature or solvent effects. Crystals of $[SbCl_3([8]aneSe_2)]$ were prepared by the reaction of one molar equivalent of $[8]aneSe_2$ with one molar equivalent of $SbCl_3$, both in rigorously anhydrous CH_2Cl_2. The solvent was reduced *in vacuo* and the solution left under an atmosphere of dry-N_2 to form orange-needles. Single crystal X-ray analysis (120K) reveals $[Sb_2Cl_6(\eta^1\text{-}[8]aneSe_2)_2]$ dimers involving edge-bridged square pyramids with *anti* $[8]aneSe_2$ ligands. Long-range secondary interactions exist between the remaining Se atoms and the open vertex of the Sb atoms, thus linking the dimers into an infinite ladder structure (Figure 3.9). This is the first example involving a *trans* deposition of the Se atom on the Sb(III) acceptor. The structure is therefore grossly similar to the ladders observed for $[AsCl_3([8]aneSe_2)]$[7] and $[BiCl_3([8]aneSe_2)]$,[16] but it is much more distorted.

Figure 3.8 View of the structure of a) $[SbCl_3([8]aneSe_2)]$ with atom numbering scheme. H atoms are omitted for clarity and 40% probability ellipsoids are drawn. [Symmetry operations: ' = -x, -y, -z, '' = x + 1, y, z].

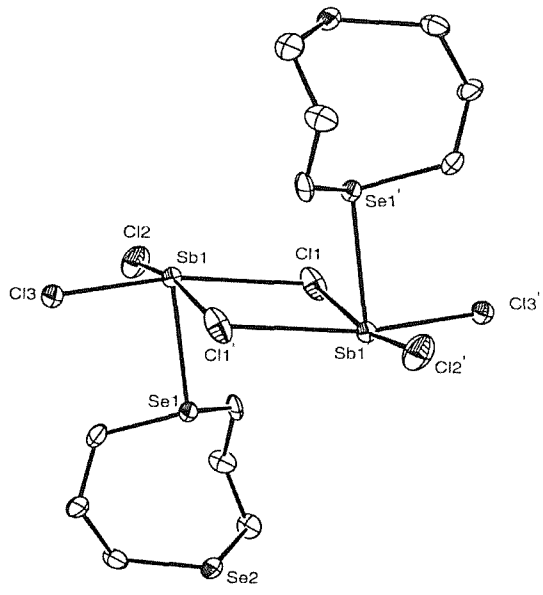

Figure 3.9 View of a portion of the infinite ladder structure formed from weakly associated dimers.

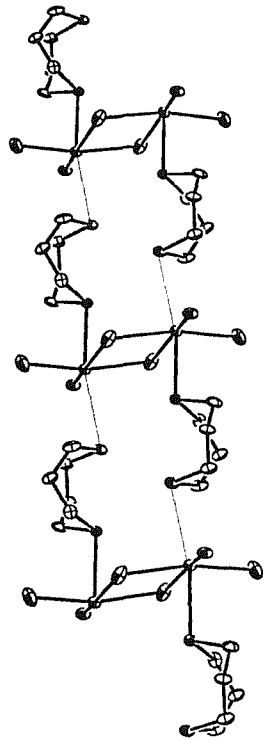

Examination of the bond length and bond angle distributions in $[SbCl_3([8]aneSe_2)]$ reveals a much less symmetrical environment surrounding the Sb(III) metal centre. The Sb(1)-Se(1) bond length, d(Sb-Se) = 2.7839(13) Å is 0.5 Å shorter than the Sb(1)-Se(2) bond length, d(Sb-Se) = 3.2904(13) Å. The terminal Sb-Cl bond distances are 2.499(2) and 2.438(2), with the Sb-μ-Cl bonds (2.751(2) and 2.881(2) Å) being asymmetric. The bond angles around Sb in $[SbCl_3([8]aneSe_2)]$ are also irregular, the Se(1)-Sb(1)-Se(2) angle is 168.10(3)°, with Se(2) tilted away from the bridging Cl's. The distortion appears to be in the region of the Se(2)-Sb(1)-Cl(1)' plane and the corresponding angle at Sb(1) of 98.74(5)° is very open.

The structure adopted by $[SbCl_3([8]aneSe_2)]$ is similar to the structure observed for the Bi(III) analogue $[BiCl_3([8]aneSe_2)]$, whereby the Se-donor atoms adopt mutually *trans* coordination sites on each Bi ion, giving Bi-Se 2.988(4) and 3.044(4) Å and $Bi\text{-}Cl_{terminal}$ of *c.a* 2.5 Å and $Bi\text{-}Cl_{bridging}$ distances of *c.a* 2.8 Å The $[AsCl_3([8]aneSe_2)].CH_2Cl_2$ also adopts an infinite one-dimensional ladder motif comprising of near-planar As_2Cl_6 rungs linked by bridging $[8]aneSe_2$ molecules. The Se-donor ligands are bound to the As_2Cl_6 units in a mutually *trans* fashion, giving As-Se 2.7840(7) and As-Cl in the range 2.2734(17) – 2.7766(19) Å. In conclusion the bond lengths and bond angles at Bi(III) and As(III) appear to be fairly symmetrical.

Due to the structural distortions observed in this crystal of $[SbCl_3[8]aneSe_2)]$ we were concerned that the weak, secondary bonding interactions may be affected significantly by packing effects in the crystal lattice, thus there may be other closely related structural forms which are energetically similar. In an attempt to eliminate this possibility, X-ray analysis on a second crystal ((b) $[SbCl_3([8]aneSe_2)]$) grown under the same solvent conditions was undertaken. Structure solution and refinement revealed that the structure was identical within the normal standard deviations, and thus it was evident that the structural distortions which are evident in $[SbCl_3([8]aneSe_2)]$ but not in the As(III) or Bi(III) analogues are genuine and reproducible.

Table 3.1 Crystallographic data and refinement parameters.

	Crystal (a) **[$SbCl_3$([8]aneSe_2)]**	**Crystal (b)** **[$SbCl_3$([8]aneSe_2)]**
Formula	$C_6H_{12}Se_2Sb_1Cl_3$	$C_6H_{12}Se_2Sb_1Cl_3$
MWt	470.18	470.18
Crystal System	monoclinic	monoclinic
Space Group	$P2_1/n$	$P2_1/n$
a/Å	9.327(3)	9.331(3)
b/Å	12.165(4)	12.1716(4)
c/Å	10.998(10)	10.9992(4)
α/°	90	90
β/°	96.948(10)	96.9600(10)
γ/°	90	90
U/Å^3	1238.7(8)	1239.89(7)
Z	4	4
μ(Mo- Kα)/mm^{-1}	8.703	8.694
Unique reflections	2761	2789
Obs. reflections With [$I > 2\sigma(I)$]	2007	2516
$R1[I > 2\sigma(I)]$	0.0494	0.0326
$R1$(all data)	0.0805	0.0718
$wR2$ (all data)	0.0850	0.0746

Common Data: T = 120K; λ(Mo-Kα) = 0.71073 Å; $R1 = \Sigma||F_o|-|F_c||/\Sigma|F_o|$; $wR2 = [\Sigma w(F_o^2-F_c^2)^2/\Sigma wF_o^4]^{½}$

Table 3.2 Selected bond lengths (Å) and angles (°) for crystal (a) $[SbCl_3([8]aneSe_2)]$ and crystal (b) $[SbCl_3([8]aneSe_2)]$.

	Crystal (a) Bond Lengths/ Å	**Crystal (b) Bond Lengths/ Å**
Sb(1)-Cl(1)	2.881(2)	2.8829(12)
Sb(1)-Cl(2)	2.499(2)	2.4961(12)
Sb(1)-Cl(3)	2.438(2)	2.4396(10)
Sb(1)-Cl(1)'	2.751(2)	2.7522(12)
Sb(1)-Se(1)	2.7839(13)	2.7844(5)

	Crystal (a) Bond Angles (°)	**Crystal (b) Bond Angles (°)**
Cl(3)-Sb(1)-Cl(2)	92.71(7)	92.71(4)
Cl(3)-Sb(1)-Cl(1)'	87.10(7)	87.02(4)
Cl(3)-Sb(1)-Se(1)	90.56(5)	90.56(3)
Cl(2)-Sb(1)-Se(1)	90.13(5)	90.27(4)
Cl(1)'-Sb(1)-Se(1)	77.84(5)	77.80(3)
Cl(2)-Sb(1)-Cl(1)	94.88(7)	94.94(4)
Cl(1)-Sb(1)-Cl(1)'	83.35(6)	83.43(3)
Se(1)-Sb(1)-Cl(1)	79.26(5)	79.39(3)
Se(1)-Sb(1)-Se(2)	168.10(3)	167.38(4)

Symmetry operations: ' = -x, -y, -z; '' = x +1, y, z

In contrast to the majority of the complexes of MX_3 (M = As, Sb, or Bi; X = Cl, Br or I) characterised, which are based on pyramidal MX_3 units with secondary M---S/Se interactions completing the coordination environment, complexes of the cyclic diselenoether [8]aneSe_2 contain planar M_2Cl_6 units linked by bridging diselenoether ligands which occupy mutually *trans* coordination sites. The effects of the M based lone pair are more evident due to the complexes being more symmetrical than the common pyramidal species.

Prior to coordination each of the acceptor atoms M = Bi(III), As(III) and Sb(III) carries a lone pair of electrons, which is an important consideration in the structural chemistry. The lone pair can either occupy an s orbital, resulting in the elongation of the M-Cl and M-Se bond distances by an approximately equal amount. Alternatively, it may be directional/stereochemically active. This results either in a void in the coordination environment or distortions in bond lengths and/or bond angles in particular regions of the coordination environment at M. It is not easy to forecast when there will be a stereochemically active lone pair in these MX_3 complexes, but the following general trends can be noted.[18] Stereochemical activity of the lone pair decreases with:

1) Increasing coordination numbers
2) Increasing atomic number of the halogen
3) Increasing atomic number of E (i.e. As > Sb > Bi)

Therefore, in these chloro complexes [MCl_3([8]aneSe_2)] one might expect the lone pair to be stereochemically active in the As(III) derivative, and to be less active in the Bi(III) complex. However, in these studies it becomes apparent that the expected general trend is not observed.

The availability of X-ray structural data on this homologous series of complexes allows direct comparison of the bond length and angle patterns and allow conclusions to be made on the extent of lone pair activity within these neutral adducts. It is important to note that in complexes of this type, the presence of the lone pair is merely inferred on the basis of a void in the coordination sphere of the metal atom. In the dianionic $[M_2Cl_8]^{2-}$ (all *anti*-edge bridged square pyramids in the crystal structures)

there is an open vertex which is assumed to be occupied by the lone pair.[19] The terminal M-Cl distances in the anions are very similar to those in the corresponding $[MCl_3([8]aneSe_2)]$ compounds; however, for the neutral donor-acceptor compounds there is no open vertex available and all of the metal centres in the complexes are 6-coordinate. There is an unexpected irregular pattern in lone pair activity in this series, the coordination sphere around the 6-coordinate As(III) in the $[AsCl_3([8]aneSe_2)]$ appears to be symmetrical, suggesting that the lone pair is inactive. In contrast, in $[SbCl_3([8]aneSe_2)]$ the coordination sphere around Sb(III) is distorted and the lone pair is assumed to be stereochemically active. There is no significant distortion of the bond lengths or angles at Bi in $[BiCl_3([8]aneSe_2)]$ and the structure shows 6-coordination, it is concluded that the lone pair is probably occupying the 6s orbital, which due to relativistic effects is both stabilised and contracted.

3.2 Complexes of Antimony (V)

3.2.1 Introduction

As discussed in the previous section compounds of Group 15 acceptor ions in the +3 oxidation state are much more structurally diverse giving coordination geometries of up to 7, as a result of the presence of a non-bonded pair of electrons. However, the coordination numbers encountered for complexes in the +5 oxidation state are most commonly four, five and six. The pentahalides of group 15 - AsF_5, SbF_5 and BiF_5 are all exceptionally strong Lewis acids and form many complexes with hard donors including halide ions.[4] The pentafluorides are highly reactive and toxic, while PCl_5 is a weak acceptor and $AsCl_5$ is thermally very unstable. Thus $SbCl_5$ offers unique scope to extend coordination chemistry in this area. The MX_5 molecules adopt a trigonal bypyramidal structure and interact with an electron donor (L) to give octahedral or distorted octahedral complexes. The anions EX_6^- are obtained when L = F, Cl, Br or I and the structure is strictly octahedral.

Figure 3.10 A diagram of the structures adopted by $SbCl_5$ and $SbCl_6^-$

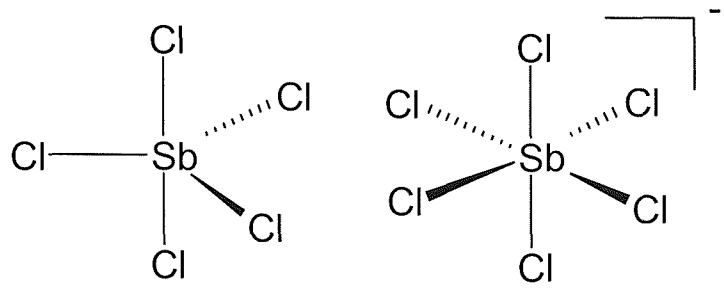

Antimony(V) complexes containing oxygen donor ligands have long been known, and the majority of the complexes have been characterised by X-ray crystallography and infrared spectroscopy. The first crystallographically characterised example $[SbCl_5(OPCl_3)]$ was reported in 1959 by Branden and Lindquist.[20] Single crystals of the very hygroscopic compound were prepared, and the crystals were stable during the time of exposure. The structure is built up of discrete $[SbCl_5(OPCl_3)]$ molecules, the coordination around Sb is octahedral with an O atom from $POCl_3$ in the sixth vertex. The approximately tetrahedral structure of $OPCl_3$ is preserved. The Sb-Cl bond distances lie in the range 2.319(6) – 2.350(6) Å, d(Sb-O) = 2.18(2) Å and d(P-O) = 1.46(2) Å. Branden and Lindquist[21] also reported the isomorphous complex $[SbCl_5(OPMe_3)]$, which also exhibits octahedral geometry about the Sb(V) metal centre. The Sb-O and P-O bond lengths are 1.99(2) Å and 1.61(2) Å, respectively, the Sb-Cl bond lengths lie in the range 2.32(12) – 2.37(12) Å.The Sb-O-P bond angle is 139.0(13)°. The donor strength of Me_3PO was proved to be greater than that of $POCl_3$ with $SbCl_5$ as the acceptor. Lindqvist and Olofsson[22] further investigated the addition compounds of phosphine oxides. The addition compound $[SbCl_5(OPPh_3)]$ was prepared by precipitating it out from cool, dilute solutions of $SbCl_5$ and $OPPh_3$ in CCl_4 (mole ratio 1:1) and was recrystallised from CH_2Cl_2 as almost colourless needle-shaped crystals. There are two symmetry independent $[SbCl_5(OPPh_3)]$ molecules in the unit cell. Distances are d(Sb-O) = 2.04(2) Å in one of the molecules in the unit cell and 1.99(2) Å for the other.[23]

Figure 3.11 View of the structure of $[SbCl_5(OPPh_3)]$[23]

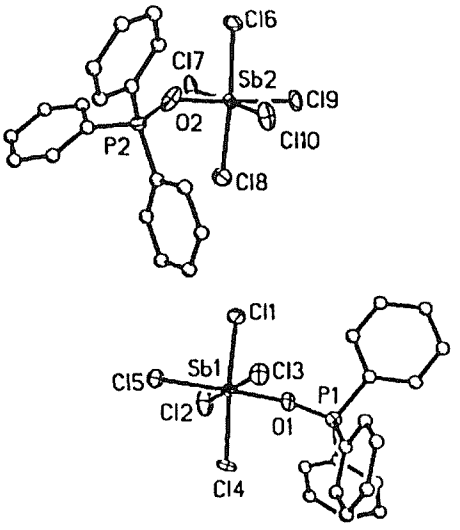

Figure 3.12 View of the crystal structure of $[SbCl_5(OPMe_3)]$[21]

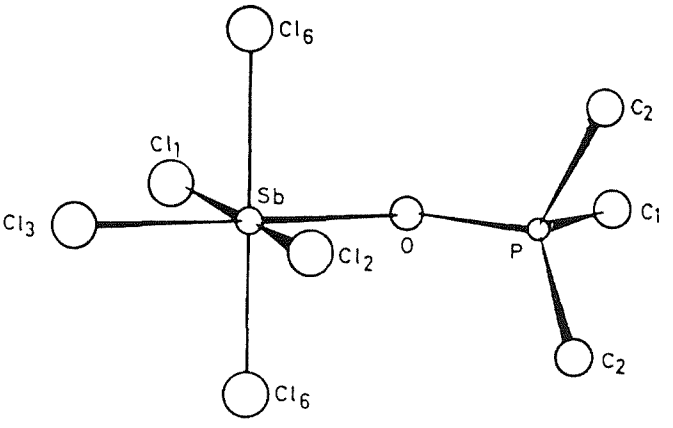

In 1966 Van Der Veer and Jellinek[24] characterised addition compounds of triphenylphosphine sulphide using infrared spectroscopy. X-ray structural analysis on the complex $[SbCl_5(SPPh_3)]$ has not been undertaken. The complex $[SbCl_5(SPPh_3)]$ was prepared by the reaction of one molar equivalent of the ligand in CS_2 or $C_2H_4Cl_2$ with one molar equivalent of $SbCl_5$ in CCl_4 or $C_2H_4Cl_2$. Infrared spectroscopy on both $[SbCl_5(OPPh_3)]$ and $[SbCl_5(SPPh_3)]$ shows that the P-S and P-O bands of the free ligands Ph_3PS (632 cm^{-1}) and Ph_3PO (1195 cm^{-1}) shift considerably upon coordination to the Sb metal centre (536 cm^{-1} and 1030 cm^{-1} respectively).

Amides are also capable of forming addition compounds with $SbCl_5$ and an adduct of acetamide with antimony(V) chloride has been prepared. X-ray structural determinations have been carried out on $[SbCl_5(HC(O)NMe_2)]$.[25] The carbonyl oxygen of the *N,N*-dimethylformamide acts as the donor atom, the Sb(V) exhibits a change of coordination from trigonal bypyramidal in free $SbCl_5$ to distorted octahedral in the adduct. The Sb-Cl bond lengths lie in the range 2.330(3) – 2.353(3) Å, and the Sb-O bond length is 2.048(6) Å. The Sb-Cl bond lengths are very similar to those of the complexes $[SbCl_5(OPCl_3)]$, $[SbCl_5(OPMe_3)]$ and $[SbCl_5(OPPh_3)]$. Dialkylnitrosamines also forms a 1:1 complex with $SbCl_5$. The complex $[SbCl_5(ONNMe_2)]$ has been formed, an O-Sb bond links the components and the complex is isostructural with that of the $SbCl_5$ complex of N,N-dimethylformamide, with d(Sb-O) = 2.113(3) Å and d(Sb-Cl) = 2.344(1) and 2.364(1) Å.[26]

Figure 3.13 View of the structure of $[SbCl_5(ONNMe_2)]$.[26]

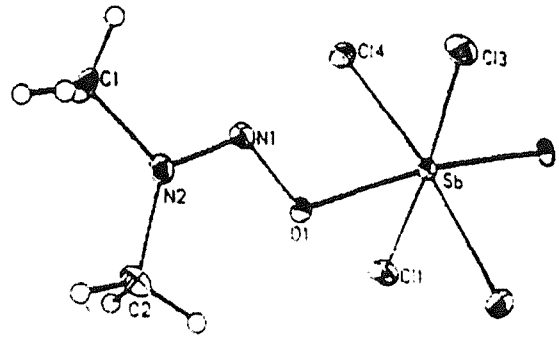

The complexes $[SbCl_5(OSMe_2)]$, $[SbCl_5(O_2SMe_2)]$, $[SbCl_5(OSeCl_2)]$ and $[SbCl_5(OSPh_2)]$ have been characterised by X-ray crystallography and infrared spectroscopy. The complex $[SbCl_5(OSPh_2)]$ is a molecular solid with coordination from the oxygen to the antimony(V) metal centre increasing the coordination number to six, while the one to one addition compound between dimethylsulfone and antimony pentachloride has only one of its two oxygen atoms coordinated. The complex $[SbCl_5(OSMe_2)]$ was formed from an equimolar mixture of Me_2SO and $SbCl_5$ in carbon tetrachloride and isolated as a white precipitate. Thin plate crystals were grown from a solution of the complex in benzene. The structure exhibits a distorted octahedral geometry about the central metal atom with five chlorine atoms and an oxygen atom of

the Me_2SO. The Me_2SO molecule is statistically disordered in the crystal. The bond distances of Sb-Cl, d(Sb-Cl) = 2.29(2) – 2.37(1) Å are in good agreement with the structure $[SbCl_5(OPMe_3)]$. The bond angles for the disordered oxygen, antimony and five chlorine atoms depart considerably from those of a regular octahedral structure. This distortion prevents the sulfur atom of Me_2SO from making abnormally short contacts with chlorine atoms.[27]

Holliday[28] and co-workers studied the crystal and molecular structure of the antimony pentachloride adducts of 10-chlorophenoxarsine oxide, $[SbCl_5(C_{12}H_8OAsClO)]$. The antimony chloride unit of the molecule compares very closely with previous structures described.

Figure 3.14 View of the structure of $[SbCl_5(C_{12}H_8OAsClO)]$.[28]

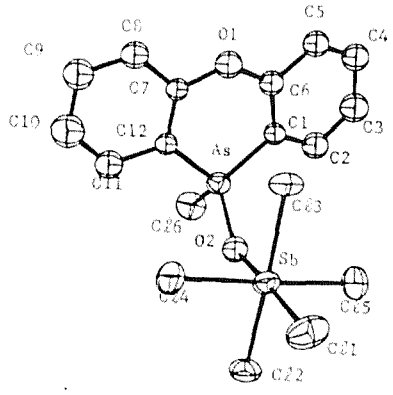

In all these complexes the formation of a coordinate bond by donation of a lone pair of electrons simply perturbs the donor molecule, no great changes in the stereochemistry are required. However, the acceptor molecule undergoes a major change in stereochemistry, in these complexes from trigonal bipyramidal (D_{3h}) to *pseudo*-octahedral (C_{4v}). Examination of the Sb-Cl stretching modes in conjunction with the ligand vibrations provide a useful tool for the investigation of the adducts in the solid state. There are no characterised examples of adducts with the soft phosphine, arsine, thioether or selenoether ligands.

3.2.2 Aims of the Study

Antimony(V) chloride complexes with phosphine oxide, phosphine sulphide and arsine oxide ligands were known as early as 1959. Many of the early studies do not include full characterisation. Therefore, the preliminary aims of this study are to re-examine specific examples and to obtain full spectroscopic analysis and to prepare specific $SbCl_5$ complexes of bidentate phosphine oxide and arsine oxides and monodentate phosphine sulfides and selenides ($R_3P{=}S$, $R_3P{=}Se$). This will provide a basis for future work, extending these studies to look at $SbCl_5$ complexes of the parent phosphine and arsine ligands.

3.2.3 Results and Discussion

3.2.3.1 Antimony (V) – Monodentate Arsine Oxide and Phosphine Oxide Complexes

A range of complexes of the type $[SbCl_5(L)]$ (where L = Me_3PO, Ph_3PO, $MePh_2PO$ and Ph_3AsO) have been prepared by the reaction of one molar equivalent of $SbCl_5$ in CH_2Cl_2 with one molar equivalent of the ligand in rigorously anhydrous CCl_4. The complexes were isolated as white solids in good yield (*ca.* 60%) following filtration, washing with CCl_4 and drying *in vacuo*. The $[SbCl_5(L)]$ complexes were formed as powdered white solids. On account of the moisture sensitivity of $SbCl_5$ and to a lesser extent the $[SbCl_5(L)]$ adducts formed, all reactions were performed under an atmosphere of dry nitrogen using standard Schlenk techniques, and the complexes were stored in a dry, N_2 filled glove box.

With Lewis bases (L:) reacting with the Lewis acid ($SbCl_5$) the obvious product is that in which a coordinate bond is formed between L: and Sb by donation of a lone pair of electrons into vacant orbitals of antimony. Antimony thus increases its coordination number from 5 to 6 (*i.e.* trigonal bypyramidal going to octahedral coordination). For molecules of the type $[SbCl_5(L)]$ with C_{4v} symmetry the reducible representation is:

	E	2C4	C2	2σV	2σd
ΓSb-Cl	5	1	1	3	1

Reduction to an irreducible representation predicts three infrared ($2A_1 + E$)) Sb-Cl stretches, observed between the range 300-400cm^{-1}.

The complexes $[SbCl_5(OPPh_3)]$ and $[SbCl_5(OPMePh_2)]$ reveal three features in the far infrared region consistent with group theory. However, in the case of the other monodentate ligand complexes the bands are not so well resolved and only one broad feature is revealed.

The P=O and As=O stretching frequencies for both 'free' and complexed ligands have been tabulated (Table 3.3). 'Free' $MePh_2PO$ reveals a strong feature at 1173 cm^{-1}, which is assigned to the P-O stretching mode. This shifts to 1125 cm^{-1} in the complex. The shift in the P-O and As-O stretching modes to lower frequency is evident for all the monodentate complexes formed. The stretching mode corresponding to P-O for the complex $[SbCl_5(OPPh_3)]$ of 1039cm^{-1} is comparable to the literature value (1030cm^{-1}).[24] The significant low frequency shift of the P-O and As-O band of the adducts relative to the P-O and As-O bands of the free ligands show that the oxygen atoms are coordinated to the metal. The majority of the bands are attributed to ligand absorptions, which are seen to shift slightly on coordination to $SbCl_5$. Importantly the absence of a stretch in the range 3600 – 3100 cm^{-1} confirms the absence of water in the samples.[29]

Table 3.3 IR spectroscopic data for the antimony(V) chloride complexes of the monodentate phosphine and arsine oxide ligands.

Complex	Colour	v(Sb-Cl)/cm^{-1}	Complex ν(As=O), ν(P=E) E = O, S or Se /cm^{-1}	Free Ligand ν(As=O), ν(P=E) E = O, S or Se /cm^{-1}
$[SbCl_5(OAsPh_3)]$	White	360(br)	835	879[30]
$[SbCl_5(OPMe_3)]$	White	351(br), 320(sh)	1040	1170[31]
$[SbCl_5(OPPh_3)]$	White	361, 342, 325	1039	1195[31]
$[SbCl_5(OPMePh_2)]$	White	358, 343, 324	1145	1170[32]

a. spectra recorded as Nujol mulls
br = broad
sh = shoulder

The complexes are soluble in halocarbon solvents and were thus amenable to both ^1H and $^{31}P\{^1H\}$ NMR spectroscopy. $^{31}P\{^1H\}$ NMR spectra were recorded in rigorously anhydrous, non-coordinating solvent (CH_2Cl_2/CD_2Cl_2) to avoid competition from the solvent for coordination to the antimony. The $^{31}P\{^1H\}$ NMR spectra of the $[SbCl_5(L)]$ (where L = Ph_3PO, Me_3PO and $MePh_2PO$) complexes at 300K each reveal a singlet, showing a considerable shift in the resonances to high frequency in comparison to the $^{31}P\{^1H\}$ NMR resonances of the free ligand (Table 3.4). This is consistent with coordination of P-O. The observation of a single resonance in the $^{31}P\{^1H\}$ NMR spectra for the phosphine oxide complex suggests the presence of only one species in solution. In the case of the complex $[SbCl_5(OAsPh_3)]$, a shift in the aromatic resonances in the ^1H NMR spectrum is apparent.

Table 3.4 $^{31}P\{^{1}H\}$ NMR spectroscopic data for the antimony(V) chloride complexes of monodentate phosphine and arsine oxide ligands.

Complex	$^{31}P\{^{1}H\}$ Complex (δ)[a]/ppm	$^{31}P\{^{1}H\}$ Free Ligand (δ)[b]/ppm
$[SbCl_5(OPMe_3)]$	71	39[33]
$[SbCl_5(OPPh_3)]$	48	26[35]
$[SbCl_5(OPMePh_2)]]$	52	29 [35]

a. Spectra recorded relative to external 85% H_3PO_4 in CH_2Cl_2/ $CDCl_3$ solution

b. Spectra recorded relative to external 85% H_3PO_4 in $CDCl_3$

3.2.3.2 Sb(V) – Bidentate Phosphine Oxide and Arsine Oxide Complexes

The complex $[(SbCl_5)_2(Ph_2P(O)CH_2P(O)Ph_2)]$ has been prepared by the reaction of two molar equivalents of $SbCl_5$ with one molar equivalent of the ligand in rigorously anhydrous CCl_4. The complex was isolated in good yield (*ca* 50%) by filtration, washing with CCl_4 and drying *in vacuo*. The white precipitate formed has been characterised by infrared spectroscopy, ^{1}H and $^{31}P\{^{1}H\}$ NMR spectroscopy.

Infrared spectroscopy on the complex $[(SbCl_5)_2(Ph_2P(O)CH_2P(O)Ph_2)]$ reveals two features in the far infrared region assigned to the Sb-Cl stretching modes of an $SbCl_5$ unit, profile and frequencies similar to the monodentates. A strong, broad peak *ca.* 1044cm^{-1} in the nujol IR spectra confirmed the presence of the coordinated diphosphine dioxide ligand, shifted from *ca.* 1187cm^{-1} [34] for the uncoordinated ligand. There are no resonances attributable to un-coordinated P=O.

The $^{31}P\{^{1}H\}$ NMR spectrum of $[(SbCl_5)_2(Ph_2P(O)CH_2P(O)Ph_2)]$ obtained in $CH_2Cl_2/CDCl_3$ at room temperature reveals a sharp singlet at δ 53. This value is considerably shifted from the resonance of the un-coordinated $Ph_2P(O)CH_2P(O)Ph_2$ (δ 25)[37]. The ^{1}H NMR spectra were recorded in anhydrous $CDCl_3$. There are no resonances attributable to 'free' ligand. However, it is apparent that the $SbCl_5$ complexes of the phosphine oxides are considerably unstable in solution, and partial dissociation of the complex $[(SbCl_5)_2(Ph_2P(O)CH_2P(O)Ph_2)]$ is observed in the ^{1}H

NMR spectrum. This is indicated by the presence of a multiplet at δ 4.8 – 4.6. A triplet at δ 5.0 is revealed corresponding to $-CH_2-$, shifted in comparison to the 'free' ligand (δ 3.5). The triplet and multiplet integrate as 1:10 with the phenyls as expected. On the basis of these data it is concluded that the structure is a ligand bridged dimer.

Figure 3.15 Diagram of the proposed structure of $[Ph_2P(O)CH_2P(O)Ph_2(SbCl_5)_2]$.

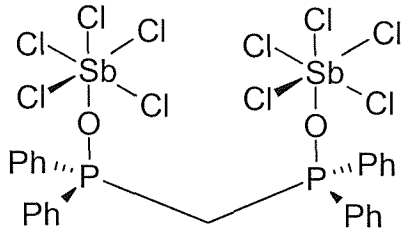

Reaction of one molar equivalent of $Ph_2As(O)CH_2As(O)Ph_2$ with two molar equivalents of $SbCl_5$ in CCl_4 formed a white precipitate. A shift in ν(As-O) from 'free' ligand (890 cm^{-1})[30] to coordinated ν(As-O) (849 cm^{-1}) is observed in the infrared spectra. There is also no evidence for free $Ph_2As(O)CH_2As(O)Ph_2$. The ^1H NMR spectrum reveals a multiplet at δ 8.0 – 7.5, a singlet at δ 4.7 corresponding to CH_2 in the complex and a singlet at δ 3.6 corresponding to CH_2 in free ligand. On the basis of these results it is suggested that the complex undergoes partial hydrolysis in solution.

Efforts to grow good quality crystals of these systems, suitable for X-ray diffraction proved unsuccessful, therefore further work on these complexes is required enabling full characterisation.

3.2.3.3 Sb(V) – Tertiary Phosphine Sulfide and Selenide Complexes

The complex $[SbCl_5(SPPh_3)]$ was prepared by the reaction of one molar equivalent of $SbCl_5$ in anhydrous CCl_4 with one molar equivalent of Ph_3PS in CH_2Cl_2, at room temperature producing a white precipitate which was filtered and washed with CCl_4. Initial attempts to react $SbCl_5$ with Ph_3PSe at room temperature in anhydrous CCl_4 formed a red solid or orange gum, possibly indicating fragmentation of the Ph_3PSe ligand releasing selenium. In order to circumvent this the reaction of $SbCl_5$ with one molar equivalent of Ph_3PSe, both in anhydrous CCl_4 was conducted at ice

temperature forming a white precipitate. The reaction was undertaken at ice temperature to control the kinetics, thus preventing the cleavage of the P-Se bond. The solids were obtained in moderate yield, by washing with CCl_4, filtration and drying *in vacuo*. Due to the extreme air/moisture sensitivity of the complexes formed the samples were manipulated in a dry-nitrogen purged glove box. The $[SbCl_5(SPPh_3)]$ adduct was stored in the dry-box, however $[SbCl_5(SePPh_3)]$ was stored in the freezer.

Infrared spectroscopy of both complexes showed a reduction in υ(P-S) = 544 cm^{-1} and υ(P-Se) = 507 cm^{-1} respectively, compared with υ(PS) = 637 cm^{-1} and υ(PSe) = 561 cm^{-1} in the free ligands [31]. The P-S stretching mode for $[SbCl_5(Ph_3PS)]$ compares with the literature value 536cm^{-1}. [24] Due to poor resolution only one infrared band is observed for the stretching modes corresponding to υ(Sb-Cl) (341 cm^{-1} for $[SbCl_5(SPPh_3)]$) and (339 cm^{-1} for the reaction of 1:1 Ph_3PSe: $SbCl_5$).

The $^{31}P\{^1H\}$ NMR spectrum of $[SbCl_5(SPPh_3)]$ at room temperature shows a singlet at δ 66, which is shifted to significantly high frequency in comparison to free ligand (δ 43),[35] suggesting coordination of the ligand to the Sb(V) metal centre. However, the $^{31}P\{^1H\}$ NMR spectrum of the $SbCl_5$ complex of Ph_3PSe shows a singlet at δ 37, this is little shifted compared to free ligand (δ 36),[35] suggesting that the complex is very labile and extensive dissociation occurs in solution.

3.3 Conclusions

The crystal structures of $[MCl_3([8]aneSe_2)]$ (M = As or Sb) reveal ladder structures comprising Cl-bridged planar M_2Cl_6 units bridged by selenoether ligands with the Se atoms (unusually) occupying mutually *trans* coordination sites. Comparison of the bond length and angle distributions in these structures with those of the heavier and structurally similar Bi(III) homologue reveals a rather unexpected and irregular trend in lone pair activity. The M-based lone pair is essentially stereochemically inactive in both the Bi and the As complexes, whereas in the Sb analogue the lone pair is apparently stereochemically active and directional, located in the region of the Se-Sb-Cl (bridging) plane.

A range of complexes of the form $[SbCl_5(L)]$ and $[(SbCl_5)_2L]$ have been formed. The complexes $[SbCl_5(OPMe_3)]$, $[SbCl_5(OPPh_3)]$ and $[SbCl_5(SPPh_3)]$ are known in the literature, however characterisation is limited to X-ray structural determinations or infrared spectroscopy. The latter were reported in the 1960's and ^1H and $^{31}P\{^1H\}$ NMR spectroscopic data were not presented. The formation of these complexes is not trivial, $SbCl_5$ and the complexes formed are very hydrolytically unstable. The aim of this study was to review the methodology employed in the synthesis of these complexes and to modify this technique to permit the preparation of a range of $SbCl_5$ complexes of bidentate phosphine and arsine oxides, and phosphine chalcogenides. This has been achieved, and the methods form the basis of further studies into this area, eventually including thio- and seleno-ether ligands and the parent phosphine and arsine ligands.

3.4 Experimental

Infrared spectra were recorded as Nujol mulls between CsI plates, using a Perkin Elmer 983G spectrometer over the range 200-4000 cm^{-1}. ^1H NMR spectra were obtained in $CDCl_3$ using a Bruker AM300 spectrometer operating at 300 MHz, while $^{31}P\{^1H\}$ and $^{77}Se\{^1H\}$ spectra were recorded on a Bruker DPX400 spectrometer operating at 162 and 149 MHz respectively and are referenced to external 85% H_3PO_4 and neat external Me_2Se respectively. Microanalyses were performed by the University of Strathclyde Microanalytical Laboratory. Antimony(V) chloride was obtained from Aldrich and used as received. Ph_3PSe[36], $Ph_2P(O)CH_2P(O)Ph_2$[37] and $Ph_2As(O)CH_2As(O)Ph_2$ were synthesised according to the literature procedures. All other ligands had been previously synthesised by other members of the research group, or obtained from Aldrich. Standard Schlenk techniques were used throughout, and all preparations and manipulations were performed under a N_2 environment, using rigorously anhydrous solvents (CH_2Cl_2 and CCl_4 distilled from CaH_2). Isolated yields were at typically 60-70% in each case. The ligands were dried *in vacuo* before use, $SbCl_5$ and isolated solids were stored in an N_2-filled glove box.

3.4.1 Preparations

Ph_3PSe[36] Freshly ground elemental selenium (1.023 g, 13 mmol) was added to a solution of triphenylphosphine (2.038 g, 7.78 mmol) in THF (35 cm^3). The reaction mixture was stirred for 24 hours and filtered. The product was subsequently recrystallised from THF. $^{31}P\{^1H\}$ NMR spectrum ($CH_2Cl_2/CDCl_3$, 300K): δ 36 (*s*). ^1H NMR spectrum ($CDCl_3$, 300K): δ 7.3-7.8 (*m*). IR/cm^{-1}: 569 (P=Se).

$Ph_2P(O)CH_2P(O)Ph_2$[37] A solution of $Ph_2PCH_2PPh_2$ (1.152 g, 3 mmol) in $CHCl_3$ (20 cm^3) was treated with a solution of diodine (1.523 g, 6 mmol) in $CHCl_3$ (5 cm^3). After stirring (24 hrs, room temperature), the solution was transferred to a separating funnel and shaken with aqueous 2M NaOH (20 cm^3). The organic phase was separated and the $CHCl_3$ removed *in vacuo*. The oil produced was recrystallised from $CHCl_3$/ EtOH to a crystalline solid. $^{31}P\{^1H\}$ NMR spectrum ($CH_2Cl_2/CDCl_3$, 300K): δ 26 ppm. ^1H NMR spectrum ($CDCl_3$, 300K): δ 7.2-7.8 (*m*), δ 3.5 (*t*). IR/cm^{-1}: 1187 (P=O).

$Ph_2As(O)CH_2As(O)Ph_2$ A solution of $Ph_2AsCH_2AsPh_2$ (2.0 g) in $CHCl_3$ (20 cm^3) was treated with a solution of diodine (2.15 g, 8.4 mmol) in $CHCl_3$ (5 cm^3). After stirring (24 hrs, room temperature), the solution was transferred to a separating funnel and shaken with aqueous 2M NaOH (20 cm^3). The organic phase was separated, dried over magnesium sulphate and the $CHCl_3$ removed *in vacuo*. ^1H NMR spectrum ($CDCl_3$, 300K): δ 7.3 – 7.9 (*m*), 3.5 (*s*, CH_2). IR/ cm^{-1}: 890 (As=O).

$[SbCl_5(OPPh_3)]$[23] Ph_3PO (0.278 g, 1 mmol) was dissolved in rigorously anhydrous CCl_4 (10cm^3) under an atmosphere of dry N_2 and the solution further degassed. $SbCl_5$ (0.299 g, 1 mmol) in CH_2Cl_2 (5 cm^3) was added to the ligand solution and stirred, forming a white precipitate, which was filtered, washed with CCl_4 and dried *in vacuo*. $^{31}P\{^1H\}$ NMR spectrum ($CH_2Cl_2/CDCl_3$, 300K): δ 47 (*s*). ^1H NMR spectrum ($CDCl_3$, 300K): δ 7.5-8.0 (*m*).

[$SbCl_5(OPMe_3)$][21] Method as for [$SbCl_5(OPPh_3)$], but using Me_3PO. A white precipitate formed, which was filtered, washed with CCl_4 and dried *in vacuo*. $^{31}P\{^1H\}$ NMR spectrum ($CH_2Cl_2/CDCl_3$, 300K): δ 71 (*s*). ^1H NMR spectrum ($CDCl_3$, 300K): δ 2.0 (*d*).

[$SbCl_5(OAsPh_3)$].1/2CH_2Cl_2 Method as for [$SbCl_5(OPPh_3)$], but using Ph_3AsO. A white precipitate formed, which was filtered, washed with CCl_4 and dried *in vacuo*. Calc. for $C_{18}H_{15}AsOSbCl_5.1/2CH_2Cl_2$: C, 34.8 H, 2.4 %; Found: C, 33.4 H, 2.2 % .^1H NMR spectrum ($CDCl_3$, 300K): δ 7.6 – 8.0 (*m*).

[$SbCl_5(OPMePh_2)$] Method as for [$SbCl_5(OPPh_3)$], but using Ph_2MePO. A white precipitate formed, which was filtered, washed with CCl_4 and dried *in vacuo*. Calc. for $C_{13}H_{13}Cl_5OPSb$: C, 30.3; H, 2.5 %, Found: C, 29.5; H, 2.8 %. $^{31}P\{^1H\}$ NMR spectrum ($CH_2Cl_2/CDCl_3$, 300K): δ 52 (*s*). ^1H NMR spectrum ($CDCl_3$, 300K): δ 7.5-8.0 (*m*, 10H, Ph_2), 2.7 (*d*, 3H, CH_3).

[$Ph_2P(O)CH_2P(O)Ph_2(SbCl_5)_2$].$CCl_4$ $Ph_2P(O)CH_2P(O)Ph_2$ (0.2 g, 0.5 mmol) was dissolved in CCl_4 (10 cm^3) under an atmosphere of dry N_2 and the solution further degassed. $SbCl_5$ (0.3 g, 1 mmol) in CCl_4 (5 cm^3) was added to the ligand solution and stirred. A white precipitate formed, which was filtered, washed and dried *in vacuo*. Calc. for $C_{25}H_{22}Cl_{10}O_2P_2Sb_2.CCl_4$: C,26.7; H,1.9 %, Found C, 26.4; H, 1.9 %. $^{31}P\{^1H\}$ NMR spectrum ($CH_2Cl_2/CDCl_3$, 300K): δ 53 ppm (*s*). ^1H NMR spectrum ($CDCl_3$, 300K): δ 7.4-8.1 (*m*), 5.0 (*t*), 4.58-4.81 (*m*). IR/cm^{-1}: 346 (br), 361 (sh) (Sb-Cl).

Reaction of $Ph_2As(O)CH_2As(O)Ph_2$ with $SbCl_5$ Method as for [$Ph_2P(O)CH_2P(O)Ph_2(SbCl_5)_2$], but using $Ph_2As(O)CH_2As(O)Ph_2$. An off-white precipitate was formed, which was filtered, washed with CCl_4 and dried *in vacuo*. ^1H NMR spectrum ($CDCl_3$, 300K): δ 8.0-7.5 (*m*), 4.7 (*s*), 3.6 (*s*) ppm. IR/cm^{-1}: 849 (As=O), 365 (sh), 343 (br) (Sb-Cl).

[$SbCl_5(SPPh_3)$][24] Ph_3PS (100 mg, 0.34 mmol) was dissolved in CH_2Cl_2 (10 cm^3) under an atmosphere of dry N_2 and the solution further degassed. $SbCl_5$ (101 mg, 0.34 mmol) in CCl_4 (5 cm^3) was added forming a yellow solution. On stirring (10 minutes) a white solid formed, which was filtered and dried *in vacuo*. Calc. for $C_{18}H_{15}Cl_5PS_1Sb.CCl_4$: C,

30.5; H, 2.0 %, Found: C, 30.8; H, 2.9 %. $^{31}P\{^{1}H\}$ NMR spectrum ($CDCl_3$, 300K): 67 ppm (*s*). ^{1}H NMR spectrum ($CDCl_3$, 300K): δ 7.7-8.8 (*m*). IR/cm^{-1}: 544 (P=S), 341 (br) (Sb-Cl).

Reaction of Ph_3PSe with $SbCl_5$ Ph_3PSe (100 mg, 0.29 mmol) was dissolved in CCl_4 (10 cm^3) under an atmosphere of N_2 and the solution further degassed and cooled to 0°C. A solution of $SbCl_5$ (87 mg, 0.29 mmol) in CCl_4 (5 cm^3) at 0°C was added forming a yellow solution. After stirring (10 minutes) an off-white solid formed which was filtered and dried *in vacuo*. $^{31}P\{^{1}H\}$ NMR spectrum ($CH_2Cl_2/CDCl_3$, 300K): δ 38 (*s*). ^{1}H NMR spectrum: δ 7.3-7.8 (*m*). IR/cm^{-1}: 507 (P=Se), 339 (Sb-Cl).

3.5 References

[1] N. W. Alcock., *Adv. Inorg. Chem. Radiochem.*, 1972, **15**, 1.

[2] P.Pyykko, *Chem. Rev.*, 1997, **97**, 597.

[3] C. K. Prout and J. D. Wright, *Angew. Chem., Int. Ed. Engl.*, 1968, **7**, 659.

[4] C. J. Carmalt and N. C. Norman, in *The Chemistry of Arsenic, Antimony and Bismuth*, N. C. Norman, ed., Blackie, London, 1998, ch. 1.

[5] N. H. Hill, W. Levason, and G. Reid, *Inorg. Chem.*, 2002, **41**, 2070.

[6] W. Levason and G. Reid, *J. Chem. Soc., Dalton Trans.*, 2001, 2953

[7] N.J. Hill, PhD Thesis, University of Southampton, 2002.

[8] A. J. Barton, N. J. Hill, W. Levason and G. Reid, *J. Am. Chem. Soc.*, 2001, **123**, 11801.

[9] A. J. Barton, N. J. Hill, W. Levason, B. Patel and G. Reid, *Chem. Commun.*, 2001, 95.

[10] G. R. Willey, M. T. Lakin, M. Ravindran and N. W. Alcock, *J. Chem. Soc., Chem Commun.*, 1991, 271.

[11] G. R. Willey, M. T. Lakin and N. W. Alcock, *J. Chem. Soc., Dalton Trans.*, 1992, 591.

[12] G. R. Willey, M. T. Lakin and N. W. Alcock, *J. Chem. Soc., Dalton Trans.*, 1992, 1339.

[13] A. J. Blake, D. Fenske, W-S. Li, V. Lippolis and M. Schröder, *J. Chem. Soc., Dalton Trans.*, 1998, 3961.

[14] A. R. J. Genge, W. Levason, and G. Reid, *Chem. Commun.*, 1998, 2159.

[15] A. J. Barton, A. R. J. Genge, W. Levason and G. Reid, *J. Chem. Soc., Dalton Trans.*, 2000, 859.

[16] A. J. Barton, A. R. J. Genge, W. Levason and G. Reid, *J. Chem. Soc., Dalton Trans.*, 2000, 2163.

[17] W. Levason, N. J. Hill and G. Reid, *J. Chem. Soc., Dalton Trans.*, 2002, 4316.

[18] F. A. Cotton and G. Wilkinson, *Advanced Inorganic Chemistry*, 5th Edition., Wiley-Interscience, New York, 1988.

[19] V. A. T. Mohammed and U. Műller, *Acta Crystallogr., Sect. C*, 1985, **41**, 329; J. Kaub and W. S. Sheldrick, *Z. Naturforsch. B*, 1984, **39**, 1252; W. Czado, S. Rabe and U. Műller, *Z. Naturforsch. B*, 1999, **54**, 288; U. Eisinger, W. Schwarz and A. Schmidt, *Z. Naturforsch. B*, 1982, **37**, 1584; B. Jaschinski, R. Blachnik and H. Reuter, *Z.*

Naturforsch. B, 1998, **53**, 565; N. Alcock, M. Ravindran and G. R. Willey, *J. Chem. Soc., Chem. Commun.*, 1989, 1063.

[20] I. Lindquist and C. I. Branden, *Acta Crystallogr.,* 1959, **12**, 642.

[21] C. I. Branden and I. Lindquist, *Acta. Chem. Scand.*, 1961, **15**, 167.

[22] I. Lindqvist and G. Olofsson, *Acta. Chem. Scand.*, 1959, **13**, 1753.

[23] B. Neumüller, R. Meyer zu Kőcker and K. Dehnicke, *Z. Kristallogr.*, 1994, **209**, 90.

[24] W. Van Der Veer and F. Jellinek, *Rec. Trav. Chim. Pays. Bas.*, 1966, **85**, 843.

[25] L. Brun and C. I. Branden, *Acta Crystallogr.*, 1966, **20**, 749.

[26] A. Schmidpeter and H. Noth, *Inorg. Chim. Acta.*, 1998, **269**, 7.

[27] J. Yamamoto, S. Ito, T. Tsuboi, T. Tsuboi and K. Tsukihara, *Bull. Chem. Soc. Jpn*, 1985, **58**, 470.

[28] R. J. Holliday, R. W. Broach, L. B. Handy, A. W. Cordes and L. Thomas, *Inorg. Chem.*, 1972, **11**, 1849.

[29] D. H. Williams and I. Fleming, *Spectroscopic Methods in Organic Chemistry.*, McGraw-Hill, London, 1995.

[30] D. J. Phillips and S. Y. Tyree, *J. Am. Chem. Soc.*, 1961, **83**, 1806.

[31] D. G. Gilheany, in *The Chemistry of Organophosphorus Compounds*, ed. F. R. Hartley, Wiley, New York, 1992, Volume 2.

[32] J. Koketsil and Y. Ihsii, *Bull. Chem. Soc.*, 1970, 2527.

[33] T. E. Műller, J. C. Green, D. M. P. Mingos, C. M. McPartlin, C. Whittingham, D. J. Williams and T. M. Woodroffe, *J. Organomet. Chem.*, 1998, **551**, 313.

[34] J. J. Richard, K. E. Burke, J. W. O'Laughlin and C. V. Banks, *J. Amer. Chem. Soc.*, 1961, **83**, 1722.

[35] T. A. Albright, W. J. Freeman and E. E. Schweizer, *J. Org. Chem.*, 1975, **40**, 3437.

[36] S. R. Foley and D. S. Richeson, *Chem. Commum.*, 2000, 1391.

[37] S. Bittner, M. Pomerantz, Y. Ascaf, P. Krief, S. Xi amd M. K. Witczak. *J. Org. Chem.*, 1988, **53**, 1.

CHAPTER 4

Catalytic Air Oxidation of Arylphosphines in the Presence of Tin(IV) Iodide

4.1 Introduction

To-date, a number of oxidants have been developed to effect the selective oxidation of P and S heteroatoms, and the most commonly used oxidants are summarised here. Looking first at phosphines, the most obvious route is air oxidation of a phosphine reagent. Tertiary phosphine oxides can be prepared by refluxing a solution of the phosphine in air.[1] Nickel(II) halides form complexes with diphosphines, which are stable in the solid state, but decompose slowly if heated above 220°C, undergoing air oxidation, to yield the diphosphine dioxide.[2]

Although dioxygen is a thermodynamically potent oxidant, its reactions are both slow and unselective. Hence catalysis of the reactions of O_2 by transition metals has been widely used to overcome these problems (Figure 4.1).[3] There are numerous well-characterised examples of catalysts that involve formation of a terminal oxo moiety by reaction of O_2 with a reduced metal centre, these catalysts transfer oxygen atoms from the oxometal complex to the substrate. For example, on stirring PPh_3 with nickelocene in benzene in the presence of oxygen gives Ph_3PO in 90% yield.[4] Ph_3P is also reported to be converted quantatively into its oxide by treatment with oxygen in the presence of $Ph_4P^+Cl^-$, whereas in the absence of the catalyst the reaction fails.[5]

Figure 4.1 Oxygen Atom Transfer-Based Strategy for Catalysed Air Oxidations.

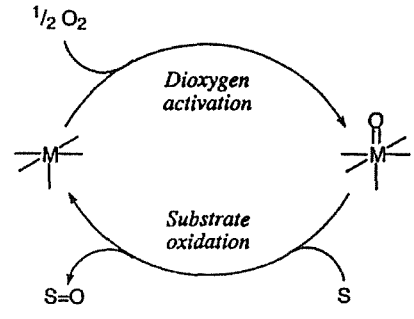

The number of examples that combine both processes at reasonable rates is low. Both thermodynamics and kinetics must be considered. Thermodynamically, to allow

dixoygen activation and substrate oxidation, the strength of the metal-oxygen bond must be strong enough to be formed exothermically from O_2, but not so strong that substrates cannot be oxidised. Kinetically, dioxygen is an electron-poor substance that reacts most favourably with electron rich metal centres, however the reactivity of oxometal complexes in oxygen atom transfer reactions is dependant on the electrophilic character in its oxidised form. The catalyst trimesityliridium(III) strikes a balance between the nucleophillic character in its reduced form and the electrophilic character in its oxidised form.[6] Oxotrimesityliridium(V) is quantatively reduced by triphenylarsine and by a variety of triaryl phosphines to give homoleptic trimesityliridium(III) and the corresponding arsine or phosphine oxide.

Figure 4.2 Proposed mechanism for $(mes)_3Ir{=}O$ catalysed aerobic oxidation of triphenylphosphine.[6]

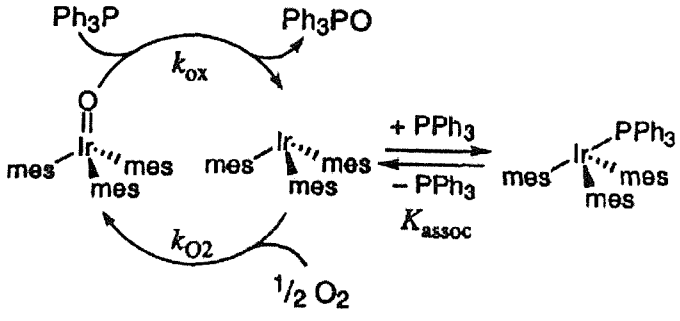

Other transition metals platinum(0),[7] cobalt(II)[8] and iridium(I),[9] in appropriate systems, can promote air oxidation of phosphines to phosphine oxides, in these cases it is likely that the metal-dioxygen complexes are intermediates. For example, the catalytic oxidation of triphenylphosphine *via* $[Pt(PPh_3)_3]$[7] may be depicted as:

$$Pt(PPh_3)_3 + O_2 \longrightarrow Pt(PPh_3)_2O_2 + PPh_3$$

$$Pt(PPh_3)_2O_2 + PPh_3 \longrightarrow [Pt(PPh_3)_3O_2] \longrightarrow Pt(PPh_3)_3 + 2Ph_3PO$$

The oxidation of triphenylphosphine may be catalysed by Vaska complexes ($[IrX(CO)(PPh_3)_2]$ (X = Cl, Br or I)) to afford triphenylphosphine oxide.[9] The catalyst is recovered without decomposition after the reaction. The oxidation reactions were

carried out under conditions where a homogenous solution of triphenylphosphine and the iridium complex in a solvent such as benzene are heated with a constant bubbling of oxygen for 8 hours. For Vaska type complexes the yield of the triphenylphosphine oxide increases in the order: X = Cl<I<Br. The fact that the Vaska complexes coordinate with the oxygen molecule easily under oxygen atmosphere suggests that the oxidation reaction occurs *via* an Ir-O_2 complex. Studies[10] show that the Vaska complex-catalysed oxidation may proceed through the coordination of both oxygen and triphenylphosphine to iridium (I).

Phosphines oxides may also be obtained *via* oxidation by a peroxy compound. Dimethylphosphine, on oxidation[11] with 7 % H_2O_2 at 20-30°C in the presence of 4 % HCl, gives the oxide in 96 % yield. $Ph_2P(O)CH_2P(O)Ph_2$ (Figure 4.3) may be prepared by oxidation of $Ph_2PCH_2PPh_2$ with H_2O_2 in acetone. Whilst this method of oxidation is effective there is a risk of explosion, thus requiring extreme care.

Figure 4.3 Hydrogen peroxide oxidation of DPPM.[12]

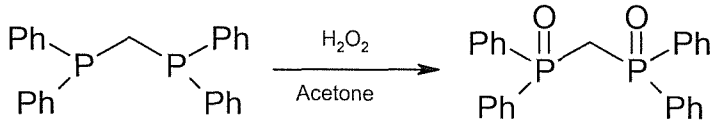

Phosphine oxides may also be synthesised *via* iodine oxidation and treatment with a strong base. For example the phosphine oxide *o*-$C_6H_4(P(O)Ph_2)_2$ is prepared by stirring *o*-$C_6H_4(PPh_2)_2$ and I_2 in chloroform followed by base hydrolysis.[13]

Compounds containing a sulfoxide moiety ($R_2S=O$) are useful synthetic molecules for the construction of various chemically and biologically significant molecules.[14] Despite myriad of oxidants that convert sulfides to the corresponding sulfoxides, most reagents require careful control of the reaction conditions, including the quantity of the oxidant, to minimise the formation of sulfones (R_2SO_2) as side products.[15] A variety of methods exist for the oxidation of sulfides to sulfoxides. The use of H_2O_2 as a terminal oxidant utilises hexafluoropropan-2-ol[16] as the catalytic solvent for efficient sulfoxidations. Tetrabromoaurate(III)[17] is a catalyst for the

oxidation of sulfides by nitric acid in a biphasic system. The combination of mercury(II) oxide/iodine[18] serves as a good oxidising agent of sulfides. Methyltrioxorhenium (CH_3ReO_3) is an effective catalyst for reactions in which a substrate, X, usually an electron-rich species (X = R_2S, PhSR, Ph_2S) is oxidised to XO by hydrogen peroxide:

$$X + H_2O_2 \longrightarrow XO + H_2O$$

In these reactions an oxygen atom is transferred from peroxide to the substrate. In studying the oxidation of the alkyl and aryl sulfides (X = R_2S, PhSR, Ph_2S) to sulfoxides, it was noted that further oxidation to sulfones ensued over longer periods of time.[19] Benzyltriphenylphosphonium peroxymonosulfate can also be used for the selective oxidation of aromatic and aliphatic sulfides and thiols to their corresponding sulfoxides and disulfides under nonaqueous and aprotic conditions without a catalyst.[20]

Figure 4.4 A scheme to show the oxidation of alkyl/aryl sulfides using benzyltriphenylphosphonium peroxymonosulfate.[20]

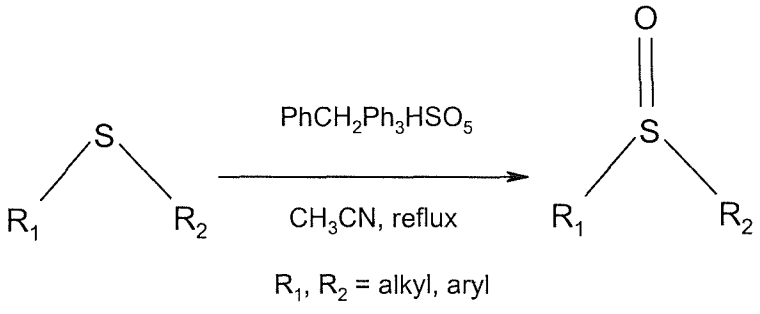

In recent years, hypervalent iodine-containing reagent systems have been employed to oxidise various organic substrates with or without a catalyst.[21] A method for the selective oxidation of sulfides to sulfoxides with periodic acid (H_5IO_6) catalysed by $FeCl_3$ in MeCN has been devised. For example, PhMeS is converted to PhMeSO.[22]

Figure 4.5 A scheme to show the transformation of sulfides into sulfoxides.[22]

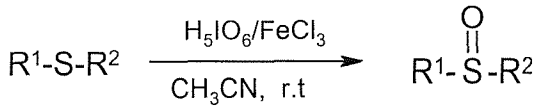

4.1.1 Aim of the Study

Triarylphosphines are usually air-stable in solid state and in solution in common organic solvents. During recent studies of tin(IV) phosphine complexes in the Southampton laboratories, it was observed that the complexes were often contaminated with the corresponding phosphine oxide unless rigorously anhydrous solvents and dry-box techniques were used. The oxidation reactions appeared particularly facile with tin(IV) iodide, and from SnI_4 and *o*-$C_6H_4(PPh_2)_2$ in dry CH_2Cl_2 solution the complex [SnI_4(*o*-$C_6H_4(P(O)PPh_2)_2$] was obtained, which was thoroughly characterised both by single-crystal X-ray diffraction and by comparison of its spectroscopic properties with a sample made directly from o-$C_6H_4(POPh_2)_2$.[13] The promotion of the oxidation by p-block metal halides was unexpected and the following work was undertaken to investigate the reaction in more detail. It also provides further examples of these oxidations occurring in SnI_4-arylphosphine systems. Recent studies have also shown that during crystallisation of the complex [SnI_4{$MeS(CH_2)_3SMe$}], oxidation of the ligand occurs forming $MeS(O)(CH_2)_3SMe$ in the complex *cis*-[SnI_4{η^1-*O*-$MeS(CH_2)_3SMe$}$_2$].[23] Therefore studies were also undertaken on the oxidation of the sulfur moiety.

4.2 Results and Discussion

4.2.1 Oxidation of Phosphine Ligands

The initial studies were carried out in 10 mm NMR tubes containing anhydrous CH_2Cl_2 with *o*-$C_6H_4(PPh_2)_2$ and SnI_4 in a (1) 1:1 molar ratio and (2) *ca.* 50:1 molar ratio and (3) as a control a solution of *o*-$C_6H_4(PPh_2)_2$ alone. The tubes were filled with dry nitrogen and monitored by $^{31}P\{^1H\}$ NMR spectroscopy; over a period of a few days no reaction occurred in any of the tubes. The tubes were then filled with dry oxygen and again monitored. Over the period of the experiment there was no change in the spectrum obtained from tube (3) containing only the diphosphine (δ –13). However, NMR studies of tube (2) show that over time the initial free diphosphine resonance decreases and a resonance at δ +31 becomes apparent. The NMR shift is consistent with the diphosphine dioxide, *o*-$C_6H_4(POPh_2)_2$[13] which after 1 day was the only phosphorus species present. In tube (1) no $^{31}P\{^1H\}$ NMR resonance was initially

observed since the complex [SnI_4(*o*-$C_6H_4(PPh_2)_2$)] undergoes rapid reversible ligand dissociation in solution at room temperatures, however when the solution is cooled to 190K a resonance for this complex is observed at δ –52.5. However, after 1 day a resonance at δ +39.8 attributable to [SnI_4(*o*-$C_6H_4(P(O)Ph_2)_2$)][13] was present, and after 5 days orange solid [SnI_4(*o*-$C_6H_4(P(O)Ph_2)_2$)] had precipitated from solution.

Reaction of Ph_3P in CH_2Cl_2 in the presence of a small crystal of SnI_4 was cleanly converted into Ph_3PO over a few days. Reaction of $Ph_2P(CH_2)_2PPh_2$ was also cleanly converted to $Ph_2P(O)CH_2CH_2P(O)Ph_2$. The $^{31}P\{^1H\}$ NMR resonances and ν(P-O) IR shifts are consistent with the literature (Table 4.1). The $^{31}P\{^1H\}$ NMR spectrum shows no other phosphorus containing species. A solution of Ph_3As in CH_2Cl_2 in the presence of a small crystal of SnI_4 was not converted into the corresponding oxide, the IR spectrum of the white solid did not show any evidence for ν(As=O), which occurs at 879 cm^{-1} for Ph_3AsO.[24]

Table 4.1 $^{31}P\{^1H\}$ NMR Spectroscopy Data for the Phosphine Oxides.

Phosphine Oxide	**$^{31}P\{^1H\}$ Free Ligand (δ)[a]**	**$^{31}P\{^1H\}$ Phosphine Oxide (δ)[a] obtained**	**$^{31}P\{^1H\}$ Phosphine Oxide (δ)[a] Literature Values**
Ph_3PO	-6[6]	+29	+29[25]
$Ph_2P(O)CH_2CH_2P(O)Ph_2$	-13[26]	+33	+33[27]
o-$C_6H_4(P(O)Ph_2)_2$	-13[13]	+31	+33[13]

a. relative to external 85% H_3PO_4 in CH_2Cl_2

Table 4.2 ν(P=O) Stretches for the Phosphine Oxides.

Phosphine Oxide	ν(P=O)/ cm^{-1} Phosphine Oxide Obtained	ν(P=O)/ cm^{-1} Phosphine Oxide, Literature Values
$Ph_3P^{16}O$	1193	1195[28]
$Ph_3P^{18}O$	1157	1148[a]
$Ph_2P(O)CH_2CH_2P(O)Ph_2$	1177	1175[29]

a = value calculated using the simple diatomic oscillator model.

The mechanism of the reactions that occur for phosphine oxidation *via* SnI_4 catalysis is unclear, and to probe the mechanism further, the reaction of a solution of Ph_3P in CH_2Cl_2 in the presence of SnI_4 was attempted using $^{18}O_2$ under rigorously anhydrous conditions. Both IR spectroscopy and EI mass spectrometry proved that $Ph_3P^{18}O$ is formed exclusively. The vibration frequency ν for a diatomic molecule A-B may be expressed as:

$$4\pi^2\nu^2 = F\left(\frac{1}{mA} + \frac{1}{mB}\right)$$

Where, F is a constant independent of isotopic mass. From that it follows that an isotopically substituted species A'-B', the corresponding frequency ν' is given by:

$$\left(\frac{V'}{V}\right)^2 = \left(\frac{1}{mA'} + \frac{1}{mB'}\right)/\left(\frac{1}{mA} + \frac{1}{mB}\right)$$

Therefore, using the simple diatomic oscillator model we predict ν(P=O) as 1148 cm-^{1}. The slightly higher value observed is a result of coupling with ν(P-C) at lower frequency.

The EI mass spectrum for $Ph_3P^{18}O$ (Figure 4.5) displays a peak at *m/z* 279 which corresponds to $[Ph_3P^{18}O\text{-}H]$; $Ph_3P^{16}O$ displays a peak at *m/z* 277 which corresponds to $[Ph_3P^{16}O\text{-}H]$[30], a theoretical EI mass spectrum is also displayed (Figure 4.6). From the EI mass spectroscopy data it is apparent than in these reactions,

air/dioxygen is the source of oxygen as opposed to water, but the mechanism is still unclear. The weak Lewis acidity of the SnI_4 may promote the oxidation, along with the extensive dissociation of the tin(IV) iodide complexes formed allowing the reaction to cycle, enabling the use of catalytic amounts of SnI_4. Although oxidation occurs for the other SnX_4 (where X = Cl, Br), the stronger Lewis acidity of these precipitate the complexed oxidised ligand, thus removing tin(IV) from the reaction.

Figure 4.5 View of the EI Mass Spectrum of $Ph_3P^{18}O$

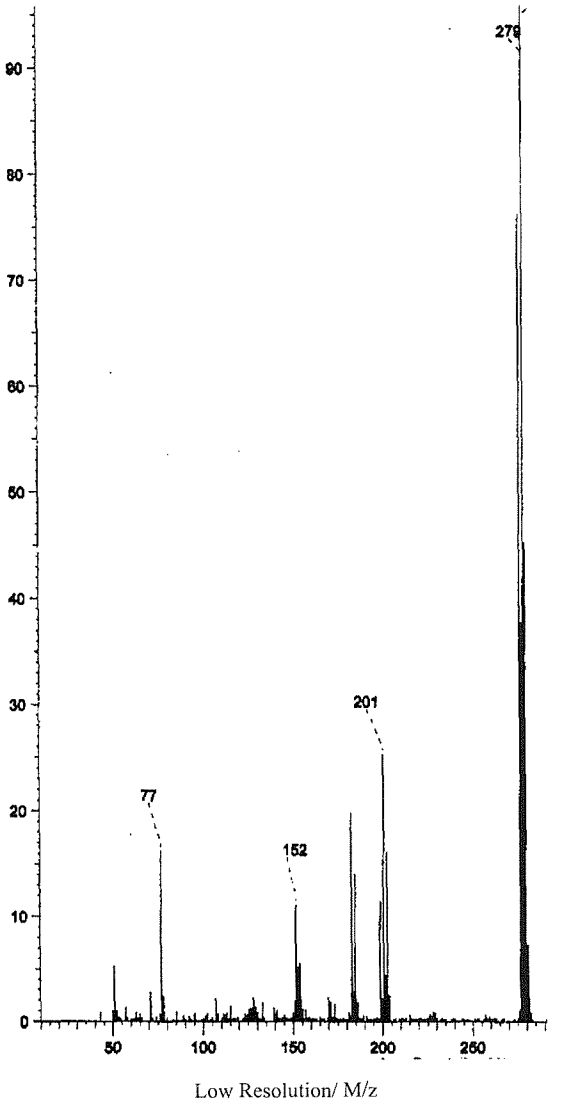

Figure 4.6 View of the simulated EI mass spectrum for $Ph_3P^{18}O$.

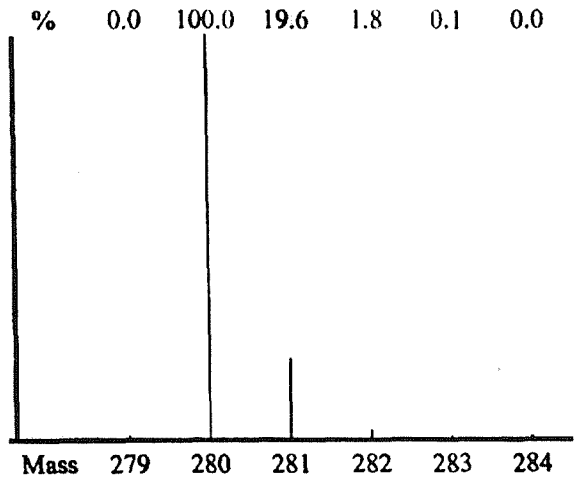

4.2.2 Attempted Oxidation of Thioether Ligands

The oxidation of mono- and bi-dentate thioethers was also attempted. A solution of one molar equivalent of Me_2S with one molar equivalent of SnI_4 in CH_2Cl_2 under O_2 was not oxidised to the corresponding sulfoxide over a period of three weeks. Due to the extreme volatility of Me_2S and the method employed for the work up procedure, the ^1H NMR of the solution was free from any resonance corresponding to free Me_2S. No strong bands in the range 900 – 1200 cm^{-1} were present in the IR spectrum as have been reported in complexes incorporating sulfoxide (S=O) functions. Specifically for the complex $[SnI_4(Me_2SO)_2]$ ν(S-O) occurs at 928 cm^{-1}.[31] A solution of one molar equivalent of $MeS(CH_2)_3SMe$ with two molar equivalents of SnI_4 in CH_2Cl_2 was also not converted. The ^1H NMR spectrum of the solution is little shifted compared to that of free ligand.[32]

4.2.3 Conclusion

Arylphosphines including Ph_3P, *o*-$C_6H_4(PPh_2)_2$ and $Ph_2PCH_2CH_2PPh_2$ are cleanly and quantatively converted into the corresponding phosphine oxides on reaction with dry air or dioxygen in CH_2Cl_2 solution in the presence of catalytic amounts of SnI_4. A detailed examination of the $^{31}P\{^1H\}$ NMR spectroscopy, IR spectroscopy and in some cases EI mass spectrometry has been presented. The triarylarsine Ph_3As, was not converted to the respective arsine oxide under similar conditions, and the IR

spectrum revealed bands consistent with free ligand. The results also confirmed that the thioethers, Me_2S and $MeS(CH_2)_3SMe$ were also not converted to the corresponding oxides.

4.3 Experimental

Infrared spectra were recorded as Nujol mulls between CsI plates, using a Perkin-Elmer 983G spectrometer over the range 180-4000 cm^{-1}. $^{31}P\{^1H\}$ spectra were obtained in anhydrous CH_2Cl_2 using a Bruker DPX400 spectrometer operating at 162 MHz and were referenced to external 85 % H_3PO_4. Mass spectra were run by low-resolution electron impact (EI) on a VG 70-SE Normal geometry double focusing spectrometer. SnI_4, Ph_3P, Ph_3PO, Ph_3As and Ph_3AsO were obtained from Aldrich and used as received. The diphosphines $Ph_2PCH_2CH_2PPh_2$, *o*-$C_6H_4(PPh_2)$ and their dioxides were synthesised according to the literature procedure.[13,33,34] $^{18}O_2$ was obtained from BOC. Schlenk techniques were used throughout and manipulations were performed under an N_2 atmosphere unless otherwise indicated. In all preparations rigorously anhydrous solvents were used (CH_2Cl_2 distilled from CaH_2). Isolated yields were typically 60 % in each case.

4.3.1 Preparations

NMR experiments (General procedure) A 10-mm OD NMR tube was charged with the phosphine (0.1 g), dry CH_2Cl_2 (4 cm^3) and an appropriate amount of SnI_4. The tube was purged with dry nitrogen, sealed and $^{31}P\{^1H\}$ spectrum recorded immediately. The tubes were then purged with dry O_2 and the $^{31}P\{^1H\}$ NMR spectrum recorded at set intervals.

Experiment 1: *o*-$C_6H_4(PPh_2)_2$ with a crystal of SnI_4. $^{31}P\{^1H\}$ NMR spectrum (CH_2Cl_2, 300K, Time=0): δ -13, (Time=24 hrs): δ -13, (Time= 5 days): δ +31.

Experiment 2: *o*-$C_6H_4(PPh_2)_2$ with a stoichiometric amount of SnI_4. $^{31}P\{^1H\}$ NMR spectrum (CH_2Cl_2, 300K, Time=24 hrs): δ + 39.8.

Experiment 3: *o*-$C_6H_4(PPh_2)_2$ (standard) $^{31}P\{^1H\}$ NMR spectrum (CH_2Cl_2, 300K, Time=0): δ –13, (Time=24 hrs): δ –13, (Time= 5 days): δ –13.

$Ph_3P^{16}O$ A solution of Ph_3P (1.0 g, 3.8 mmol) in CH_2Cl_2 (20 cm^3) was treated with a single small crystal of SnI_4 under an atmosphere of dry N_2. The gas atmosphere was then replaced by dry O_2 by flushing. On completion of the reaction the solution was transferred to a separating funnel and shaken with aq. NaCl solution (30 cm^3). The colourless organic phase was separated, dried over $MgSO_4$ and filtered. The solvent was removed under reduced pressure, and the residue recrystallised from ethanol. $^{31}P\{^1H\}$ NMR (CH_2Cl_2, 300 K): δ 29. ^1H NMR (CD_2Cl_2, 300 K): δ 7.3-7.9 (m). IR/cm^{-1}: 1193 (P=O).

$Ph_3P^{18}O$ A solution of Ph_3P (1.0 g, 3.8 mmol) in CH_2Cl_2 (20 cm^3) was treated with a crystal of SnI_4, under an atmosphere of dry N_2. The gas atmosphere was then replaced by dry O_2 by flushing. On completion of the reaction the solution was transferred to a separating funnel and shaken with NaCl solution (30 cm^3). The colourless organic phase was separated, dried over $MgSO_4$ and filtered. The solvent was removed under reduced pressure, and the residue recrystallised from ethanol. IR/cm^{-1}: 1157 (P=O).

$Ph_2P(O)CH_2CH_2P(O)Ph_2$ A solution of $Ph_2P(O)CH_2CH_2P(O)Ph_2$ (1.0 g, 2.3 mmol) in CH_2Cl_2 (20 cm^3) was treated with a crystal of SnI_4 under an atmosphere of dry N_2. The gas atmosphere was then replaced by dry O_2 by flushing. The solution was transferred to a separating funnel and shaken with NaCl solution (30 cm^3). The colourless organic phase was separated, dried over $MgSO_4$ and filtered. The solvent was removed under reduced pressure, and the residue recrystallised from ethanol. $^{31}P\{^1H\}$ NMR (CH_2Cl_2, 300 K): δ 31. IR/cm^{-1}: 1177 (P=O).

Attempted synthesis of Ph_3AsO Procedure as for $Ph_3P^{16}O$, but using Ph_3AsO.

Attempted synthesis of Me_2SO A solution of dimethyl sulfide (100 mg, 1.3 mmol) in anhydrous CH_2Cl_2 (15 cm^3) was treated with one molar equivalent of SnI_4 (200 mg, 0.3 mmol) under an atmosphere of dry N_2. The gas atmosphere was then replaced by dry O_2 by flushing. On stirring (room temperature, 3 weeks), an orange precipitate formed, and the solvent was removed under reduced pressure.

Attempted synthesis of $MeS(O)(CH_2)_3S(O)Me$ A solution of 1,3-bis(methylthio)propane (100 mg, 0.6 mmol) in anhydrous CH_2Cl_2 ($15cm^3$) was treated with two molar equivalents of SnI_4 (751 mg, 1.2 mmol) under an atmosphere of dry N_2. The gas atmosphere was then replaced by dry O_2 by flushing. On stirring (room temperature, 3 weeks), an orange precipitate formed, and the solvent was removed *in vacuo*. ^1H NMR ($CDCl_3$, 300K): δ 2.55 (*t*, SCH_2, 4H), 2.2 (*s*, SCH_3, 6H), 1.8 (*qnt*, CH_2, 2H).

4.4 References

[1] K. Weinburg, *US Pat.*, 1973, 3751482; *Chem. Abstr.*, 1973, **79**, 9237n

[2] C. Ercolani, J. V. Quagliano and L. M. Vallarino, *Inorg. Chim. Acta*, 1973 **7**, 413.

[3] D. H. R. Barton, A. E. Martell and D. T. Sawyer, Eds. *The Activation of Dioxygen and Homogenous Catalytic Oxidation*; Plenum Press, New York, 1993.

[4] N. Hagiwara, N. Takahashi and H. Kojima, *Jpn. Pat.*, 1974, 7424900; *Chem. Abstr.*, 1975, **82**, 86404n.

[5] R. K. Poddar and U. Agarwala, *Inorg. Nucl. Chem. Lett.*, 1973, **9**, 785.

[6] B. G. Jacobi, D. S. Laitar, L. Pu, M. F. Wargocki, A. G. Dipasquale, K. C. Fortner, S. M. Schuck and S. N. Brown, *Inorg. Chem.*, 2002, **41**, 4815.

[7] J. Halpern and A. L. Pickard, *Inorg. Chem.*, 1970, **9**, 2798.

[8] J. Halpern, B. L. Goodall, G. P. Khare, H. S. Lim and J. J. Plath, *J. Am.Chem. Soc.*, 1975, **97**, 2301.

[9] K. Takao, Y. Fujiwara, T. Imanaka and S. Teranishi, *Bull. Chem. Soc. Jap.*, 1970, **43**, 1153.

[10] S. J. LaPlaca and J. A. Ibers, *J. Am. Chem. Soc.*, 1965, **87**, 2581; J. A. McGinnety, R. J. Doedens and J. A. Ibers, *Inorg. Chem.*, 1967, **6**, 2243.

[11] H. Staendeke and W. Klose, *Ger. Pat.*, 1973, 2156203; *Chem. Abstr.*, 1973, **79**, 53553v.

[12] W. Hewartson, *Chem. Abstr.*, 1970, **73**, 56570k.

[13] A. R. J. Genge, W. Levason, G. Reid, *Inorg. Chim. Acta*, 1999, **288**, 142.

[14] M. C. Careno, *Chem. Rev.*, 1995, **95**, 1717.

[15] M. Hudlicky, Oxidations in *Organic Chemistry*, ACS Monograph Series, American Chemical Society, Washington. DC, 1990, 252-261; D. J. Procter, *J. Chem. Soc., Perkin Trans.*, 1999, 641; E. G. Mata, *Phosphorus Sulfur Relat. Elem*, 1996, **117**, 231; M. Madesclaire, *Tetrahedron*, 1986, **42**, 5459.

[16] K. S. Ravikumar, J. –P. Bégué, D. Bonnet-Delpon, *Tetrahedron Lett.*, 1998, **39**, 3141.

[17] F. Gasparrini, M. Giovannoli and D. Misiti, *J. Org. Chem.*, 1990, **55**, 1323.

[18] K. Orito, T. Hatakeyama, M. Takeo and H. Suginome., *Synthesis*, 1995, 1357; and references therein.

[19] D. W. Lahti and J. H. Espenson, *Inorg. Chem.*, 2000, **39**, 2164.

[20] A. R. Hajipour, S. E. Mallakpour and H. Adibi, *J. Org. Chem.*, 2002, **67**, 8666.

[21] C. Srinivasan, A. Chellamani and P. Kuthalingam, *J. Org. Chem.*, 1982, **47**, 428; M. Ochiai, A. Nakanishi and T. J. Ito, *J. Org. Chem.*, 1997, **62**, 4253; D. H. R. Barton, W. Li and J. A. Smith, *Tetrahedron Lett.*, 1998, **39**, 7055; H. Tohma, S. Takizawa, H. Watanabe, Y. Fuckuoka, T. Maegawa and Y. Kita, *J. Org. Chem.*, 1999, **64**, 3519.

[22] S. S. Kim, K. Nehru, S. S. Kim, D. W. Kim and H. C. Jung, *Synthesis*, 2002, 2484.

[23] A. R. J. Genge, PhD Thesis, University of Southampton, 1999.

[24] D. J. Philips and S. Y. Tyree, Jr, *J. Amer. Chem. Soc.*, 1961, **83**, 1806.

[25] T. A. Albright, W. J. Freeman and E. E. Schweizer, *J. Org. Chem.*, 1975, **40**, 3437.

[26] J. A. Davies, S. Dutremez and A. A. Pinkerton, *Inorg. Chem.*, 1991, **30**, 2380.

[27] P. Calcagno, B. M. Kariuki, S. J. Kitchin, J. M. A. Robinson, D. Philip and K. D. M. Harris, *Chem. Eur. J.*, 2000, **6**, 2338.

[28] D. G. Gilheany in F. R. Hartley (Ed), *The Chemistry of Organophosphorus Compounds*, vol 2, Wiley, New York, Chapter 1.

[29] U. Sartorelli, F. Canziani and F. Zingales, *Inorg. Chem.*, 1966, **5**, 2233.

[30] C. Glidewell, *J. Organomet. Chem,* 1964, **29**, 1660.

[31] T. Tonaka, *Inorg. Chim. Acta*, 1967, **1**, 217.

[32] K. Griesbaum, A. A. Oswald, E. R. Quiram and W. Naegele, *J. Org. Chem.*, 1963, 1952.

[33] A. M. Aguiar and J. Beisler, *J. Org. Chem.*, 1964, **29**, 1660.

[34] H. C. E. McFarlane and W. McFarlane, *Polyhedron*, 1983, **2**, 303.